Improving volcanic ballistic hazard assessment through field and laboratory approaches

---

A thesis

submitted in partial fulfilment of the requirements for the degree

of

Doctor of Philosophy in Geology

at the

University of Canterbury

by

Rebecca Hanna Fitzgerald

UNIVERSITY OF CANTERBURY

2019

Frontispiece

A Strombolian explosion at dusk, Yasur Volcano, Vanuatu. This long exposure image highlights the rapid rise of incandescent bombs along ballistic trajectories, posing a risk to visitors. Photo credit: Ben Kennedy

Abstract

Direct impact from volcanic ballistic projectiles, fragments of solid rock or molten lava, are one of the most common causes of fatalities and injuries on volcanoes and have caused substantial damage and destruction of property and infrastructure. Despite this, ballistic hazard, impact and risk research trails behind other volcanic hazards. There is a good understanding of how ballistics are transported, how far they travel and their size, though little is understood of how they are distributed within a ballistic field, the intensity of ballistic hazard within the field, and how the spatial distribution changes over time. Consequently, when ballistic hazard has been included in hazard and risk assessments and management decisions, it is managed by placing a precautionary zone around the volcano, often based on the maximum travel distance.

In addition, it is well known that an impact by a ballistic can cause injury or death, yet this is not the only aspect of the hazard footprint from an individual ballistic. Other aspects such as impact ejecta (surface debris and/or shrapnel from the ballistic) also contribute to the hazard footprint size and little is known about their ability to cause death or injury and how this changes over the hazard footprint. It is critical for hazard and risk managers to know the potential size of the hazard footprint that a person could be affected by and the hazard intensity that may be experienced to calculate risk effectively. Previously only direct impact and impact angle have been considered in risk calculations. This thesis aims to improve our understanding of ballistic hazard so that a more risk-based approach to hazard and risk assessment and management can be applied. This is achieved through review of ballistic hazard characteristics, hazard and risk assessments, maps, management and communication literature to get an overview of the topic and determine knowledge gaps; and field and experimental work to investigate the ballistic hazard footprint and hazard intensity.

To assess how ballistic distribution and intensity change over a ballistic field, the ballistic hazard footprint at Yasur Volcano, Vanuatu was mapped from drone-captured orthophotos taken in two field campaigns two months apart. Mapping revealed that the spatial density of ballistics changed over small areas. Spatial density and ballistic size decreased with distance from the crater, while an increased spatial density was also noted to the S – SSE of the vent area indicating explosion directionality. When compared with eruption footage captured over a

three-day period, it was found that explosion directionality slightly differed between the two data sets (mapping and video analysis) taken over different timescales suggesting that directionality may evolve over time.

The size of the hazard footprint from an individual ballistic was found to be influenced by impact energy of the ballistic, ballistic diameter, crater diameter, ejecta travel distance, ejecta impact energy, ballistic density, substrate hardness, impact angle and slope. Pneumatic cannon experiments were used to investigate the contribution of impact ejecta to the hazard footprint. The kinetic energy and travel distance of impact ejecta produced from varying ballistic densities impacting different surfaces were analysed and findings showed that ejecta have the potential to cause injury or fatality on impact (based on hazard intensity values found in the literature). However, this was greatly dependent on the density of the impacting ballistic, the surface hardness, ballistic impact energy and where along the ejecta trajectory it impacted. Initial kinetic energy values were not retained over the entire ejecta trajectory, indicating that hazard intensity varies over the individual ballistic hazard footprint.

To make the most effective risk management decisions it is important to understand both the hazard footprint and the hazard intensity. Ballistic hazard and risk assessments should be conducted over as much of the volcano as possible and assess the spatial density (hazard intensity) as well as the extent. Additionally, assessments should include all temporal hazard changes that may occur in the timeframe relevant to the assessment to get the greatest understanding of the spatial and temporal aspects of the hazard. When calculating hazard intensity, vulnerability and risk to people from ballistics on volcanoes, the kinetic energy of the impact ejecta should be included in the hazard footprint in addition to ballistic energy and impact angle. Improving current understanding of how ballistics are distributed in space and time, and how hazard intensity varies over the ballistic hazard footprint will vastly improve our ability to assess ballistic hazard and risk.

Acknowledgements

A huge thank you goes to my supervision team: Ben Kennedy, Tom Wilson and Graham Leonard, for being so encouraging and supportive. I'm so thankful for all the fieldwork, conference and travel opportunities that you have provided and supported. Ben, thanks for always being super positive, full of ideas (even though I'm sure I shot a lot of them down!), for always championing me, being so patient, and for always being available to answer questions. Tom, I couldn't have done this without your natural hazards brain. Thanks for your enthusiasm, for challenging me, and for believing in me even when I didn't. Graham, I really appreciated your task-master ways, making me plan out step-by-step how I was going to do things, it made it a lot easier to attack my thesis.

To the techs and staff at UC, none of my fieldwork and lab work would have been possible without you. Thanks to Matt Cockcroft and Peter Jones for helping build, fix and troubleshoot with the cannon. Thanks to Sacha, Cathy and Sarah for fulfilling my always last-minute equipment needs. To Chris for showing me the basics of the seds lab. To Jim for reading through my draft papers (even though you didn't have to!) and culling all the unnecessary words. Rebekah and Pat for the travel bookings, Mason Trust questions and admin help. To Nick Key for coming with me to Vanuatu and flying the drone.

My PhD wouldn't have been possible without funding. Thanks to the Ngāi Tahu Research Centre for offering me a Doctoral Scholarship, and to EQC (Biennial Grant 16/727) for funding my fieldwork in Japan and Vanuatu.

Thanks to all the helpers I've had along the way. To Shanelle, my GIS hero, even though I may not have used half the stuff we tried, I'm so thankful to you for answering my basic questions, showing me step-by-step how to do things and brainstorming ways for me to better analyse my data. To my cannon helpers Ame, Waddo, George, Josh, Luke, Ian and Steph. I couldn't have dug so much sand, fixed the cannon so many times, and DCP'd without you all.

Thanks to my friends, Huntingdon Country Club members, officemates (412, 311 and 260), CoUGARs, and Volc Group. Especially AJ, Emma, Liv, Josh, Tyler, Ali, Tom, Heather, Grant, SamTram, Lorelei, and George. Thanks for listening to me rant, keeping me socialised and

sane, for the discussions (both work-related and, more often than not, procrastination), laughs, help, coffee breaks, and encouragement.

Last but definitely not least, I'm especially grateful to my family. Mum, Steve, Sam, Dad and Juliet thanks for checking I'm staying healthy, for the food deliveries, for reminding me to keep checking boxes, for the FaceTime's, encouragement, and for just being there.

Co-authorship Forms

UNIVERSITY OF CANTERBURY
Te Whare Wānanga o Waitaha
CHRISTCHURCH NEW ZEALAND

Deputy Vice-Chancellor's Office
Postgraduate Research Office

Co-Authorship Form

Chapter 2: The communication and risk management of volcanic ballistic hazards

Published in: Fearnley C, Bird D, Jolly G, Haynes K and McGuire B (Eds), Observing the Volcano World: Volcano Crisis Communication, Advances in Volcanology, Springer International Publishing, ISBN 978-3-319-44095-8.

The published manuscript was compiled and written by Rebecca Fitzgerald. The concept of the manuscript was developed by Rebecca Fitzgerald in discussion with Ben Kennedy, Thomas Wilson and Graham Leonard. Kae Tsunematsu and Harry Keys provided expertise and situational knowledge for the Japanese volcanoes and Tongariro Volcano, respectively. All co-authors reviewed draft versions of the manuscript before submission by Rebecca Fitzgerald.

Certification by Co-authors:
If there is more than one co-author then a single co-author can sign on behalf of all
The undersigned certifies that:

- The above statement correctly reflects the nature and extent of the PhD candidate's contribution to this co-authored work
- In cases where the candidate was the lead author of the co-authored work he or she wrote the text

Name: *Ben Kennedy* Signature: Date: *22/05/2019*

UNIVERSITY OF CANTERBURY
Te Whare Wānanga o Waitaha
CHRISTCHURCH NEW ZEALAND

Deputy Vice-Chancellor's Office
Postgraduate Research Office

Co-Authorship Form

Chapter 3: Volcanic ballistic projectile deposition from a continuously erupting volcano: Yasur Volcano, Vanuatu

Submitted to: Volcanica

Rebecca Fitzgerald compiled and wrote the manuscript, analysed GoPro footage and catalogued explosions, mapped the ballistic distributions and analysed the results. Ben Kennedy, Thomas Wilson and Graham Leonard provided advice and discussion on the concept of the manuscript, fieldwork planning and support with writing the manuscript. Chris Gomez processed drone imagery and created the orthophotos and DEMs. Robin Matoza provided supporting infrasound data and created Figure 5. Ben Simons provided observation logs between two trips. Art Jolly provided seismic data from YASH station. Esline Garaebiti coordinated fieldwork and provided local hazard management context. All authors assisted in discussions and reviewed the manuscript before submission.

Certification by Co-authors:
If there is more than one co-author then a single co-author can sign on behalf of all
The undersigned certifies that:

- The above statement correctly reflects the nature and extent of the PhD candidate's contribution to this co-authored work
- In cases where the candidate was the lead author of the co-authored work he or she wrote the text

Name: *Ben Kennedy* Signature: Date: *22/05/2019*

UNIVERSITY OF CANTERBURY
Te Whare Wānanga o Waitaha
CHRISTCHURCH NEW ZEALAND

Deputy Vice-Chancellor's Office
Postgraduate Research Office

Co-Authorship Form

Chapter 4: Using pneumatic cannon experiments to understand ballistic hazard footprints
Prepared for submission to: Journal of Applied Volcanology

The concept of the manuscript was developed through discussion between all authors (Rebecca Fitzgerald, Ben Kennedy, Tom Wilson and Graham Leonard). Writing of the manuscript was undertaken by Rebecca Fitzgerald. Ben Kennedy provided valuable contribution to the structure of the paper and discussion of results. Experimental design was discussed between Rebecca Fitzgerald and Ben Kennedy, with help from Tom Wilson. All experiments, modelling and analysis were performed by Rebecca Fitzgerald. Tom Wilson suggested creating damage states and fragility functions to better analyse and present this work.

Certification by Co-authors:
If there is more than one co-author then a single co-author can sign on behalf of all
The undersigned certifies that:

- The above statement correctly reflects the nature and extent of the PhD candidate's contribution to this co-authored work
- In cases where the candidate was the lead author of the co-authored work he or she wrote the text

Name: *Ben Kennedy* Signature:  Date: *25/05/19*

UNIVERSITY OF CANTERBURY
Te Whare Wānanga o Waitaha
CHRISTCHURCH NEW ZEALAND

Deputy Vice-Chancellor's Office
Postgraduate Research Office

Co-Authorship Form

Appendix A: Capturing the Acoustic Radiation Pattern of Strombolian Eruptions using Infrasound Sensors Aboard a Tethered Aerostat, Yasur Volcano, Vanuatu

Published in: Geophysical Research Letters, 44(19), 9672-9680.

Rebecca Fitzgerald was the 6th author on this paper. She provided analysis of video footage of eruptions which were used to check eruption directionality and reviewed the manuscript. Art Jolly conceived and wrote the paper. He also collected and analysed the infrasound data. Robin Matoza and David Fee wrote a section of the manuscript and, along with Ben Kennedy, provided discussion of results. Richard Johnson, Alexandra Iezzi and Allison Austin provided technical and field assistance.

Certification by Co-authors:
If there is more than one co-author then a single co-author can sign on behalf of all
The undersigned certifies that:

- The above statement correctly reflects the nature and extent of the PhD candidate's contribution to this co-authored work
- In cases where the candidate was the lead author of the co-authored work he or she wrote the text

Name: *Ben Kennedy* Signature: Date: *25/05/19*

UNIVERSITY OF CANTERBURY
Te Whare Wānanga o Waitaha
CHRISTCHURCH NEW ZEALAND

Deputy Vice-Chancellor's Office
Postgraduate Research Office

Co-Authorship Form

Appendix B: A progress report on the assessment of ballistic hazard and impacts from the 2000 eruption of Usu, Japan and the 2014 eruption of Mt Ontake, Japan

Submitted to: EQC for Biennial Grant 16/727

Rebecca Fitzgerald was the lead author and wrote the majority of this report. She analysed the aerial photos and mapped the ballistic distribution. George Williams wrote sections 1.5.3 and 1.5.4 and conducted the data analysis for these sections. Rebecca Fitzgerald, George Williams, Ben Kennedy, Graham Leonard, Kae Tsunematsu and Hiromu Okada conducted fieldwork. Tom Wilson and Koshun Yamaoka provided input into fieldwork planning. Koshun Yamaoka provided data from Mt Ontake. Hiromu Okada provided aerial photos from Usu Volcano. Thomas Wilson and Ben Kennedy helped structure the report and provided useful discussion of the results.

Certification by Co-authors:
If there is more than one co-author then a single co-author can sign on behalf of all
The undersigned certifies that:

- The above statement correctly reflects the nature and extent of the PhD candidate's contribution to this co-authored work
- In cases where the candidate was the lead author of the co-authored work he or she wrote the text

Name: *Ben Kennedy* Signature: Date: *25/05/19*

UNIVERSITY OF CANTERBURY
Te Whare Wānanga o Waitaha
CHRISTCHURCH NEW ZEALAND

Deputy Vice-Chancellor's Office
Postgraduate Research Office

Co-Authorship Form

Appendix C: The DEVORA Scenarios: Multi-hazard eruption scenarios for the Auckland Volcanic Field
Submitted to: GNS Science report; 2018/29

Rebecca Fitzgerald was 3rd author of this report. She conducted all ballistic hazard modelling and wrote the section on it in the report. Josh Hayes was lead author and conceptualised, compiled and wrote the majority of the report. He also conducted all modelling (with the exception of ballistics and lava flows) and data analysis. Sophia Tsang conducted all lava flow modelling. Daniel Blake contributed to early scenario development. Natalia Deligne, Angela Doherty, Jenni Hopkins, Tony Hurst, Nicolas Le Corvec, Graham Leonard, Jan Lindsay, Craig Miller, Karoly Nemeth, Elaine Smid, James White and Thomas Wilson reviewed the manuscript and contributed their specialised knowledge to the report.

Certification by Co-authors:
If there is more than one co-author then a single co-author can sign on behalf of all
The undersigned certifies that:

- The above statement correctly reflects the nature and extent of the PhD candidate's contribution to this co-authored work
- In cases where the candidate was the lead author of the co-authored work he or she wrote the text

Name: *Josh L. Hayes* Signature:  Date: *25/05/2019*

UNIVERSITY OF CANTERBURY
Te Whare Wānanga o Waitaha
CHRISTCHURCH NEW ZEALAND

Deputy Vice-Chancellor's Office
Postgraduate Research Office

Co-Authorship Form

Appendix D: Buildings vs. ballistics: Quantifying the vulnerability of buildings to volcanic ballistic impacts using field studies and pneumatic cannon experiments
Submitted to: Journal of Volcanology and Geothermal Research, 343, 171 – 180.

Rebecca Fitzgerald was the 4th author of this paper and helped in experimental and field data collection and manuscript review. George Williams wrote the manuscript, conducted the experiments, collected field data and analysed all data. Ben Kennedy and Thomas Wilson assisted with the structure and conceptual framing of the paper. Kae Tsunematsu and Adrian Teissier assisted in field and experimental work.

Certification by Co-authors:
If there is more than one co-author then a single co-author can sign on behalf of all
The undersigned certifies that:

- The above statement correctly reflects the nature and extent of the PhD candidate's contribution to this co-authored work
- In cases where the candidate was the lead author of the co-authored work he or she wrote the text

Name: *Ben Kennedy* Signature: Date: *25/05/19*

Table of Contents

List of Figures

List of Tables

Chapter One – Introduction

Volcanic eruptions produce multiple geological phenomena such as ash, pyroclastic density currents, and ballistics. These phenomena can be considered hazards, where they may negatively affect societal elements, such as people and infrastructure which may be susceptible to damage or loss (UNDRR 2017). Worldwide, over 29 million people live within 10 km of an active volcano (Brown et al. 2015). Active volcanoes also attract scientists, tourists and climbers. An increasing global population and an increasing number of visitors to active volcanoes means the number of people exposed to volcanic hazards will likely continue to rise (Erfurt-Cooper, Sigurdsson and Lopes 2015).

1.1. Disaster risk reduction

To combat negative consequences to society and the environment from volcanic hazards and a global need to reduce disaster consequences, disaster risk reduction (DRR) is used as the global unifying framework. DRR is the reduction of disaster risk through methodical analysis and management of the factors that cause disasters (UNDRR 2017).

The United Nations Office for Disaster Risk Reduction (UNDRR) has outlined how disaster risk and the subsequent consequences can be reduced in the Sendai Framework for Disaster Risk Reduction (UNISDR 2015). Priority 1: Understanding Disaster Risk states that “Policies and practices for disaster risk management should be based on an understanding of disaster risk in all its dimensions of vulnerability, capacity, exposure of persons and assets, hazard characteristics and the environment” and encourages “the use of and strengthening of baselines and periodically assess disaster risks, vulnerability, capacity, exposure, hazard characteristics and their possible sequential effects at the relevant social and spatial scale on ecosystems, in line with national circumstances” (UNISDR 2015 pg. 9).

1.2. Disaster risk assessment

A core principle of DRR is to take a scientific approach to understanding the disaster risk (UNISDR 2015). DRR strategies should be based on science and this approach should be systematic, repeatable and transparent. Disaster risk is the potential of death, injury, damage, and/or loss over a specified period of time from a hazardous event (UNDRR 2017). It is the product of the hazard (process or phenomenon that can cause negative consequences such as damage or death) interacting with assets exposed to the hazard (exposure), such as infrastructure and people, and the vulnerability or susceptibility of the exposed assets to damage by the hazard (UNDRR 2017).

$$Risk = Hazard \times Exposure \times Vulnerability$$

A volcanic risk assessment determines the probability of the adverse consequences occurring to exposed assets from hazardous events (Blong 1996). This typically includes: assessing the hazard by 1) reviewing the eruptive history of the volcano to ascertain eruptive frequency and magnitude, 2) field mapping, remote sensing and/or literature review to determine the nature and extent of the hazard, and 3) modelling of the hazard to explore future hazard extent (Sparks et al. 2013); assessing exposure by identifying which assets are exposed; and assessing vulnerability through vulnerability models informed from post-eruption impact assessments, empirical experiments, theoretical modelling and expert judgement (Rossetto and Elnashai 2003; Wilson et al. 2017). Figure 1.1 conceptualises the risk assessment framework. Hazard informs vulnerability through hazard intensity metrics (HIMs) which are a measure of a hazard property linked to adverse consequences (Wilson et al. 2014). For example, an HIM that may be used to assess building vulnerability to ashfall is tephra thickness. A greater thickness (hazard property) of ash would likely result in damage (adverse consequence) to the building (Wilson et al. 2017). Exposure is linked to vulnerability by the relevant attributes of the exposed element. For example, when considering buildings, the attributes might be the type and strength of roofing or cladding of the exposed building. One way to express the potential consequence or risk is by using the concept of 'Damage or Impact States'. They describe the scale of impact (e.g. damage) in terms of severity (Blong 2003). While Damage or Impact States are typically described in qualitative terms, they can also include or be related to a quantitative measure of risk e.g. percentage of damage or replacement cost (Blong 2003; Wilson et al. 2017). Risk

assessments can be both deterministic (scenario) or probabilistic, with pros and cons to both approaches (Marzocchi et al. 2004). Risk-to-life assessments, which are most relevant to ballistic risk assessments, are typically probabilistic so as to most effectively account for scientific and modelling uncertainties (Sparks et al. 2013). Once risk has been assessed, disaster risk reduction strategies (risk treatment) can be evaluated and applied if appropriate.

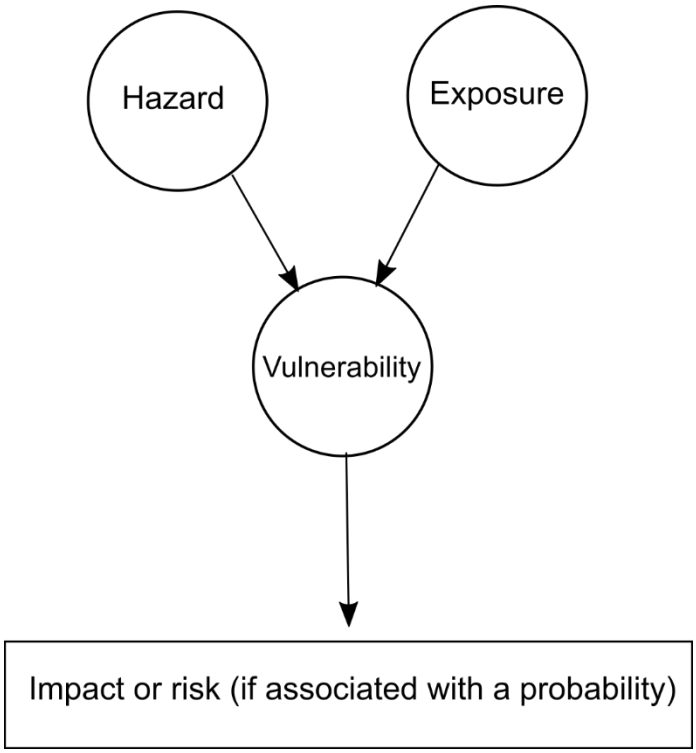

Figure 1.1 Risk assessment framework where hazard and exposure are related by vulnerability to assess impact or risk (if there is an associated probability).

1.3. Volcanic ballistic hazard and risk

One volcanic hazard that has received less research attention than others, despite being the most common cause of volcano fatalities for tourists and scientists (Brown et al. 2017), is volcanic ballistic projectiles. Ballistics are fragments of molten lava or solid rock ejected in explosive eruptions. Diameters can range from a few centimetres to tens of metres (Nairn and Self 1978; Bower and Woods 1996; Swanson et al. 2012). They travel on ballistic trajectories, separating early from the eruptive column. Projectiles typically land within the first 5 km from the vent,

however they have been recorded up to ~10 km away (Blong 1984; Alatorre-Ibargüengoitia et al. 2012). Initial velocities can also range up to hundreds of metres per second (Harris et al. 2012; Maeno et al. 2013). They therefore present a substantial risk to both life and infrastructure.

Records show that ballistics have killed at least 367 people and injured hundreds more (Brown et al. 2017). A relatively unheralded eruption in 2014 from Mt Ontake, Japan, ejected ballistics which killed 55 people who were hiking around the summit (Tsunematsu et al. 2016). Injuries can be due to the kinetic energy on impact or from the thermal energy from molten bombs (Baxter and Gresham 1997). In addition to human impacts, ballistics have also caused loss and damage to buildings (Blong 1984; Williams et al. 2017), cars (Wardman et al. 2012), radio antenna (Wardman et al. 2012), aircraft (Blong 1984) and vegetation (Alatorre-Ibargüengoitia et al. 2012).

Traditionally a precautionary approach to ballistic risk management has been taken where zonation was used to avoid the hazard (i.e. restriction or exclusion zones, as seen at Sakurajima Volcano (Kagoshima City 2010) and Yasur Volcano (Vanuatu Meteorology and Geo-hazards Department 2019)). This zone was often based on the hazard footprint (the spatial extent of the area affected by the hazard). Hazard footprints reported in literature include the maximum travel distance of a ballistic (Robertson et al. 1998; Alatorre-Ibargüengoitia et al. 2012), mapped edges of ballistic fields (Minakami 1942), and distribution of ballistic size (Houghton et al. 2011). Rarely do they contain details of the spatial distribution within these areas such as spatial density of impacts (Fitzgerald et al. 2014). While a ballistic may travel 3 km, there may only be one ballistic landing at this distance over a 1 km^2 area, thus the risk of being hit is extremely low. Further review of ballistic hazard and risk management and communication is provided in Chapter 2.

With an increased need for DRR (due to population growth, land use, tourism, and legislature) there is a need for a more risk-based approach to assessment and management. This means that not only hazard, but exposure and vulnerability need to be incorporated into ballistic DRR and for those aspects to feed in and interact with each other. Human exposure to ballistic hazard is difficult to assess in detail due to the lack of knowledge on human behaviour on a volcano,

especially our movement during non-eruption and rapid onset eruption situations. There is also uncertainty surrounding the areas of the body that would be exposed to ballistic impact. Additionally, to assess human vulnerability properly would require medical knowledge of the human body and its susceptibility to injury, which is beyond the scope of this geology PhD. Therefore, this thesis focuses on improving our understanding and assessment of ballistic hazard, both spatial and temporal, and how hazard interacts with exposure and vulnerability.

While it is well known how far ballistics can travel (Minakami 1942; Blong 1984; Kilgour et al. 2010; Alatorre-Ibargüengoitia et al. 2012; Gurioli et al. 2013), little is known about how they are distributed within the ballistic field (Fitzgerald et al. 2017). Spatial density is an important hazard intensity metric to use for considering the hazard of a ballistic field. Are there areas that may receive less ballistics than others and can therefore be deemed safer? And is this constant or does the spatial density change over time? Only a few ballistic fields have been mapped in detail and/or spatial density considered (Swanson et al. 2012; Gurioli et al. 2013; Fitzgerald et al. 2014; Kaneko et al. 2016). Three of these fields are from phreatic and phreatomagmatic events and one from a strombolian eruption. A larger dataset is needed to understand the spatial distribution and how this changes with distance and direction in a ballistic field and over time.

Additionally, it is assumed that the hazard footprint of an individual ballistic impact consists only of the ballistic (i.e. a direct strike to the person). However, ballistics have been observed to produce impact craters (Maeno et al. 2013; Breard et al. 2014), roll and bounce out of impact craters (Bernard 2018; Taddeucci et al. 2017), produce ejecta (Waitt et al. 1995; Rosi et al. 2006) and impact at an angle (Minakami 1942; Maeno et al. 2013; Fitzgerald et al. 2014). These factors can create their own hazard and/or change the size of the footprint. Can the size of the hazard footprint be quantified? How hazardous are these factors? Records show deaths and injuries from impacts with ballistics (Baxter and Gresham 1997; Brown et al. 2017) but can these factors also cause these outcomes? Does the level of hazard intensity (in this case kinetic energy) change over the footprint? By understanding the size of the hazard footprint, the hazard intensity exposure (the area that people are exposed to) and vulnerability (the level of hazard intensity that may cause susceptibility to an asset) can then be assessed. Many of these questions have led to the overall aim and specific objectives of this thesis.

1.4. Thesis aims and objectives

The overarching aim of this research is to improve our understanding of volcanic ballistic hazard so that it can be better assessed and managed. Currently there is limited understanding of the distribution of ballistics within a ballistic field, the hazard intensity within the field, and how the spatial distribution changes with time. Furthermore, little research has been completed on the hazard footprint of an individual ballistic, what factors influence it and how hazard intensity varies within it. These knowledge gaps affect the way ballistic hazard is managed. To achieve this overall aim, six objectives will be addressed (Figure 1.2):

1) A review of ballistic hazard and risk characteristics, management and communication to provide an overview of the topic and recommendations for how management and communication could be improved.
2) Determine the size and spatial distribution of ballistics from a complex, cumulative ballistic field through detailed mapping, to understand the spatial and temporal distribution of hazard intensity across the hazard footprint.
3) Using an integrative approach, assess temporal ballistic hazard and how this is affected by eruption dynamics.
4) Review and understand the factors that contribute to the hazard footprint from an individual ballistic impact.
5) Quantify the size and hazard intensity of the hazard footprint from an individual ballistic from impact ejecta associated with ballistics of different density and different substrates to improve ballistic hazard and risk assessments.

It is important to note that this thesis has been completed as a geology (not a disaster risk reduction) PhD thesis. As such it focusses on the geological phenomena which influence hazard. The above review of risk assessment and management is used to acknowledge and place this research in the wider disaster risk reduction context.

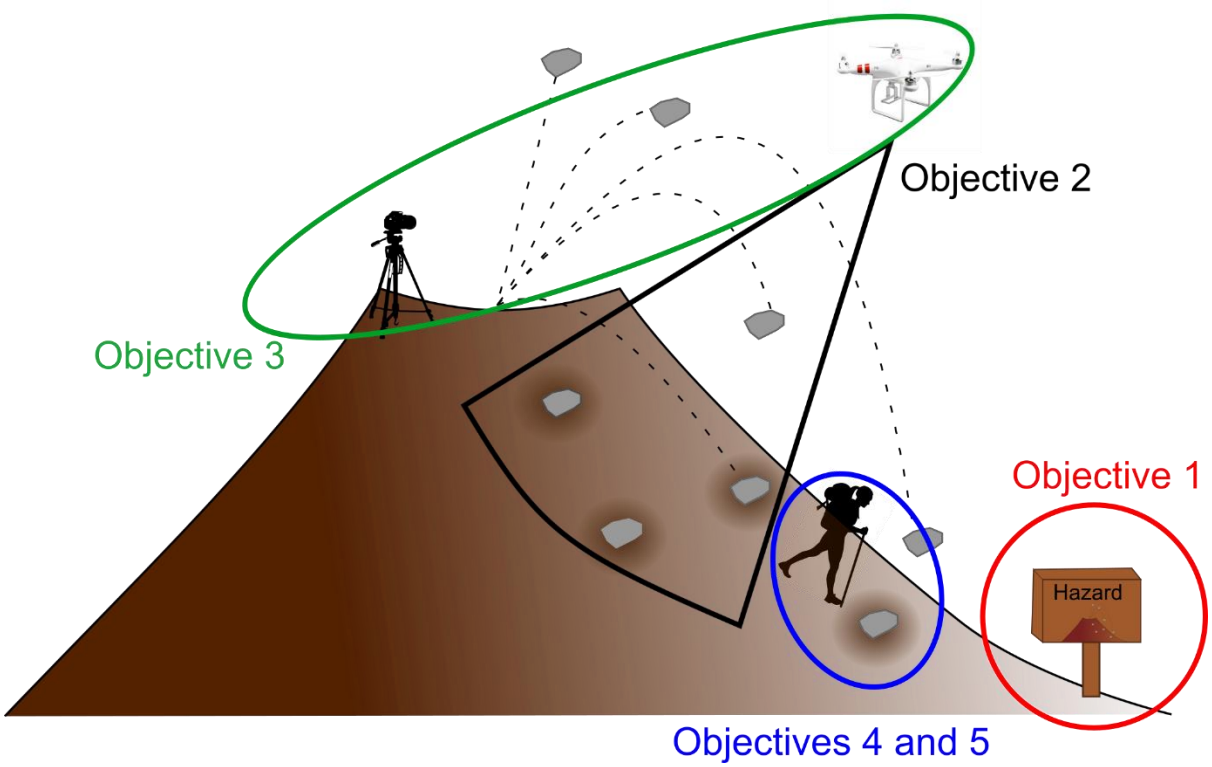

Figure 1.2 Conceptual diagram of thesis objectives

1.5. Thesis structure

This thesis is structured into six chapters, three of which are stand-alone papers with their own introductions. Chapter 1 provides a broad introduction to the disaster risk reduction framework, research objectives and thesis structure. Chapter 2 reviews the various processes and products used to manage and communicate ballistic hazard and risk and provides a detailed overview of ballistic hazard and risk assessments (Objective 1). It was published as a chapter in Observing the Volcano World: Volcano Crisis Communication, part of the IAVCEI series Advances in Volcanology. Chapter 3 uses Yasur Volcano, Vanuatu as a case study to understand ballistic distribution from a frequently erupting volcano (Objective 2). It examines how eruption dynamics influence the spatial distribution and how this changes over time (Objective 3). This chapter was submitted to the journal Volcanica and has been accepted pending minor revisions. Chapter 4 reviews the various factors that influence the size of the hazard footprint from an individual ballistic impact (Objective 4), presents results from pneumatic cannon testing to analyse hazard intensity (kinetic energy) of ejecta produced from a ballistic impact with varying

surfaces, and introduces damage states and hazard intensity metrics for ballistics (Objective 5). It will be submitted to the Journal of Applied Volcanology. The thesis is then summarised, and conclusions drawn in Chapter 5. The content of these chapters is my own work; however, my co-authors did provide data, editing, analysis, guidance, and useful discussions. Their contributions are listed in the preceding co-authorship forms.

The appendices contain further lead and co-authored work on ballistic hazard and risk that were undertaken during this PhD, although though not within the scope of this thesis:

- Appendix A is a co-authored paper that describes the acoustic radiation pattern from explosions at Yasur Volcano recorded using a tethered aerostat. The video footage of ballistic explosions used to analyse explosion directionality in Chapter 3 was additionally used in this paper to confirm directionality observed in the acoustic data.
- Appendix B is a lead-author EQC funding report detailing the ballistic hazard and impact assessment trip to Japan in 2015. The ballistic distributions and damage to buildings from the 2000 eruption of Usu Volcano and the 2014 eruption of Mt. Ontake were investigated. See Appendix D for the published article on the building damage.
- Appendix C contains a co-authored published report outlining eruption scenarios created for the Auckland Volcanic Field with the expectation that they will be used in impact and risk studies. Each scenario included modelling of the ballistic hazard.
- Appendix D is a co-authored paper published in the Journal of Volcanology and Geothermal Research on the vulnerability of buildings to ballistic impact. It combines field measurements (see Appendix B), data reported in literature, and experimental results to develop fragility functions for various building typologies.

1.6. References

Alatorre-Ibargüengoitia MA, Delgado-Granados H, Dingwell DB (2012). Hazard map for volcanic ballistic impacts at Popocatépetl volcano (Mexico). Bulletin of Volcanology 74(9), 2155–2169

Baxter P, Gresham A (1997). Deaths and injuries in the eruption of Galeras Volcano, Colombia, 14 January 1993. Journal of Volcanology and Geothermal Research 77, 325–338

Bernard B (2018). Rapid hazard assessment of volcanic ballistic projectiles using long-exposure photographs: insights from the 2010 eruptions at Tungurahua volcano, Ecuador. Volcanica, 1(1), 49–61. https://doi.org/https://doi.org/10.30909/vol.01.01.4961

Blong RJ (1984). Volcanic hazards: A sourcebook on the effects of eruptions. Orlando: Academic Press

Blong RJ (1996). Volcanic hazards risk assessment. In: Scarpa R, Tilling RI (ed) Monitoring and Mitigation of Volcanic Hazards, Springer, Berlin, pp 675–698

Blong R (2003). A review of damage intensity scales. Natural Hazards, 29, 57–76

Bower S, Woods A (1996). On the dispersal of clasts from volcanic craters during small explosive eruptions. Journal of Volcanology and Geothermal Research 73, 19–32

Breard ECP, Lube G, Cronin SJ, Fitzgerald R, Kennedy B, Scheu B, Montanaro C, White JDL, Tost M, Procter JN, Moebis A (2014). Using the spatial distribution and lithology of ballistic blocks to interpret eruption sequence and dynamics: August 6 2012 Upper Te Maari eruption, New Zealand. Journal of Volcanology and Geothermal Research 286, 373–386

Brown SK, Auker MR, Sparks RSJ (2015). Populations around Holocene volcanoes and development of a Population Exposure Index. In: Loughlin SC, Sparks RSJ, Brown SK, Jenkins SF, Vye-Brown C (eds). Global Volcanic Hazards and Risk. Cambridge: Cambridge University Press, 223–232

Brown SK, Jenkins SF, Sparks RSJ, Odbert H, Auker MR (2017). Volcanic fatalities database: analysis of volcanic threat with distance and victim classification. Journal of Applied Volcanology, 6, 15

Erfurt-Cooper P, Sigurdsson H, Lopes RMC (2015). Volcanoes and Tourism. In: Sigurdsson H (ed), The Encyclopedia of Volcanoes, Academic Press, 1295-1311

Fitzgerald RH, Kennedy BM, Wilson TM, Leonard GS, Tsunematsu K and Keys H (2017). The communication and risk management of volcanic ballistic hazards. In: Fearnley C, Bird D, Jolly G, Haynes K and McGuire B (Eds) Observing the Volcano World: Volcano Crisis Communication, Advances in Volcanology, Springer International Publishing, ISBN 978-3-319-44095-8

Fitzgerald RH, Tsunematsu K, Kennedy BM, Breard ECP, Lube G, Wilson TM, Jolly AD, Pawson J, Rosenberg MD, Cronin SJ (2014). The application of a calibrated 3D ballistic trajectory model to ballistic hazard assessments at Upper Te Maari, Tongariro. Journal of Volcanology and Geothermal Research 286, 248–262

Gurioli L, Harris AJL, Colo L, Bernard J, Favalli M, Ripepe M, Andronico D (2013). Classification, landing distribution, and associated flight parameters for a bomb field emplaced during a single major explosion at Stromboli, Italy. Geology 41(5), 559–562

Harris AJL, Ripepe M, Hughes EA (2012). Detailed analysis of particle launch velocities, size distributions and gas densities during normal explosions at Stromboli. Journal of Volcanology and Geothermal Research, 231–232, 109–131. https://doi.org/10.1016/j.jvolgeores.2012.02.012

Houghton BF, Swanson DA, Carey RJ, Rausch J., Sutton AJ (2011). Pigeonholing pyroclasts: Insights from the 19 March 2008 explosive eruption of Kilauea volcano. Geology 39(3), 263–266

Kagoshima City (2010). Sakurajima Volcano Hazard Map. http://www.city.kagoshima.lg.jp/soumu/shichoshitu/kokusai/en/emergency/documents/sakurazimahm_eng.pdf. Accessed 19 October 2015

Kaneko T, Maeno F, Nakada S (2016). 2014 Mount Ontake eruption: characteristics of the phreatic eruption as inferred from aerial observations. Earth, Planets and Space 68, 72-82

Kilgour G, Della Pasqua F, Hodgson KA, Jolly GE (2010). The 25 September 2007 eruption of Mount Ruapehu, New Zealand: Directed ballistics, surtseyan jets, and ice-slurry lahars. Journal of Volcanology and Geothermal Research 191(1-2), 1–14

Maeno F, Nakada S, Nagai M, Kozono T (2013). Ballistic ejecta and eruption condition of the vulcanian explosion of Shinmoedake volcano, Kyushu, Japan on 1 February, 2011. Earth, Planets and Space 65(6), 609–621

Marzocchi W, Sandri L, Gasparini P, Newhall C, Boschi E (2004). Quantifying probabilities of volcanic events: the example of volcanic hazard at Mount Vesuvius. Journal of Geophysical Research: Solid Earth, 109, 1–18

Minakami T (1942). 5. On the distribution of volcanic ejecta (Part I.): The distributions of volcanic bombs ejected by the recent explosions of Asama. Bulletin of Earthquake Research Institute 20, 65 – 92

Nairn IA, Self S (1978). Explosive eruptions and pyroclastic avalanches from Ngauruhoe in February 1975. Journal of Volcanology and Geothermal Research 3, 36–60

Robertson R, Cole P, Sparks RSJ, Harford C, Lejeune AM, McGuire WJ, Miller AD, Murphy MD, Norton G, Stevens NF, Young SR (1998). The explosive eruption of Soufriere Hills Volcano, Montserrat, West Indies, 17 September, 1996. Geophysical Research Letters 25(18), 3429–3432

Rosi M, Bertagnini A, Harris AJL, Pioli L, Pistolesi M, Ripepe M (2006). A case history of paroxysmal explosion at Stromboli: Timing and dynamics of the April 5, 2003 event. Earth and Planetary Science Letters, 243, 594 – 606

Rossetto T, Elnashai A (2003). Derivation of vulnerability functions for European-type RC structures based on observational data. Engineering Structures, 25, 1241–1263

Sparks RSJ, Aspinall WP, Crosweller HS, Hincks TK (2013). Risk and uncertainty assessment of volcanic hazards. In: Sparks RJS, Hill L (eds) Risk and uncertainty assessment for natural hazards, Cambridge University Press

Swanson DA, Zolkos SP, Haravitch B (2012). Ballistic blocks around Kīlauea Caldera: Their vent locations and number of eruptions in the late 18th century. Journal of Volcanology and Geothermal Research 231-232, 1-11

Taddeucci J, Alatorre-Ibargüengoitia MA, Cruz-Vázquez O, Del Bello E, Scarlato P, Ricci T (2017). In-flight dynamics of volcanic ballistic projectiles. Reviews of Geophysics, 55(3), 675–718. https://doi.org/10.1002/2017RG000564

Tsunematsu K, Ishimine Y, Kaneko T, Yoshimoto M, Fujii T, Yamaoka K (2016). Estimation of ballistic block landing energy during 2014 Mount Ontake eruption. Earth, Planets and Space 68, 88

UNDRR (2017). Terminology. Retrieved from https://www.unisdr.org/we/inform/terminology

UNISDR (2015). Sendai Framework for Disaster Risk Reduction (2015-2030). United Nations International Strategy for Disaster Reduction, Geneva, Switzerland. Retrieved from http://www.unisdr.org/we/coordinate/sendai-framework

Vanuatu Meteorolgy and Geo-Hazards Department (2019). Yasur visitor fact sheet. Retrieved from https://www.vmgd.gov.vu/vmgd/index.php/geohazards/volcano/volcano-info/resources

Waitt RB, Mastin LG, Miller TP (1995). Ballistic showers during crater peak eruptions of Mount Spurr volcano, summer 1992. USGS Bulletin, 2139

Wardman J, Sword-Daniels V, Stewart C, Wilson T (2012). Impact assessment of the May 2010 eruption of Pacaya volcano, Guatemala. GNS Science Report 2012/09, 90p

Williams GT, Kennedy BM, Wilson TM, Fitzgerald RH, Tsunematsu K, Teissier A (2017). Buildings vs. ballistics: Quantifying the vulnerability of buildings to volcanic ballistic impacts using field studies and pneumatic cannon experiments. Journal of Volcanology and Geothermal Research 343, 171-180

Wilson G, Wilson TM, Deligne NI, Blake DM, Cole JW (2017). Framework for developing volcanic fragility and vulnerability functions for critical infrastructure. *Journal of Applied Volcanology*, *6*, 14–38. https://doi.org/10.1186/s13617-017-0065-6

Wilson G, Wilson TM, Deligne NI, Cole JW (2014). Volcanic hazard impacts to critical infrastructure: A review, Journal of Volcanology and Geothermal Research, 286, 148–182

Preamble (Chapter 2)

In Chapter 1 I summarised what disaster risk reduction is, the importance of understanding ballistic hazard and how it has been approached using disaster risk reduction measures, and the knowledge gaps that led to the research objectives being addressed in this thesis. This chapter reviews the current research on ballistic distributions, consequences, hazard and risk assessments, hazard maps, and processes and products used to communicate and manage ballistic risk. Recommended strategies for communicating and managing ballistic hazard are also provided.

Chapter 2 has been published in the book Observing the Volcano World: Volcano Crisis Communication: Fitzgerald RH, Kennedy BM, Wilson TM, Leonard GS, Tsunematsu K and Keys H (2017). The communication and risk management of volcanic ballistic hazards. In: Fearnley C, Bird D, Jolly G, Haynes K and McGuire B (Eds) Observing the Volcano World: Volcano Crisis Communication, Advances in Volcanology, Springer International Publishing, ISBN 978-3-319-44095-8.

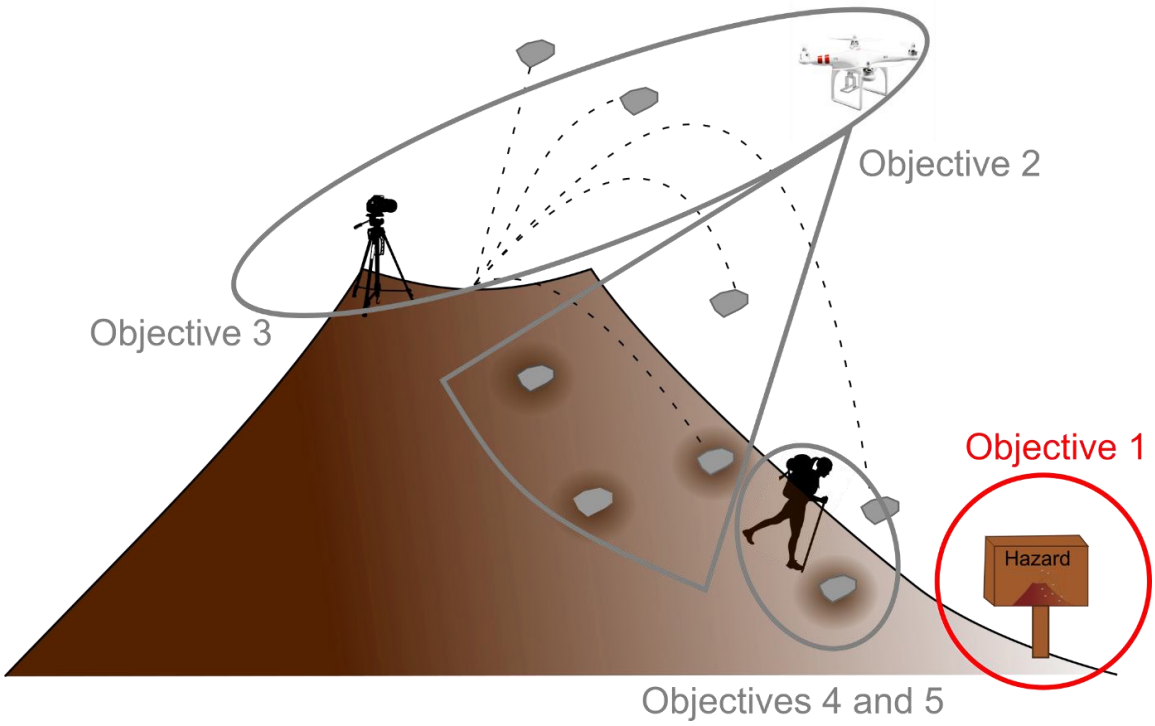

Conceptual diagram showing the objectives of the thesis with the objective addressed in Chapter 2 in red.

Chapter Two – The communication and risk management of volcanic ballistic hazards

2.1. Abstract

Tourists, hikers, mountaineers, locals and volcanologists frequently visit and reside on and around active volcanoes, where ballistic projectiles are a lethal hazard. The projectiles of molten lava or solid rock, ranging from a few centimetres to several metres in diameter, are erupted with high kinetic, and sometimes thermal, energy. Impacts from projectiles are amongst the most frequent causes of fatal volcanic incidents and the cause of hundreds of thousands of dollars of damage to buildings, infrastructure and property worldwide. Despite this, the assessment of risk and communication of ballistic hazard has received surprisingly little study. Here, we review the research to date on ballistic distributions, impact consequences, hazard and risk assessments and maps, and methods of communicating and managing ballistic risk including how these change with a changing risk environment. The review suggests future improvements to the communication and management of ballistic hazard.

2.2. Introduction

Ballistic projectiles are one potentially lethal and damaging hazard produced in volcanic eruptions. Ballistics are fragments of molten lava (bombs) or solid rock (blocks) ejected in explosive eruptions (Figure 2.1a and b). Projectiles range from a few centimetres to tens of metres in diameter and separate from the eruptive column to follow nearly parabolic trajectories (Wilson 1972; Fagents and Wilson 1993; Bower and Woods 1996). Their exit velocities can reach hundreds of metres per second and land up to ~10 km from the vent, although typically within five kilometres (Blong 1984; Alatorre-Ibargüengoitia et al. 2012). Ballistics are associated with all forms of explosive eruptions but are considered major hazards of hydrothermal, phreatic, phreatomagmatic, Strombolian and Vulcanian eruptions, especially those which have little to no precursory signals of volcanic unrest. Managing ballistic hazard and risk on active volcanoes, particularly those permanently occupied or regularly visited,

presents considerable challenges: it requires good information and specialist communication strategies around risk mitigation, preparedness, response, and recovery dependent on the state of the volcano, e.g. pre-, during- and post-eruption. In this chapter, we present an overview of volcanic ballistic hazards and consequences and the communication strategies used to manage risk on active volcanoes.

Figure 2.1: Types of ballistic particles and their consequences: a. Ballistic bombs from Yasur Volcano, Vanuatu (photo credit: Ben Kennedy), b. Ballistic blocks (1.4 m diameter block) from the August 2012 Upper Te Maari eruption, c. Damage to a building from ballistics ejected in the 2000 Mt. Usu, Japan eruption, d. Damage to the environment illustrated by a 4.4 m wide crater from the August 2012 Upper Te Maari, Tongariro eruption, e. Damage to a hiking hut from 2012 Upper Te Maari ballistics (photo credit: Nick Kennedy)

2.3. Ballistic hazard and risk management

Ballistic projectiles are a risk to life on active volcanoes and can cause substantial damage to exposed infrastructure and the environment due to their high kinetic energy, mass, and often high temperatures (Blong 1984). Volcanic ballistic projectiles are amongst the most frequent

causes of fatal incidents on volcanoes, with at least 76 recorded deaths at six volcanoes (Galeras, Yasur, Popocatepetl, Pacaya, Raoul Island and Ontake) since 1993 (Baxter and Gresham 1997; Cole et al. 2006; Alatorre-Ibargüengoitia et al. 2012; Wardman et al. 2012; Tsunematsu et al. 2016). Many more people have been injured as a result of ballistic impacts, frequently suffering from blunt force trauma (broken bones), lacerations, burns, abrasions and bruising (Blong 1984; Baxter and Gresham 1997). Additionally, damage to buildings (Figure 2.1c and e), infrastructure, property and the surrounding environment (Figure 2.1d) are also common occurrences from ballistics during explosive eruptions. The high kinetic and thermal energy of ballistics can puncture, dent, melt, burn and knock down structures and their associated systems, such as power supply and telecommunication masts; crater roads; and crush and ignite vegetation (Booth 1979; Calvari et al. 2006; Pistolesi et al. 2008 Alatorre-Ibargüengoitia et al. 2012; Wardman et al. 2012; Andronico et al. 2013; Maeno et al. 2013; Fitzgerald et al. 2014; Jenkins et al. 2014). Blong (1981), Pomonis et al. (1999) and Jenkins et al. (2014) estimate a ballistic only needs 400-1000 J of kinetic energy to penetrate a metal sheet roof, far less than the estimated kinetic energy of ballistics (~10^6 J) from VEI 2-4 eruptions (Alatorre-Ibargüengoitia et al. 2012).

The distribution (distance from vent, direction, area and density) of ejected ballistics is controlled by the explosivity, type, size and direction of explosive eruptions, and usually creates spatially variable deposits (Gurioli et al. 2013; Breard et al. 2014; Fitzgerald et al. 2014). Generally, the distance travelled, and the total area impacted by ballistics increases with increasing explosivity, i.e. particles generally travel further and cover a greater area in Vulcanian eruptions (Nairn and Self 1978; Alatorre-Ibargüengoitia et al. 2012; Maeno et al. 2013) compared with Strombolian eruptions (Harris et al. 2012; Gurioli et al. 2013; Turtle et al. 2016). However, eruptions can be directed, ejecting ballistics at low angles and at distances greater than those from more vertically directed eruptions (Fitzgerald et al. 2014; Tsunematsu et al. 2016). The directionality of these blasts is often unpredictable and can be influenced by external factors such as landslides (Christiansen 1980; Breard et al. 2014), making it difficult to deterministically forecast future ballistic distributions. Mapped deposits from past eruptions are often not symmetrical around the vent, reflecting this directionality (Minakami 1942; Fudali and Melson 1972; Steinberg and Lorenz 1983; Kilgour et al. 2010; Houghton et al. 2011; Gurioli et al. 2013; Fitzgerald et al. 2014), and are sometimes the result of the crater and

surrounding topography (Breard et al. 2014; Tsunematsu et al. 2016). Detailed descriptions and maps of ballistic impact distributions are rare, but those published may contain some of the following data: maximum ballistic travel distances (Steinberg and Lorenz 1983; Robertson et al. 1998; Kaneko et al. 2016); the outer edges of a ballistic field (Minakami 1942; Nairn and Self 1978; Yamagishi and Feebrey 1994); and/or maximum particle (Nairn and Self 1978; Steinberg and Lorenz 1983; Robertson et al. 1998; Swanson et al. 2012) or crater size (Robertson et al. 1998; Maeno et al. 2013; Kaneko et al. 2016). When isopleths of particle size are included these rarely contain individual measurements and may be severely limited by the availability of only specific mapped locations (e.g., Kilgour et al. 2010; Houghton et al. 2011). For this reason, the number of particles, sizes of particles, and spatial density per unit area is rarely reported (only four publications could be found with this level of detail - Pistolesi et al. 2008; Swanson et al. 2012; Gurioli et al. 2013; Kaneko et al. 2016). This leads to a limited understanding of the hazard and risk posed to the area.

Though work has been completed on ballistic hazard (e.g., mapping deposits, better understanding eruption dynamics and the factors that influence ballistic distribution, recording particle velocities, the creation and use of ballistic trajectory models, and the production of hazard maps either focussed solely on ballistics or as an aspect of a multi-hazard map), very little has been focussed on the management of ballistic risk, leaving a large knowledge gap and a need for research in this area. Risk management strategies and mitigation systems are key to protecting life and infrastructure from ballistic hazards (Leonard et al. 2008; Bertolaso et al. 2009; Bird et al. 2010; Jolly et al. 2014b). Table 2.1 lists some of the strategies and tools used at volcanoes around the world.

Table 2.1: Risk management and communication strategies with selected example volcanoes where they have been employed

Risk management strategy	Description	Selected examples of volcanoes where strategy has been used	References
Hazard and risk assessments	Hazard assessments determine the likelihoods of hazard producing events and the areas that may be impacted. These can be expanded to risk assessments to determine the likelihood of consequences to people and/or other	Tongariro Mt Fuji Popocatepetl El Chichon	Mount Fuji Disaster Prevention Council 2004; Alatorre-Ibargüengoitia et al. 2012; Jolly et al. 2014b; Alatorre-Ibargüengoitia et al. 2016

	societal assets. They underpin and inform other risk management strategies		
Hazard and risk maps	Identify zones of relative hazard and/or risk, typically in a two-dimensional representation	Popocatepetl Mt Fuji	Mount Fuji Disaster Prevention Council 2004; Alatorre-Ibargüengoitia et al. 2012
Volcano monitoring and research	Systems deployed on and around a volcano to monitor volcanic activity and indicate when the volcano is in unrest or eruption. Research is also conducted on the eruptive behaviour (e.g. magnitude and style) and eruption frequency of a volcano	Mt Etna Tongariro Sakurajima Mt Ontake Stromboli	https://www.geonet.org.nz/volcano/info/tongariro; http://www.ct.ingv.it/en/mappa-stazioni.html; JMA 2013a; JMA 2013b
Real-time warning systems	To monitor and detect a hazardous event (e.g. eruption) and communicate a warning to those potentially exposed.	Ruapehu	Leonard et al. 2008; Keys and Green 2010
Volcanic alert levels, bulletins and media advisories	Formal communications from a volcano observatory which communicate changes in volcano behaviour, notify emergency managers and the population of an eruption and advise on mitigation.	Yasur Tongariro	https://www.geonet.org.nz/volcano/info/tongariro; http://www.geohazards.gov.vu/
Emergency response plans	Plan for directing response actions which aim to reduce the consequences of an eruption. Plans are best executed with training and exercises in their use	Ruapehu Sakurajima	Leonard et al. 2008; http://www.city.tarumizu.lg.jp/kikikanri/kurashi/bosai/bosai/taisaku/sakurajima.html
Rescue services	Deploy in emergencies to provide aid to affected persons and properties, e.g. Search and Rescue, police, ambulance, and fire services	Ontake Ruapehu	Kilgour et al. 2010; The Japan Times 27/9/15
Land use planning	Policy and regulations used to minimise or exclude the development of settlement and construction of high-value assets in hazard zones.	Usu Volcano Tongariro Ruapehu	Becker et al. 2010; Keys and Green 2010
Construction of protective shelters	Structures designed to withstand specific hazards e.g. ballistic shelters in high-risk areas	Sakurajima Aso Stromboli	Bertolaso et al. 2009; Erfurt-Cooper 2010
Exclusion or restriction zones	Area restrictions commonly used temporarily during eruptions or unrest. Permanent zones may be required when risk is sufficiently high or frequent	Sakurajima Stromboli	Bertolaso et al. 2009; Kagoshima City 2010
Stakeholder engagement	Involvement of stakeholders (e.g. people and organisations potentially affected by an eruption) in planning and activities to manage the risk. This is essential for effective hazard and risk communication, and to establish appropriate and acceptable risk management strategies	Tongariro Sakurajima	Williams and Keys 2013; Jolly et al 2014b; http://www.data.jma.go.jp/svd/vois/data/fukuoka/506_Sakurajima/506_bousai.html
Hazard and risk education resources	Education resources which aid communication of hazard and risk information, often developed specifically for non-expert stakeholders. These can include pamphlets and brochures, websites, warning signs, videos, and public talks and meetings.	Auckland Volcanic Field, Tongariro	DOC 2012; Wilson et al. 2014

Effective communication of ballistic hazard and risk to end-users such as the public, stakeholders in the area and emergency managers underpins effective development and implementation of these risk management strategies. However, ballistic hazard and risk are not and should not be treated the same at all volcanoes. The risk environment (the hazard, the number of people and assets exposed and their associated vulnerability) will determine the strategies, tools and methods of communication, and their relative importance, utilised in the overall risk management strategy. The volcano tourism industry is also growing (Sigurdsson and Lopes-Gautier 1999, Erfurt-Cooper 2011), increasing the number of people exposed to ballistic hazard in proximal areas. In addition, population growth in many volcanic regions means increasing numbers of people are settling closer to and on volcanoes (Small and Naumann 2001; Ewart and Harpel 2004). This creates an increasing demand for ballistic hazard and risk assessments coupled with effective communication strategies to manage ballistic risk at volcanoes. Ballistics are not a hazard in isolation. Their management needs to be integrated with that of other volcanic hazards (especially pyroclastic density currents in terms of near-vent life safety, but also landslides, lahars, lava flows, and volcanic gas emissions/areas of hot ground), and other life safety issues such as severe weather and mountain safety.

2.4. Assessments of ballistic hazard and risk

Successful management of the risk from ballistic hazards typically requires first assessing the level of risk. This may range from the simple recognition that ballistics may endanger people or their activities on a volcano to a sophisticated quantitative hazard or risk assessment (e.g. Alatorre-Ibargüengoitia et al. 2012; Jolly et al. 2014b). Ballistic hazard assessments determine the likelihood of ballistic-producing eruptions and the areas that may be affected (Thouret et al. 2000; Alatorre-Ibargüengoitia et al. 2012). Risk assessments estimate the likelihood of consequences (i.e. death, injury, damage) from exposure to ballistics, typically with an associated probability of occurrence (Blong 1996). Once the level of risk has been assessed it can be used as the robust basis for risk management strategies, such as exclusion zones, hazard/risk maps and signs, and land-use planning. Ideal assessments involve a number of steps including: (1) a review of the eruption history of the volcano to determine past eruption frequencies and magnitudes, thus informing future eruption probabilities; (2) field mapping,

remote sensing and/or review of past reports and literature to determine the nature and extent of past ballistic distributions; (3) utilising ballistic trajectory models to explore possible future distributions and areas of hazard; (4) identifying exposed assets in the area such as humans (visitors and inhabitants) and infrastructure; and (5) estimating their vulnerability to the hazard i.e. likelihood of fatality or damage (Nadim 2013). Assessments are ideally probabilistic, providing spatially varying probabilities of occurrence and damage from a range of scenarios varying in frequency and magnitude, and accounting for model and input parameter uncertainty. They should be constantly refined and improved as new information becomes available.

A hazard map is a primary tool used to present hazard and risk information (Sparks et al. 2013). Zonation is generally used as a means to distinguish areas of hazard, exposure, vulnerability and risk (Sparks et al. 2013). Ballistic hazard map zones may be classified by maximum travel distance of particles (either any size or a specific sized particle; Alatorre-Ibargüengoitia et al. 2012), number of ballistic impacts per unit area (Gurioli et al. 2013), probability of a specific size of ballistics reaching a given area (Artunduaga and Jimenez 1997), or probability of a specific consequence occurring e.g. death, injury, damage (Fitzgerald et al. 2014). A good example of a ballistic hazard map that follows the best-practice steps above was created by Alatorre-Ibargüengoitia et al. (2012) of Popocatepetl Volcano, Mexico. In this example, eruption history and frequency of occurrence are used to define three eruption scenarios (High: VEI 2 – 3 (as they are more frequent), Intermediate: 4, and Low: 5 (though an eruption of this size would affect more people and impact a larger area, it has a much lower likelihood of occurring). The maximum travel distance of ballistic projectiles from each scenario (based on field and model distributions) is then used to define the extent of the hazard zones. Additionally, the map identifies nearby towns and roads exposed to ballistic hazard.

In many instances, it may not be possible or warranted to complete all of the steps involved in an ideal risk assessment. For example, Gareloi Volcano, Alaska is located on an uninhabited island, thus a detailed ballistic hazard assessment was not the priority of initial hazard assessments. Coombs et al. (2008) explore the eruptive history of Gareloi Volcano, though eruption frequency is only narrowed down to one eruption every 20 – 50 years and is not broken down into eruption magnitudes. Ballistic hazard is confined to one hazard zone (a 5 km concentric radius around the vent), whose extent is based on Blong's (1996) assessment that

ballistics generally do not travel further than 5 km from vent. It is also mentioned that recent ballistic distributions have not travelled further than several hundred metres from vent. Neither a deterministic or probabilistic approach was taken, instead a value was adopted from other eruptions around the world.

Very few studies exist on ballistic risk or vulnerability. We summarise the three that could be found. Booth (1979) presents an example of a volcanic risk map for the La Primavera Volcanic Complex, Mexico. Though ballistics are included, they are not ascribed a probability of occurrence, instead, one zone at risk of ballistic fall is defined by the maximum travel distance for ballistics up to 0.1 m in diameter. The equation that Booth used to calculate risk includes probability of occurrence, indicating that eruption frequency has been examined; however, neither the probability used nor the description of prior eruptive history are provided in the publication. Thus, though an end-product of a risk map is produced, the process itself is not documented. Pomonis et al. (1999) utilise the Blong (1981) impact energy thresholds for roof perforation to assess building vulnerability from an eruption of Furnas Volcano, the Azores. Two risk zones are assigned (moderate and high) based on the statement that ballistics generally land within 5 km of the vent, but sometimes up to 10 km. The study only considers one eruption (the last major eruption), thus is lacking eruption frequency and magnitude, and does not provide any probabilities of building damage occurring. Building vulnerability to ballistic impact has been assessed by Jenkins et al. (2014) for Kanlaon and Fogo volcanoes (Philippines and Cape Verde, respectively) using estimates of energy required to penetrate roof materials by Blong (1981) and Pomonis et al. (1999). This study, however, focussed only on the vulnerability of the built environment and did not include an overall assessment of hazard or risk. Eruption frequency and magnitude, the extent of past ballistic distributions, and modelling of possible future trajectories were not investigated.

Assessments may also vary depending on the state of the volcano. Volcanoes in a state of quiescence allow for (and call for) more in-depth, preferably probabilistic, assessment to be completed, ideally following the steps outlined earlier. However, quiescent volcanoes may not be the primary target for in-depth assessment. Conversely, renewed volcanic activity, especially when unexpected, urgently demands rapid hazard assessments which may, as a result, be too simplistic, overly conservative or lacking sufficient detail to be considered complete. They also

need to be focussed on the range of scenarios presenting the risk in that crisis (e.g. from one vent), rather than the entire background risk from that volcano (e.g. from multiple vents). Leonard et al. (2014) describe the process of creating a crisis hazard map for the 2012 Upper Te Maari eruption, comparing this to the existing background hazard map. In the case of a volcano in a state of unrest, assessments may be limited by the availability of safe locations to survey, and this is especially likely once an eruption episode has commenced as evident during the 2012 Upper Te Maari, Tongariro eruptions and assessments presented later. Odbert et al. (2015) have been developing updateable hazard forecast estimates using Bayesian belief networks, which may help to improve rapid hazard assessments in times of crisis.

2.5. Communication and risk management strategies

Effective communication is essential in managing ballistic hazard and risk (Barclay et al. 2008; Leonard et al. 2014). Science needs to be communicated to decision-makers, stakeholders, and the public and understood and absorbed by them so they can make informed decisions. Similarly, the public, stakeholders, and decision-makers should communicate to scientists what type of information they need to make decisions relevant to their situations. Methods used to communicate ballistic hazard and risk at volcanoes include hazard and risk assessments, hazard maps, volcano monitoring and research, real-time warning systems, volcanic alert levels; volcano warnings, alert bulletins and communication with agencies; response exercises, education materials, response plans, exclusion and evacuation zones, instructions and signage for what to do in the event of an eruption around the volcano, community engagement, educational materials, and land-use planning and infrastructure design. These methods typically fall under four aspects of emergency management: Mitigation (Reduction), Preparedness, Response and Recovery (UNISDR 2009). Methods must also be integrated with the management of other risks, ideally in one cohesive approach. Ballistic communication strategies will also vary with eruption frequency, the risk context (quiescence or crisis; Figure 2.2), whether volcanoes are frequently visited or inhabited, and the availability of resources. This equally applies to volcanoes at which ballistics are/are not the main hazard.

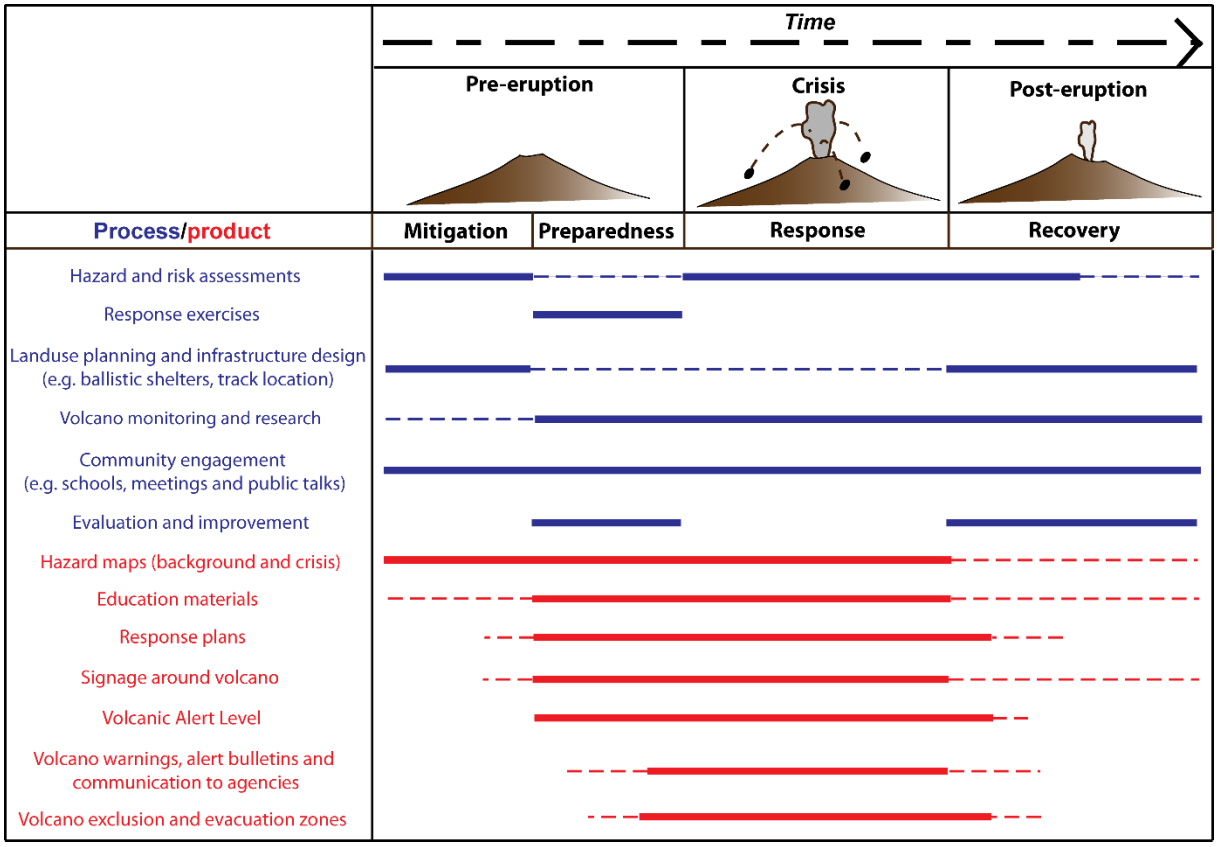

Figure 2.2: Various ballistic hazard and risk communication processes (blue) and products (red) implemented over the changing state of the volcano and the stage of risk or emergency management. The level of activity/importance is indicated by line style, with solid lines indicating higher use or importance

Effective risk management is built on communication, hazard education and engagement with the at-risk communities (Johnston et al. 1999; Johnston et al. 2000; Paton et al. 2001; Twigg 2002; Gregg et al. 2004; Leonard et al. 2008; Dohaney et al. 2015). Appropriate risk management actions by stakeholders, emergency managers and the public require an adequate perception of the risk and the correct actions to take in a crisis, with perception dependent on the hazard information received and exposure to consequences (Johnston et al. 1999; Leonard et al. 2014). Knowledge and understanding of volcanic hazards allows individuals to better decide whether to undertake preparedness and response measures, and if so, which are required, thus reducing their vulnerability to the hazard(s) (Siegrist and Cvetkovich 2000; Paton et al. 2008; Bird et al. 2010).

Scientific information can be misunderstood, misrepresented or distorted when passed from scientists to end-users (stakeholders, emergency managers and the public; Barclay et al. 2008). This can occur when end-users do not comprehend or are unaware of the science being

presented, the information is not what is actually needed by end-users, the science is communicated poorly to end-users, or there is a lack of trust between groups (Haynes et al. 2007). All groups therefore need to communicate with each other, preferably prior to a volcanic crisis, with communication products tailored to the audience (Haynes et al. 2007; Leonard et al. 2008). Following the 1979 eruption of Mt. Ontake, Japan the National Research Institute for Earth Science and Disaster Prevention in Japan (NIED, though now renamed to National Research Institute for Earth Science and Disaster Resilience) completed a report recommending: regulations on development and land-use, building of ballistic shelters and evacuation facilities, and the development of emergency plans, as an eruption in the summer hiking season would likely result in human casualties (NIED 1980). However, the report may not have been suitable or communicated well to the local municipalities responsible for disaster management as these recommendations were not adopted prior to the 2014 eruption, indicating the need for communication to ensure the information is relevant, understood and acted upon (Barclay et al. 2008; The Japan News, 27/10/2014). Communication delivered jointly by scientists and the local community is also advisable as community members may be better trusted and better communicators to their community than scientists in isolation. Users must be able to trust the source of the information being released as well as how and what is presented (Slovic 2000; Haynes et al. 2008). It is also therefore important for scientists and emergency managers to be honest about what is/is not known to maintain credibility and trust (Lindell 2013).

Best practice suggests the use of multiple sources to disseminate hazard and risk information as preferred forms of media accessed for information vary (Sorensen 2000; Mileti et al. 2004; Haynes et al. 2007; Bird et al. 2010). The public's response to volcanic hazard communication is influenced by the content and attractiveness of the message (which should include a description of the hazard, its consequences, hazard extent, and advice on what to do and when), how comprehensible it is, and the frequency and number of channels the message is received from, as well as the extent of public belief that safety actions are possible and will be effective (Leonard et al. 2008; Sorensen 2013).

2.5.1. Ballistic communication processes and products in different risk contexts

2.5.1.1. Volcano quiescence

Communication and risk management methods vary with changing eruptive states. In times of quiescence focus is placed on risk mitigation and preparedness, with access generally allowed into the hazard zone. In terms of ballistics this includes the completion of ballistic hazard and risk assessments; volcano monitoring and research; land-use and building planning i.e. the building of ballistic shelters capable of withstanding ballistic impacts or the reinforcement of existing structures to specific building standards, and the choice of location for hiking trails, viewing platforms or other visitor facilities; the creation of well distributed hazard maps with instructional text with what to do or where to go in an event of an eruption; and engagement with the local communities including exercises and evaluation (Figure 2.2).

Hazard and risk assessments are useful starting points for all communication and management strategies as the nature, extent and consequences of the hazard need to be understood prior to any decisions being made. The assessment should be made available to relevant decision makers, with the authors and science advisors available to advise or answer questions about the assessments. Scientists/authors should always strive to be transparent in their methodology. Transparency builds trust and credibility. It is important that stakeholders know the limitations of the information presented to them and/or informing decisions which affect them. It may not be needed or appropriate for the methods to be presented to the stakeholders in depth but instead it be communicated that they are available if requested. However, it is imperative to think of the risk context when making these decisions, as every situation is different. Methods and assessments should also be made fully available to other scientists so that these methods can be adopted at other volcanoes if chosen, which would increase best-practice and encourage similar and comparable methodologies. These assessments also need to be communicated to the public so that they can make informed decisions about the hazard and risk in the area they choose to enter as well as what steps they need to take to protect themselves.

The main way assessments are communicated is through a map (Haynes et al. 2007). Ballistic hazard maps are rare as they are typically not the only hazard produced in an eruption. Instead

ballistics are typically included in ‘all-hazard’ or ‘multi-hazard’ maps (Figure 2.3) depicting the general hazard for all active vent(s) (Neal et al. 2001; Hadisantono et al. 2002; Mount Fuji Disaster Prevention Council 2004; Kagoshima City 2010; Leonard et al. 2014). Ballistics are usually represented by one hazard zone, often based on the maximum or expected travel distance of a ballistic clast. This is, in part, because the public require concise, easily comprehensible information, rather than being distracted or overloaded with specifics of individual hazards (Haynes et al. 2007; Leonard et al. 2014). An effective hazard map for the public contains clear information on what are the consequences of the hazard(s), where they occur, and what to do (Leonard et al. 2014). For ballistics, consequences may be death or injury; impact locations are usually within 5 km of the vent; and advice may include “if ballistics are landing around you, move out of their oncoming path, seek shelter and make yourself a small target.” Advice on actions to be taken may vary at different volcanoes. It would be beneficial for testing of suggested actions to occur to ensure that the safest and most successful measures are being advised. For example, where frequent Strombolian explosions are the main source of ballistics, it may be possible to watch the low velocity ballistics and move out of their path. However, in many other eruption styles multiple particles may be ejected rapidly toward a person, presenting a situation in which dodging one ballistic may put you in the path of another. It may be more beneficial to make yourself as small a target as possible, seek shelter and use your backpack as a protective shield. Additionally, ballistics may be accompanied by a surge as seen in the 2014 Mt Ontake (Kaneko et al. 2016; Oikawa et al. 2016) and August 2012 Te Maari eruptions (Breard et al. 2014), inhibiting the ability to see ballistics until it is too late to act.

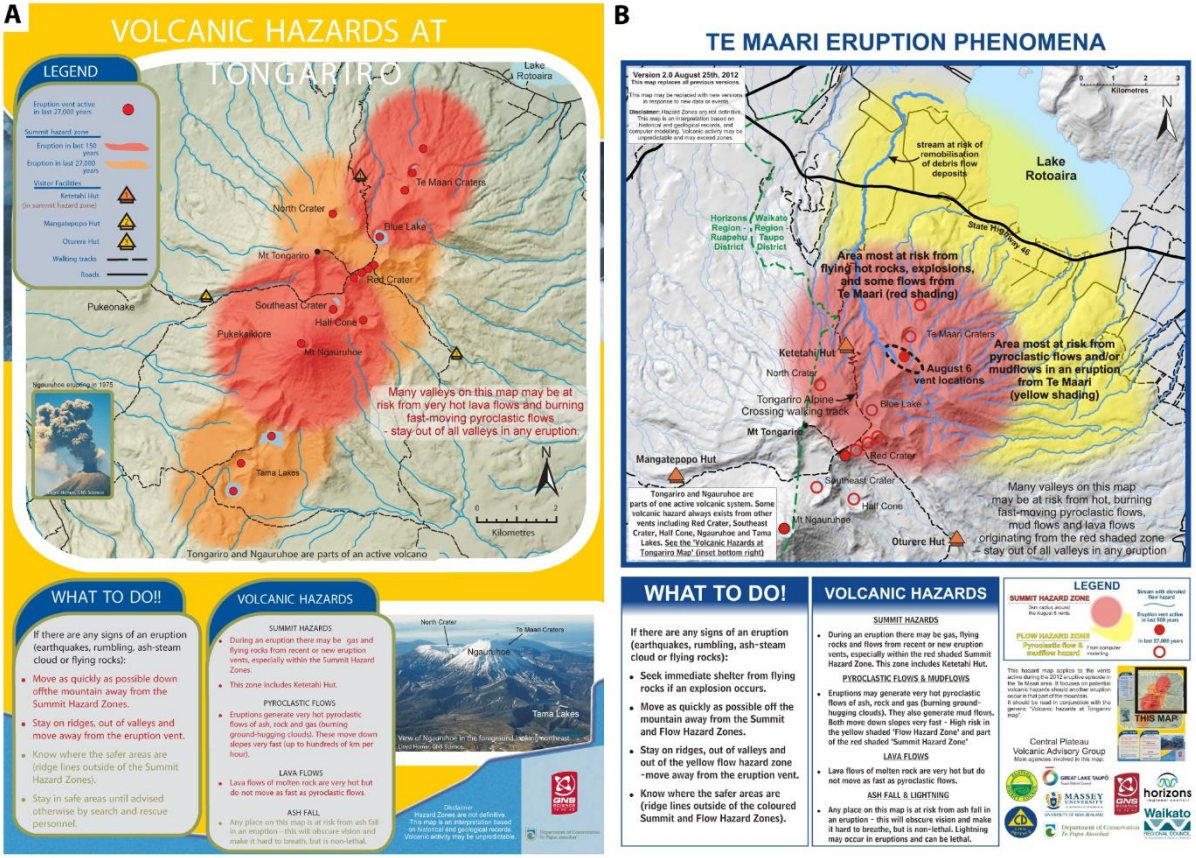

Figure 2.3: Volcanic hazard maps of Tongariro volcano, New Zealand: a. General background hazard map used in quiescent periods (GNS Science 2007), focussed on hazards from events up to a scale that may not have significant precursors to enable warning; b. Event-specific crisis hazard map following the 2012 eruptions of Upper Te Maari (GNS Science 2012). Note that map A is shown as an inset on map B with an explanation as to the complementary but differing nature of the two communication products

Map design should also take into account the effect of map properties on communication (understanding/comprehension) such as data classification, basemap or image, colour scheme (e.g. for colour blind readers), content, and key expression (Haynes et al. 2007; Thompson et al. 2015). Haynes et al. (2007) evaluated the effectiveness of volcanic hazard maps as communication tools on Montserrat, West Indies and found that the use of aerial photographs as a basemap improved people's ability to comprehend hazard information compared to traditional contour basemaps. In general, it has been found the public do not comprehend maps well and professional design input guided by iterative evaluation of map comprehension is wise (Haynes et al. 2007; Thompson et al. 2015). In contrast to the public, more specialist stakeholders such as infrastructure managers may require more detailed and hazard specific information about the consequences, location and recommended actions to inform decisions on land-use and building strength e.g. ballistic impacts in zone 1 can be expected to have sufficient energy to cause severe damage to nearly all types of infrastructure

below a certain design standard. Multiple zones of different impact intensity may be shown (e.g. travel distance, density of impacts in an area, size and or energy of expected ballistics in given scenarios). All end-user maps should successfully balance adequate detail and maximum clarity. Hazard maps and additional information should be made available and accessible to the public, and if different maps are made for, or directed to, different audiences their content must be consistent. Public availability may include being posted on signs around the volcanoes entrance(s), in a pamphlet or similar printed media at tourist facilities (e.g. information centres, tourism businesses, hotels, backpackers accommodation, transport operators), and on relevant websites such as volcano observatories and those charged with managing natural hazards.

Additionally, community engagement and participation in meetings with scientists and managers is encouraged as a means of risk communication, and discussion around management strategies, especially for communities at risk (i.e. tourism providers and those living near or on the volcano) (Cronin et al. 2004; Williams and Keys 2013). Ballistic hazards lend themselves to this type of community engagement because many open system volcanoes that may be constantly erupting but not considered to be in a state of volcanic crisis (e.g. Stromboli, and Yasur) have frequent ballistic-producing explosions that provide an attraction to tourists and employment for the local community. Ballistics at these constantly erupting volcanoes provide tangible hazards that the community can both relate to and provide valuable observational data on. Meetings should be sufficiently regular to update residents when the status of a volcano is changing and to remind them when necessary of the hazards and risks. Briefing those new to the area, especially the transient visitor, may be the biggest challenge. Engagement allows the community to be prepared in the event of an eruption and to know what to do in the event that they are within hazard areas.

2.5.1.2. Volcanic crisis

In a volcanic crisis (when the volcano is showing signs of unrest or is in eruption) communication and emergency management processes and products move toward response (Figure 2.2). Real-time warning systems triggered by monitoring equipment, such as the EDS (Eruption Detection System) system installed on Mt Ruapehu, New Zealand (Leonard et al.

2008), are used to communicate an eruption to those in the immediate vicinity. Wider communication occurs when an event is communicated from monitoring equipment to scientists, then onto emergency managers and decision-makers. Part of this process is the release of alert bulletins/warnings to advise the public of unrest, eruption phenomena, affected areas, and should always include instructions on what to do. Alert bulletins, existing hazard maps and risk and hazard assessments provide emergency managers with information to make decisions on limiting access to parts of the volcano. In the case of ballistics, limits or restrictions on access or development are usually achieved via creation of an exclusion zone, typically 1 – 4 km in radius (Kagoshima City 2010; Jolly et al. 2014b), or by reducing exposure by limiting the time spent or number of individuals allowed within a zone (Bertolaso et al. 2009).

During the crisis, hazard maps are typically updated, and hazard and risk assessments modified. Maps are generally event-specific and only used over a short time-frame, reverting back to the original background hazard maps once the crisis period is over (Leonard et al. 2014; Figure 2.3). However, ballistic hazard mapping during a crisis can be limited by access restrictions due to the possibility of further eruptions, though as time progresses more detailed mapping is able to be completed (Fitzgerald et al. 2014). The ongoing work by Odbert et al. (2015) in developing a real-time updateable probabilistic risk assessment may prove useful in these situations. The event-specific hazard maps are generally shared around the various media outlets (e.g., television, radio, newspapers, Facebook, Twitter) to inform the public of the updated hazard, as well as through the usual means of communication. They may be augmented by specific life safety signage (e.g. Figure 2.4).

Figure 2.4: Crisis communication sign temporarily used at Ruapehu volcano following a small eruption in 2007, while it was considered there was an elevated risk of further eruptions

Meetings and consultations with local communities, emergency managers and other stakeholders should also occur during and following volcanic crises. The objectives of such meetings are to update communities on the evolving eruptive hazards, build relationships and trust, reduce any miscommunication or misinformation passed along, and to make sure the information being presented is what the end-members need (Barclay et al. 2008; Bertolaso et al. 2009).

Communication of ballistic hazards and risk management vary at frequently erupting volcanoes that commonly enter in and out of crisis, such as Sakurajima in Japan. Access is generally controlled at all times (even during periods of quiescence), sometimes with permanent restriction zones in which nobody is allowed to enter due to the risk of being struck by ballistics (Kagoshima City 2010). In these cases, different hazard scenarios may be pre-prepared and communication strategies reused with a population that is well educated about the volcano.

2.5.2. Ongoing challenges in ballistic risk communication

Many volcanoes are tourist destinations with associated tourist facilities such as ski fields, accommodation and walking tracks (Erfurt-Cooper 2011). One challenge of communicating ballistic risk is to transient populations, especially tourists and other visitors. Tourists spend only a short amount of time in areas (hours to weeks) and often have little knowledge of the hazards or the available protection resources (Murphy and Bayley 1989; Drabek 1995; Burby and Wagner 1996; Bird et al. 2010). They often rely on tourism operators/employees/guides to inform them of volcanic hazards and the correct actions to take in an eruption (Leonard et al. 2008; Bird et al. 2010). This is evident at Yasur Volcano, Vanuatu where guides are frequently relied on to communicate ballistic hazard and safe areas to approach around the volcano, and at Tongariro Volcano, New Zealand where transport operators can give important information to 85% of all those hiking the Tongariro Alpine Crossing (TAC). However, tourism staff may also be somewhat transient, meaning that they may need to be regularly educated, trained or updated on volcanic hazards, appropriate responses and emergency procedures so that they can pass the message down to their patrons (Leonard et al. 2008; Bird et al. 2010; Williams and Keys 2013). Additionally, education material such as pamphlets and hazard maps on volcanic hazards should not only be available at tourism businesses but mechanisms should be in place than ensure that the hazard information is relayed to these transient populations.

Another ongoing challenge in communicating ballistic hazard is the lack of warning time associated with events that have little precursory activity, in which ballistics are typically one of the main hazards. In this scenario volcanic alert levels and bulletins may not be released prior to eruption. Instead, visitors and stakeholders would have to rely on their knowledge of the potential hazards and the response actions to take, especially if there are no real-time warning systems. This places more emphasis and weight on the availability of background hazard maps with messaging covering actions in events up to this size, signage around the volcano (in language(s) appropriate for the audience to comprehend, especially if there is a large proportion of visitors who speak a different language), on pamphlets distributed to businesses and visitors actually reading them, and through communication with their guides. Many visitors to the TAC

still assume that they do not need to be concerned because they expect the area to be closed if it is unsafe or to be advised it was unsafe (Keys 2015).

We present the various ballistic risk management and communication approaches taken at four volcanoes: Upper Te Maari, Tongariro Volcanic Complex, New Zealand; Yasur Volcano, Vanuatu; Sakurajima Volcano, Japan and Mt. Ontake, Japan (Table 2.2). These volcanoes have been chosen for their variation in: frequency of eruption (Sakurajima and Yasur frequently erupt, while Upper Te Maari and Mt Ontake have longer repose periods), available resources (Yasur has less monitoring equipment and hazard information available than the other three examples), eruptive styles – Yasur predominantly erupts bombs from small Strombolian explosions; compared with phreatic eruptions from Mt Ontake and Upper Te Maari and Vulcanian eruptions from Sakurajima that erupt blocks over a larger area, and the similarity in eruptions but with very different consequences between Upper Te Maari and Mt Ontake. Additionally, all of these volcanoes are relatively accessible and attract large numbers of tourists each year.

Table 2.2: Comparison of the four case studies and their risk management and communication strategies

	Upper Te Maari	Yasur	Sakurajima	Mt Ontake
Dominant eruptive style	Hydrothermal	Strombolian	Vulcanian	Phreatic
Recurrence interval	~16 years	Frequently erupting	Frequently erupting	~13 years
Duration of precursory activity	3 weeks of seismicity, 5 minutes of increasing seismicity			2014: 16 days seismicity, 11 minutes increasing seismicity and inflation
Number of visitors	100,000 visitors/year	20,000 visitors/year	3,702,000 visitors/year	Hundreds of visitors per day
Hazard map with ballistics	Background and crisis	Yes	Yes	Two background maps
Volcano exclusion and evacuation zones	Yes	Yes	Yes	Yes
Volcanic Alert Levels	Yes	Yes	Yes	Yes
Education material	Yes	Yes	Yes	Yes
Volcano monitoring	Yes	Yes	Yes	Yes

Land-use planning and infrastructure design	Ketetahi Hut (not reinforced). TAC runs through summit hazard zone	No shelters or buildings. Track and viewing platforms along rim of volcano	Concrete shelters around island, evacuation ports	Mountain lodges and shrines (not reinforced). Tracks near active craters
Community engagement	Yes	In progress	Yes	Yes
Response exercises	No	No	Yes	Yes
Evaluation and improvement	Assessments updated post-eruption, creation of crisis hazard map	Currently assessments and maps are being updated	Last update of hazard map was in 2010.	New hazard map released November 2015
Signage around volcano	Yes	Yes	Yes	Yes
Volcano warnings, alert bulletins and communication with external agencies	Yes	Yes	Yes	Yes

2.6. Case studies

2.6.1. 2012 eruptions of Upper Te Maari, Tongariro, New Zealand

On the 6th August 2012, Upper Te Maari Crater, one of the many vents on Tongariro volcano, New Zealand, erupted for the first time in over 100 years (Scott and Potter 2014). The hydrothermal eruption produced multiple pyroclastic surges, an ~8 km high ash plume and ejected thousands of ballistic blocks (Fitzgerald et al. 2014; Lube et al. 2014; Pardo et al. 2014). Blocks were distributed over a 6 km^2 area, affecting ~2.6 km of the popular Tongariro Alpine Crossing (TAC), a walking track frequented by around 100,000 people a year (Fitzgerald et al. 2014). Additionally, Ketetahi Hut, an overnight hut along the TAC, was severely damaged by ballistics. Fortunately, the eruption occurred at night, in winter (the low season) and in bad weather, resulting in no hikers along the TAC or staying at Ketetahi Hut (both around 1.5 km away from the vent and well within the affected area). A smaller eruption followed on 21 November 2012, though ballistics and pyroclastic surges were confined to within a well posted risk management zone 1 km from the vent and did not affect the TAC.

Ballistics were a known hazard from the active vents of Tongariro, witnessed in the 1974-5 Ngauruhoe eruptions (Nairn and Self 1978). As such they were described on the background hazard map for the volcano (Figure 2.3a). The map, published in 2007, consists of a summit hazard zone around each active vent, encompassing gas and ballistics at radii of 2-3 km for different vents based on experience of ballistic ranges in past eruptions at Tongariro National Park. Work is underway to develop ballistic and life safety models to better inform zone radius. Pyroclastic density currents (PDC's) and lava flows are not included in a hazard zone but are mentioned as a possibility in all valleys. Ashfall is stated as a hazard that could occur any place on the map. Text is provided, with instructions including to move quickly down off the mountain and away from summit hazard areas, though ballistics-specific advice was not provided (GNS Science 2007). The background hazard map with associated instructions was permanently posted at the entrances to the walking tracks up the volcano, was available on the GNS and DOC websites as well as on flyers at many of the tourist hubs (Leonard et al. 2008; 2014). The TAC hiking track cuts through most of the summit hazard zones, where access has been open at background levels. One hut, Ketetahi Hut, is located within the summit hazard zone, though is not reinforced to protect against ballistic impact.

Unrest was observed at the volcano up to three weeks before the eruption, initially in the form of increased seismicity and then increased magmatic gas content (Jolly et al. 2014a). In response the Volcanic Alert Level was raised from 0 to 1 (indicating unrest). Seismicity declined in the days prior to eruption and thus the TAC remained open to tourists (Jolly et al. 2014b), with seismicity reoccurring only ~5 minutes before the event (Jolly et al. 2014a). In the build-up to the eruption, a decision was made to complete response plans and create a crisis hazard map initially for the whole volcanic massif with some focus on the northern flank of Tongariro. However, it was not publicly available before the August 6th eruption (Leonard et al. 2014). GNS volcanic alert bulletins were also produced, communicating updates on the precursory phenomena observed at Tongariro (Volcanic Alert Bulletins TON-2012/01 – 04; Figure 2.5e). Meetings and other discussions were held with the local residents and businesses involved with the TAC to discuss the situation and future scenarios. Being wintertime, there was very little use of the track. As there was no one on the hiking trail during the eruption it is difficult to

assess the success of the hazard communication strategies, and these strategies would have been different during summer months with heavy track use.

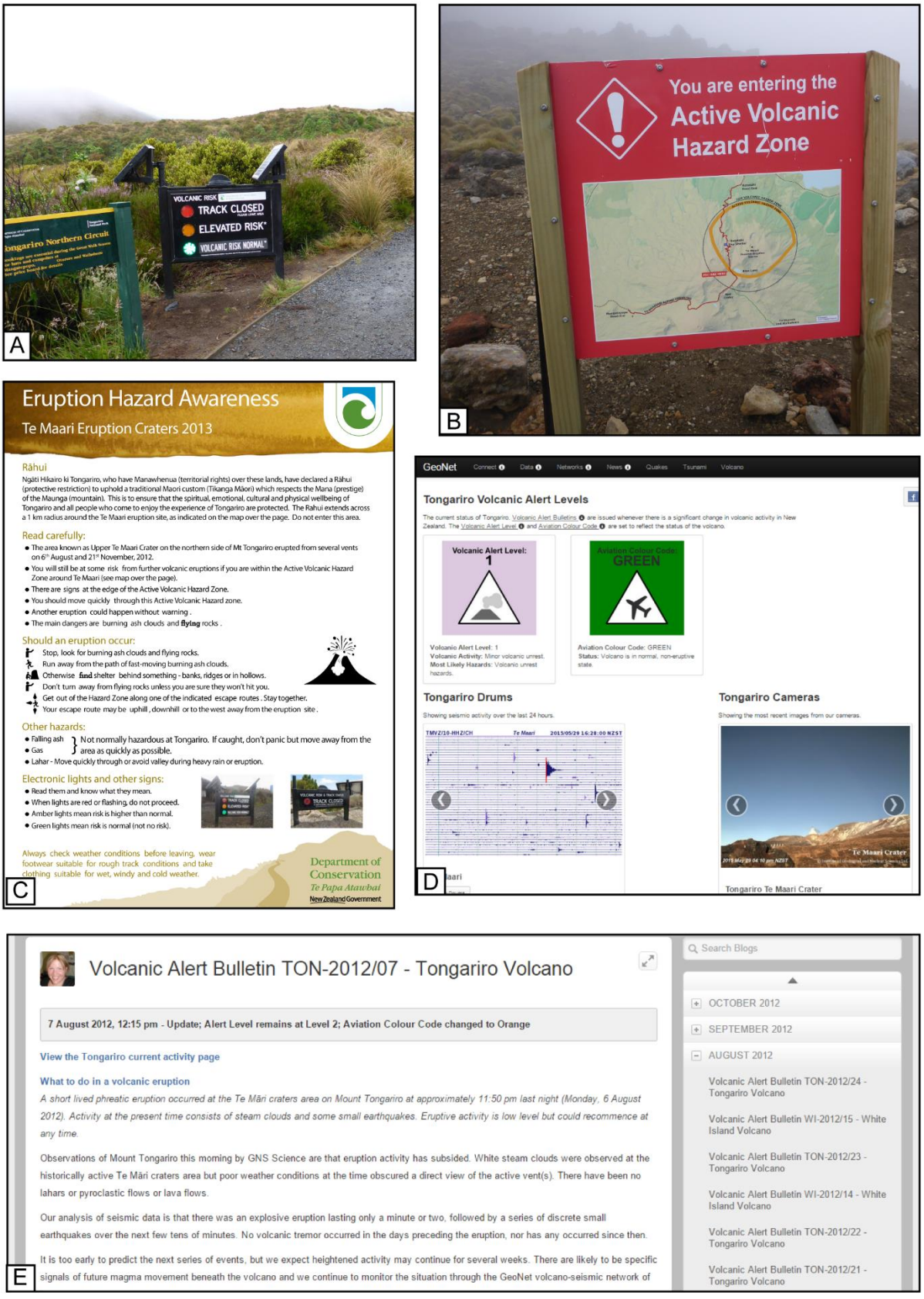

Figure 2.5: Risk communication methods used at Tongariro, New Zealand. A. Electronic signs communicating risk level and track closure at entrances to the volcano and where it crosses the AVHZ. B.

Signs advising area of increased hazard including a track-specific AVHZ hazard map. C. Additional information on volcanic hazards at Tongariro (including ballistics), initially handed out to all hikers, provided on Department of Conservation website. D. Geonet website showing monitoring data such as Volcanic Alert Level, seismic drums and visuals of the volcano. E. A Volcanic Alert Bulletin issued on the GeoNet website and distributed to media following the 2012 Upper Te Maari eruption

Following the August event, some of the local population evacuated for the night and the TAC was closed for two months due to the risk of further eruption. Within this two-month period an updated hazard and risk assessment was completed (Jolly et al. 2014b). This involved a combination of reviewing the eruptive record to understand eruption frequency and magnitude, and expert elicitation by GNS staff (the institute responsible for monitoring volcanoes and assessing their hazard/risk) working closely with the land manager (Department of Conservation) to produce three possible future eruption scenarios (a 21 November size eruption, a 6 August size eruption, and a magnitude larger eruption) and associated probabilities of these occurring. Probabilities were re-assessed every week immediately after eruption, which was subsequently extended to every month, then every three months as time passed. Hazard extent was considered for ballistics and PDC's for each scenario, exposure time along the affected area, and the vulnerability (probability of fatality) of an individual to each hazard (using the area of hazard around an individual impact for ballistics, and the presence of a person in the path of a PDC), to calculate the combined risk of fatality for all scenarios (Jolly et al. 2014b).

Initial assessments suggested that ballistics were the main hazard to life from the eruption, though detailed mapping was not able to be carried out until months later when risk levels had decreased (Fitzgerald et al. 2014; Jolly et al. 2014b). The Department of Conservation (DOC), the agency responsible for hazard and risk management at Tongariro, began to implement risk management as part of a recovery programme. The risk assessments by Jolly et al. (2014b) became an important tool for making decisions about reopening. A new, event-specific Te Maari hazard map was created using mapped deposits and the most likely hazard scenarios, in which the main hazard zone was increased to a 3km radius (choosing the larger potential radius based on historic events) down-slope and deliberately renamed the Active Volcanic Hazard Zone (AVHZ) to distinguish it from the former map (Figure 2.3b). It included ballistics, explosions, pyroclastic density currents, lahars, gas and rockfall (Jolly et al. 2014b). The accompanying text to the crisis hazard map was also updated, with a ballistic specific instruction to 'seek immediate shelter from flying rocks if an explosion occurs' (GNS Science 2012). The map was released to the public alongside a Volcanic Alert Bulletin describing the

changes made to the map and the source of the data (Volcanic Alert Bulletin TON-2012/23). This was distributed to the media (print, television, web and radio) to inform a wider audience (Leonard et al. 2014). Additionally, the map was posted at either ends of the track and where it crossed the boundaries of the AVHZ. Cordons, initially manned, were established at either ends of the TAC to prevent hikers from entering. Later, the cordon was moved to Emerald Lakes (on the edge of the 3 km Volcanic Hazard Zone) as the track was partially reopened. With declining risk of further eruption (based on the trend of the eruption probability estimates made by GNS to estimate how the expert elicitation might evolve over time), the track was fully opened 5 ½ months after the 21 November eruption.

DOC also published educational information on the eruption hazard at Te Maari including further advice on actions to take in an eruption (Figure 2.5c). This included to 'stop, look for flying rocks', to 'find shelter behind something – banks, ridges or in hollows', to not turn away from 'flying rocks unless you are sure they will not hit you' and to 'get out of the Hazard Zone along one of the indicated escape routes' (Department of Conservation 2012). In October 2013 electronic warning signs were installed that informed hikers of the status of the volcano – a red flashing light meant danger-turn back, orange elevated risk and green normal volcanic activity (Jolly et al. 2014b, Figure 2.5a). A survey of 203 hikers on the TAC in March – May 2014 indicated that most people saw these signs when activated red and understood the messages irrespective of their native language (Keys 2015). A reinforced public shelter and warden's quarters was one option being considered to replace the damaged Ketetahi Hut. Now the favoured option is to replace it with facilities outside the AVHZ.

2.6.2. Yasur Volcano, Vanuatu

Yasur Volcano is a frequently erupting basaltic scoria cone located on Tanna Island, Vanuatu (Cronin and Sharp 2002). Strombolian and Vulcanian eruptions have been relatively continuous since 1774 (Eissen et al. 1991). Ballistics are the main hazard produced by these eruptions, responsible for multiple fatalities in the past (Baxter and Gresham 1997). Yasur is one of Vanuatu's main tourist attractions with some twenty thousand people visiting the crater rim each year. The vast majority of people are guided up the volcano by local guides to watch the

explosions occur, with a main viewing area only 150 m from the crater's inner rim. As the majority of people in the area are transient tourists, guides are often relied upon to relay hazard and risk information to their patrons. Volcanic alert levels (VALs) and bulletins are posted on the Vanuatu Meteorology and Geo-Hazards Department (VMGD) website when the behaviour of the volcano changes. These sometimes include hazards maps that provide the locations of where bombs have been observed or are likely to impact, and often caution the public to approach the crater or hazardous areas with care. Maps also urge visitors, tourist agencies and communities to seriously consider the information provided prior to ascending Yasur (Vanuatu Geohazards Observatory 2009). However, advice or instructions are not given for what to do if caught in an area where ballistics are landing. A hazard map is displayed at the carpark before the ascent up the cone, highlighting the 1999 lava bomb impact zone and the observation location for each volcanic alert level – as the alert level increases so does the distance of the observation position from the cone (i.e. restriction zones are emplaced). In addition, visitors to Yasur are warned by a sign to 'Think Safety' before ascending the crater rim, though no further instructions or information is provided. As it is frequently erupting, it is assumed that visitors accept the risk that they are entering into an active volcanic hazard zone.

An updated risk management framework has been developed from 2012 to 2016 including updated bulletins and VALs, background and safety (crisis) hazard maps, and tourist information including education and safety map information. This is associated with an upgrade of Vanuatu's active volcanoes to real-time warning (at the time of writing this included a seismometer and webcam on Yasur and daily OMI satellite monitoring of SO_2 emissions; VGO 2014), supported by the New Zealand Aid Programme and GNS Science in partnership with VMGD. This integrated framework allows for pre-planning of safety zones related to ballistics and other hazards, and integration with warning products such as bulletins, VAL and tourist information. Ballistic zone ranges will initially be based on historic event ranges but will be updated to include the modelling being developed in New Zealand, once available.

2.6.3. Sakurajima Volcano, Japan

Another frequently active volcano in which ballistics are a major hazard is Sakurajima Volcano, Japan. Continuous Vulcanian eruptions have occurred since 2009 from the andesitic composite cone (Japan Meteorological Agency 2013b). Sakurajima is constantly monitored by the Sakurajima Volcano Observatory and is considered to be one of the best monitored volcanoes in Japan (GSJ 2013). When activity changes, alert levels are posted on the Japan Meteorological Agency (JMA) website for the public to view. Many people live in close proximity to the volcano (~4,900 within 5 km of the volcano) and millions visit the Kagoshima-Sakurajima area each year (3,702,000 in 2010; Japan Meteorological Agency 2013b), thus JMA and Kagoshima City released a volcanic hazard map with additional information in 2010. This map was distributed to local citizens and posted around the volcano. Three relevant zones are delineated on the map: the first is a 2 km radius (from the active craters) restricted area in which both residents and tourists are restricted from entering at all times; the second is ~3 km away from the active vents showing the area expected to be inundated with volcanic bombs in a 'strong eruption', and lastly a 6 km radius extends around the active vents where 'volcanic rock' is likely to impact from a 'great eruption' (Kagoshima City 2010). Definitions for 'strong eruption' and 'great eruption' are not provided, nor is an explanation of the data that these zones are based on. The hazard map also includes societal components such as important landmarks i.e. schools and the visitor centre, and evacuation buildings and ports. The other half of the map consists of information on precursory phenomena likely to be felt and who to call if detected; how volcanic warnings will be disseminated, and the measures needed to be taken; what the five volcanic alert levels are/what activity is expected and the consequent actions needed to be taken; information on major historic eruptions and recent activity; and evacuation procedures. An English version of the map is available in addition to the original in Japanese. This information is also available on the official tourism website of Kagoshima City (http://www.city.kagoshima.lg.jp/soumu/shichoshitu/kokusai/en/emergency/sakurajima.html). Ballistics (called 'cinders') are additionally listed on the site as a possible volcanic hazard accompanied by a description, particle size and travel distance. To prepare for a future eruption from Sakurajima, Tarumizu City (Kagoshima Prefecture) runs an emergency response exercise every year (http://www.city.tarumizu.lg.jp/kikikanri/kurashi/bosai/bosai/taisaku/sakurajima.html).

Three other notable risk communication and mitigation measures have been implemented at Sakurajima. A Volcano Disaster Prevention Council was created as a means of communication to discuss disaster prevention measures between volcanologists, local government, JMA, and other invested agencies (http://www.data.jma.go.jp/svd/vois/data/fukuoka/506_Sakurajima/506_bousai.html). Secondly, signs instructing people on the distance and direction to the nearest eruption safe house and evacuation port have been posted around the volcano. Lastly, concrete roofed shelters have been built around the island to protect visitors from falling ballistics (Erfurt-Cooper 2010).

2.6.4. 2014 eruption of Mt Ontake, Japan

Mt Ontake is a stratovolcano located on the island of Honshu, Japan (Japan Meteorological Agency 2013a). It is not a continuously active volcano with four eruptions (all phreatic) in its historic record (1979, 1991, 2007 and 2014; Japan Meteorological Agency 2013a; Smithsonian Institution 2013). Mt Ontake straddles the boundary of two prefectures – Gifu and Nagano, with trails on either side. Both prefectures have developed hazard maps for two eruption scenarios that include ballistics – the first a phreatic eruption similar in size to the 1979 eruption (VEI 2) and the second a larger eruption on the scale of 90,000 – 20,000-year recurrence interval (Nagano hazard map: vivaweb2.bosai.go.jp/v-hazard/L_read/53ontakesan/53ontake_2h03-L.pdf; Gifu hazard map: http://vivaweb2.bosai.go.jp/v-hazard/L_read/53ontakesan/53ontake_2h01-L.pdf). In both maps, ballistic hazard is defined by a 4 km asymmetric zone around an asymmetric vent area encompassing the 1979 vents - the same vents that erupted in the 1991 and 2007 eruptions. The parameter by which the zone is based on is not provided (e.g. maximum travel distance, spatial density of impacts) and no advice accompanies the hazard map, though a residents' handbook was printed that included examples of what ballistics are and how far they can travel. The maps and handbooks are available on the NIED database and the prefectural government websites, though the map is not signposted around the volcano.

Mt Ontake is constantly monitored by the JMA, with seismometers, GPS stations, tiltmeters, cameras and infrasonic microphones (Japan Meteorological Agency 2013a). In addition, preparedness communication measures also include Volcanic Alert Levels, in place since 2008

(Japan Meteorological Agency 2013a). Similarly to other volcanoes, these VALs range from 1 – 5 and include whether the alert level is a warning or forecast, the target area (e.g. crater area or more distal residential areas), the expected volcanic activity and phenomena with examples of previous cases, actions needed to be taken and also keywords accompanying the level (e.g. level 5 with 'evacuate').

The 27 September 2014 phreatic eruption occurred at lunchtime on a busy autumn day when ~340 hikers were on the mountain (Tsunematsu et al. 2016). Multiple pyroclastic surges were produced, travelling up to 2.5 km from vent, in addition to ballistics that impacted up to 1 km from the vent (Kaneko et al. 2016; Tsunematsu et al. 2016). Fifty-eight people were killed in the eruption, 55 most likely the result of ballistic trauma relatively close to the summit, with five still missing (as of 24 June 2016; Tsunematsu et al. 2016). An increase in summit seismicity was noted 16 days prior to the eruption resulting in the JMA releasing notices about volcanic activity, though activity was not at levels significant enough to raise the Volcanic Alert Level (there needed to be signs of deformation, which were not recorded until just prior to eruption; The Japan News, 26/10/14; Ui 2015). The eruption was largely unexpected with 11 minutes of precursory tremor, and uplift detected only seven minutes before the event (Ui 2015). This was a much shorter period of precursory activity than previous eruptions. The 1979 eruption was preceded by earthquake swarms for a year and five months. A month of seismicity was noted prior to the 1991 eruption, increasing in frequency just days before the event. And the 2007 eruption was preceded by inflation and seismicity for three months, accompanied by increasing fumarolic activity the week prior (Japan Meteorological Agency 2013a). Longer periods of precursory activity allow time for warnings to be issued. JMA released warnings prior to the 1991 and 2007 events, although the resulting eruptions were very small, only affected the immediate area and occurred in winter outside the climbing season (Japan Meteorological Agency 2013a). However, if it had been possible to issue a warning when the precursory activity increased on the day of the 2014 eruption, it is unlikely that it would have resulted in no fatalities. Any evacuation warning prior to an event would need to occur at least an hour before the event and be immediately transmitted to all hikers on the summit area as it takes over an hour for hikers to move out of the ballistic hazard zone. Nonetheless, even a short warning time may have provided more hikers time to get to shelter.

Following the eruption, the Volcanic Alert Level was increased to 3, warning people not to approach the volcano (as access was restricted), and that blocks may be ejected up to 1 km from vent (based on previous eruptions). Signs were posted around the volcano telling people to "keep out" of the restricted area. Search and Rescue teams were deployed to rescue the injured hikers and those that sheltered in the buildings at the summit, and to recover the dead. Those that sheltered in the buildings around the summit survived the 2014 eruption, while many of the fatalities occurred due to hikers choosing to take photos and video of the eruption outside instead of running to the nearest hut. Half of the people autopsied by one doctor were found with cell phones in hand while one person's camera was found with a photo taken four minutes after the eruption occurred (Mainichi Shimbun 10/10/14). Some then attempted to shelter around the summit shrine which they could not gain access to (the summit shrine is only open from the beginning of July to early September). Fatalities also occurred in exposed areas where there were no buildings in sight to shelter within. Personal safety measures taken by exposed hikers saved lives. This included sheltering behind large rocks, placing backpacks on heads, and wearing hard hats provided inside the mountain huts (NHK 2015).

Numerous risk management and communication tools have since been adopted. Prior to the eruption, Gifu and Nagano prefectures had separate commissions to manage volcanic activity from Mt Ontake. Following the 2014 eruption they have combined to form one commission for the entire volcano, improving communication between the prefectures and subsequently to the public. The commission, similar to the Sakurajima council, is comprised of volcanologists, local government, JMA and other interested agencies (http://www.pref.nagano.lg.jp/kisochi/kisochi-seisaku/ontakesan/kazanbousaikyougikai.html). The council ran its first eruption evacuation drill on 4th June 2015.

Interviews conducted post-eruption showed that many climbers were unaware of the volcanic activity notices released, while of those that were aware 76% did not consider that they needed to be prepared for an eruption (The Japan News 26/10/14; Shinano Mainichi Shimbun 2015). JMA subsequently launched a website to provide climbers with its observations of the volcanic activity around Japan, in an attempt to improve communication to climbers. From the 1st April, 2015 the Gifu Prefectural Government made it mandatory for all climbers of Ontake to submit a mountain climbing notification form prior to ascending Mt. Ontake, in an effort to improve

knowledge of the number and location of people on the mountain, and to improve communication in times of crisis by recording their emergency contact information (http://www.pref.gifu.lg.jp/English/tourism/mountain/). Kiso, a town in the Nagano Prefecture responsible for one of the mountain trails, has also installed loudspeakers in the mountain cabins prior to easing restrictions in September 2015 (The Japan Times 27/09/15).

In November 2015, a new hazard map was released by the Ontakesan Volcano Disaster Prevention Council (the combined commission mentioned previously). It provides two ballistic hazard zones – one for a phreatic eruption that extends 2 km from the vent area, and one for a larger magmatic eruption, extending 4 km from the vent area (http://www.city.gero.lg.jp/hazardmap/#12/35.9073/137.5203). The zones are based on research completed for Mt Fuji on past ballistic distributions from phreatic and magmatic eruptions in Japan and around the world (Mount Fuji Disaster Prevention Council 2004). The asymmetric vent area has also been increased significantly, encompassing 3 km in length and ~2 km in width. In addition, further research has been completed on the ballistic hazard produced in the eruption. Tsunematsu et al. (2016) describe an elongated distribution toward the N-NE resulting from an inclined ejection and topographic controls such as the shape of the valley the vents formed in. The spatial distribution was mapped from aerial photos by Kaneko et al. (2016) and delineated into four zones. The densest zone (A) encompasses areas with impact densities > 10 impacts per 5 x 5 m, decreasing in density with distance from the vent to Zone C which has between 0 and 2 impacts per 5 x 5 m.

2.7. Discussion

2.7.1. Understand the context and assess the risk

We identify from review of literature and analysis of the four case study volcanoes (Table 2.2) that understanding the risk context is highly important for effective communication associated with ballistic hazard and risk. Establishing this context and identifying potential risks requires engagement with potential stakeholders, such as those which may be exposed or affected by ballistic, or other, volcanic hazards. Effective communication is an essential component of this.

Once these steps are complete, we then suggest that a ballistic risk assessment is undertaken to help underpin effective management and communication of ballistic hazard and risk. Best-practice ballistic risk assessment generally consists of: 1) reviewing the volcano's eruptive history to establish eruption frequency and eruption magnitude; 2) determining the nature and extent of past ballistic distributions; 3) exploring possible future ballistic distributions; 4) identifying assets exposed in the area; and 5) estimating the asset's vulnerability. Once complete, risk can be evaluated, and appropriate management and communication strategies implemented. However, we stress that risk assessment alone cannot underpin effective communication of ballistic hazard and risk. But must be carried out in conjunction with the tools and strategies listed in Table 2.1 and Figure 2.2.

It is important to remember that every context is different and what works at one volcano does not necessarily mean it will work or is needed at another. An assessment for a frequently erupting, highly visited volcano where risk management organisations are well resourced will require a different approach compared with an infrequently active, rarely visited volcano in a country where there are few resources available for risk management. The scope and scale of risk management activities should be guided by the risk context and determine which and how risk management tools and strategies are used.

2.7.2. Reflections on the four case study volcanoes

All of the volcanoes studied are capable of causing injuries and fatalities from ballistics. The Mt Ontake 2014 eruption resulted in the most fatalities from any of the case studies and provides a chance to analyse why this was so with the aim of preventing it from occurring again. Multiple factors contributed to the high fatality rate:

- The eruption happened in peak season when ~340 people were on the mountain.
- Precursory activity only increased 11 minutes prior to eruption, resulting in an unexpected eruption. This meant no warning was able to be issued to the people on the summit and no closure of the summit prior to the event occurred. Previous eruptions had precursory events that gave more warning of the impending eruption underscoring that past history should not be solely relied on to predict outcomes of future unrest.

- The Alert Level was not raised following increased seismicity beginning 16 days before the eruption. A requirement for this to occur is the presence of ground deformation, which was not recorded until 7 minutes before the eruption.

- Hikers chose to take images and video of the eruption instead of finding shelter. This decision may have been different had hazard maps been posted around the volcano with instructions on actions to take in an eruption.

Fatalities from ballistics could occur at all of the case study volcanoes. However, a scenario with fatalities on the scale seen at Ontake is unlikely from Sakurajima due to the 2 km restriction zone. Yasur is visited by much fewer tourists than Ontake so it is unlikely to see as many fatalities from one event as occurred at Ontake, although the lack of shelter, lack of hazard advice, and proximity to the vent means that ballistic casualties are still relatively likely at this volcano. Work is ongoing to reduce this risk. The August 2012 eruption of Upper Te Maari is the most comparable to the Ontake eruption as it was largely unheralded and of the same explosivity. If the August 2012 eruption had occurred in peak tourist season, then a similar amount of fatalities as Ontake potentially could have occurred.

2.7.3. Critical issues

We identify the following critical issues for contemporary and future communication of volcanic ballistic risk, based on our review of literature and analysis of the four case study volcanoes. We note many of these issues transcend volcanic ballistics to include nearly all volcano types and volcanic hazards:

- What is the most effective way to manage and communicate risk from volcanoes which are (highly) visited and/or settled which experience eruptions with very short and/or no meaningful warnings (e.g. Ontake, Te Maari)? This is a critical issue for managing ballistic risk, as eruptions with longer unrest phases typically allow evacuation of ballistic hazard zones before the eruption.

- What are the most appropriate risk management and communication strategies for volcanoes where ballistic (and other) risk is present which have poorly understood eruptive histories and/or monitoring systems?

- Effective ballistic risk assessment requires greater understanding of a) the distribution of ballistic from a range of potential eruption styles, b) the effect of ballistics to people and other societal assets (vulnerability/fragility characteristics), and c) identification and (crucially) evaluation of what are the most appropriate mitigation actions to reduce ballistic risks before, during and after an eruption.

- Successful management of ballistic risk requires effective engagement (of which communication is a keystone) between authorities responsible for managing risk at volcanoes, those people and organisations who may have economic, cultural and social connections with a volcano, and the scientific community who can help inform hazard and (sometimes) risk considerations. Organisational and governance frameworks to allow and facilitate this seem to be highly variable globally, but some relatively successful examples do exist (e.g. New Zealand).

- How to manage future risk, particularly for volcanoes where there is significant existing use and/or strong pressure to utilise the resources through tourism (increasing visitor numbers to high risk areas), and agricultural and settlement pressure from population growth.

2.8. Conclusions

Ballistic projectiles ejected in explosive eruptions present a major proximal hazard to life, infrastructure and the environment. An increasing population living on or close to active volcanoes and a growing volcano tourism industry give rise to an increased number of people exposed to ballistic hazard, presenting a considerable need for detailed ballistic hazard and risk assessments, and specialised communication and management strategies. Recommended strategies would include at least the following:

1) Hazard and risk assessments (ideally probabilistic) specific to the volcano in question, which include ballistics where appropriate, that are made available to emergency managers and decision makers with authors/scientists available to answer questions and advise where necessary and practical;
2) The inclusion of ballistic hazard zones in hazard maps with accompanying advice on what to do. Maps should be updated in a crisis to reflect new information and readily

available through a range of media. These maps should continue to be updated after the event when detailed scientific studies are complete;

3) Volcano monitoring systems to monitor volcanic activity and indicate when a volcano is in unrest;
4) The use of signage around the volcano to communicate ballistic hazard and risk, integrated with other hazard advice, including warning systems where practical, and with a focus on effectiveness of communication rather than just providing information;
5) The use of volcanic alert bulletins, media releases or reports to communicate ballistic hazard and risk in crisis phases;
6) Open, sufficiently frequent communication between scientists, stakeholders, emergency managers and local communities in which updates and training are provided, and informed input made into management and mitigation measures.

These strategies may vary with eruptive state (quiescence or crisis), frequency of eruptions, availability of resources, and whether ballistics are the main hazard at the particular volcano. In addition to the strategies mentioned in this chapter, further work is needed to test and update the advice provided to visitors on the actions to take in a ballistic eruption, in particular personal protective measures. Effort should also be made to provide consistent advice at all volcanoes on the actions to be taken, depending on the volcanic hazards involved. This way the information would be reinforced with visits to different volcanoes and increase the likelihood of visitors acting correctly.

2.9. Acknowledgements

Funding for this study was provided by DeVoRA (Determining Volcanic Risk in Auckland) and a New Zealand Earthquake Commission (EQC) Biennial Grant (E6493). RHF is also supported by a doctoral scholarship from the Ngāi Tahu Research Centre. We wish to thank Bill McGuire and an anonymous reviewer for their thorough and constructive reviews.

2.10. References

Alatorre-Ibargüengoitia MA, Delgado-Granados H, Dingwell DB (2012) Hazard map for volcanic ballistic impacts at Popocatépetl volcano (Mexico). Bulletin of Volcanology 74(9):2155–2169

Alatorre-Ibargüengoitia MA, Morales-Iglesias H, Ramos-Hernández SG, Jon-Selvas J, Jiménez-Aguilar JM (2016) Hazard zoning for volcanic ballistic impacts at El Chichón Volcano (Mexico). Natural Hazards, DOI 10.1007/s11069-016-2152-0.

Andronico D, Taddeucci J, Cristaldi A, Miraglia L, Scarlato P, Gaeta M (2013) The 15 March 2007 paroxysm of Stromboli: video-image analysis, and textural and compositional features of the erupted deposit. Bulletin of Volcanology 75:733

Artunduaga A, Jimenez G (1997) Third version of the hazard map of Galeras Volcano, Colombia. Journal of Volcanology and Geothermal Research 77:89–100

Barclay J, Haynes K, Mitchell T, Solana C, Teeuw R, Darnell A, Crosweller HS, Cole P, Pyle D, Lowe C, Fearnley C, Kelman I (2008) Framing volcanic risk communication within disaster risk reduction: finding ways for the social and physical sciences to work together. Geological Society, London, Special Publications, 305(1):163–177

Baxter P, Gresham A (1997) Deaths and injuries in the eruption of Galeras Volcano, Colombia, 14 January 1993. Journal of Volcanology and Geothermal Research 77:325–338

Becker JS, Saunders WSA, Robertson CM, Leonard GS, Johnston DM (2010) A synthesis of challenges and opportunities for reducing volcanic risk through land use planning in New Zealand. The Australasian Journal of Disaster and Trauma Studies 2010-1

Bertolaso G, De Bernardinis B, Bosi V, Cardaci C, Ciolli S, Colozza R, Cristiani C, Mangione D, Ricciardi A, Rosi M, Scalzo A, Soddu P (2009) Civil protection preparedness and response to the 2007 eruptive crisis of Stromboli volcano, Italy. Journal of Volcanology and Geothermal Research 182(3-4):269-277

Bird DK, Gisladottir G, Dominey-Howes D (2010) Volcanic risk and tourism in southern Iceland: Implications for hazard, risk and emergency response education and training. Journal of Volcanology and Geothermal Research 189:33–48

Blong RJ (1981) Some effects of tephra falls on buildings. In: Self S, Sparks RSJ (ed) Tephra Studies, Proceedings NATO Advanced Studies Institute, Laugarvatn and Reykjavik, June 18–29, 1980, pp 405–420

Blong RJ (1984) Volcanic hazards: A sourcebook on the effects of eruptions. Orlando: Academic Press

Blong RJ (1996) Volcanic hazards risk assessment. In: Scarpa R, Tilling RI (ed) Monitoring and Mitigation of Volcanic Hazards, Springer, Berlin, pp 675–698

Booth B (1979) Assessing volcanic risk. Journal of the Geological Society 136(3):331–340

Bower S, Woods A (1996) On the dispersal of clasts from volcanic craters during small explosive eruptions. Journal of Volcanology and Geothermal Research 73:19–32

Breard ECP, Lube G, Cronin SJ, Fitzgerald R, Kennedy B, Scheu B, Montanaro C, White JDL, Tost M, Procter JN, Moebis A (2014) Using the spatial distribution and lithology of ballistic blocks to interpret eruption sequence and dynamics: August 6 2012 Upper Te Maari eruption, New Zealand. Journal of Volcanology and Geothermal Research 286:373–386

Burby RJ, Wagner F (1996) Protecting tourists from death and injury in coastal storms. Disasters 20(1):49–60

Calvari S, Spampinato L, Lodato L (2006) The 5 April 2003 vulcanian paroxysmal explosion at Stromboli volcano (Italy) from field observations and thermal data. Journal of Volcanology and Geothermal Research 149(1-2):160–175

Christiansen RL (1980) Eruption of Mount St. Helens – Volcanology. Nature 285:531-533

Cole JW, Cowan HA, Webb TA (2006) The 2006 Raoul Island Eruption–a Review of GNS Science's Actions. GNS Science Report 2006/7 38

Coombs ML, McGimsey RG, Browne BL (2008) Preliminary Volcano-Hazard Assessment for Gareloi Volcano , Gareloi Island. Alaska Scientific Investigations Report 2008-5159

Cronin SJ, Sharp DS (2002) Environmental impacts on health from continuous volcanic activity at Yasur (Tanna) and Ambrym, Vanuatu. International Journal of Environmental Health Research 12(2):109–123

Cronin SJ, Gaylord DR, Charley D, Alloway BV, Wallez S, Esau JW (2004) Participatory methods of incorporating scientific with traditional knowledge for volcanic hazard management on Ambae Island, Vanuatu. Bulletin of Volcanology 66(7):652-668

Department of Conservation (2012) Volcanic Risk in Tongariro National Park. http://www.doc.govt.nz/parks-and-recreation/places-to-go/central-north-island/places/tongariro-national-park/know-before-you-go/volcanic-risk-in-tongariro-national-park/. Accessed March 2015

Dohaney J, Brogt E, Kennedy B, Wilson TM, Lindsay JM (2015) Training in crisis communication and volcanic eruption forecasting: design and evaluation of an authentic role-play simulation. Journal of Applied Volcanology 4:12

Drabek TE (1995) Disaster responses within the tourist industry. International Journal of Mass Emergencies and Disasters 13(1):7–23

Eissen JP, Blot C, Louat R (1991) Chronologie de l'activité volcanique historique de l'arc insulaire des Nouvelles-Hébrides de 1595 à 1991. Rapp. Scientifiques Technique, Sci. Terre Geol.-Geophys. – ORSTOM (Noumea) 2

Erfurt-Cooper P (2010) Volcano and geothermal tourism in Kyushu, Japan. Volcano and Geothermal Tourism: Sustainable Geo-resources for Leisure and Recreation, Earthscan, p.142

Erfurt-Cooper P (2011) Geotourism in volcanic and geothermal environments: playing with fire? Geoheritage 3:187-193

Ewart JW, Harpel CJ (2004) In harm's way: Population and volcanic risk. Geotimes, American Geological Institute. http://www.geotimes.org/apr04/feature_VPI.html. Accessed 15 June 2016

Fagents S, Wilson L (1993) Explosive volcanic eruptions—VII. The ranges of pyroclasts ejected in transient volcanic explosions. Geophysical Journal International 113:359–370

Fitzgerald RH, Tsunematsu K, Kennedy BM, Breard ECP, Lube G, Wilson TM, Jolly AD, Pawson J, Rosenberg MD, Cronin SJ (2014) The application of a calibrated 3D ballistic trajectory model to ballistic hazard assessments at Upper Te Maari, Tongariro. Journal of Volcanology and Geothermal Research 286:248–262

Fudali R, Melson W (1972) Ejecta velocities, magma chamber pressure and kinetic energy associated with the 1968 eruption of Arenal volcano. Bulletin of Volcanology 35:383 – 401

Geological Survey of Japan (2013) Sakurajima Volcano – 2nd Edition. https://gbank.gsj.jp/volcano/Act_Vol/sakurajima/text/eng/exp01-5e.html. Accessed February 2015

GNS Science (2007) Volcanic Hazards at Tongariro. http://info.geonet.org.nz/download/attachments/8585571/Tongariro_Poster_A4.pdf. Accessed March 2015

GNS Science (2012) Te Maari Eruption Phenomena. http://info.geonet.org.nz/download/attachments/8585571/Northern_Tongariro_eruption_phenomena.pdf. Accessed March 2015

Gregg CE, Houghton BF, Paton D, Swanson DA, Johnston DM (2004) Community preparedness for lava flows from Mauna Loa and Hualālai volcanoes, Kona, Hawai'i. Bulletin of Volcanology 66:531–540

Gurioli L, Harris AJL, Colo L, Bernard J, Favalli M, Ripepe M, Andronico D (2013) Classification, landing distribution, and associated flight parameters for a bomb field emplaced during a single major explosion at Stromboli, Italy. Geology 41(5):559–562

Hadisantono RD, Andreastuti MCHSD, Abdurachman EK, Sayudi DS, Nursusanto I, Martono A, Sumpena AD, Muzani M (2002) Peta Kawasan Rawan Bencana Gung Api Merapi, Jawa Tengah dan Daerah Istimewa Yogyakarta scale 1:50 000 Direktorat Vulkanologi dan Mitigasi Bencana Geologi, Bandung

Harris AJL, Ripepe M, Hughes EA (2012) Detailed analysis of particle launch velocities, size distributions and gas densities during normal explosions at Stromboli. Journal of Volcanology and Geothermal Research 231-232:109–131

Haynes K, Barclay J, Pidgeon N (2007) Volcanic hazard communication using maps: an evaluation of their effectiveness. Bulletin of Volcanology 70(2):123-138

Haynes K, Barclay J, Pidgeon N (2008) The issue of trust and its influence on risk communication during a volcanic crisis. Bulletin of Volcanology 70(5):605-621

Houghton BF, Swanson DA, Carey RJ, Rausch J., Sutton AJ (2011) Pigeonholing pyroclasts: Insights from the 19 March 2008 explosive eruption of Kilauea volcano. Geology 39(3):263–266

Japan Meteorological Agency (2013a) 53 Ontakesan. National Catalogue of the active volcanoes in Japan (The fourth edition). http://www.data.jma.go.jp/svd/vois/data/tokyo/STOCK/souran_eng/souran.htm#kantotyubu. Accessed November 2014

Japan Meteorological Agency (2013b) 90 Sakurajima. National Catalogue of the active volcanoes in Japan (The fourth edition). http://www.data.jma.go.jp/svd/vois/data/tokyo/STOCK/souran_eng/souran.htm#kantotyubu. Accessed November 2014

Jenkins SF, Spence RJS, Fonseca JFBD, Solidum RU, Wilson TM (2014) Volcanic risk assessment: Quantifying physical vulnerability in the built environment. Journal of Volcanology and Geothermal Research 276:105–120

Johnston DM, Bebbington MS, Lai CD, Houghton BF, Paton D (1999) Volcanic hazard perceptions: comparative shifts in knowledge and risk. Disaster prevention and management 8:118–126

Johnston DM, Houghton BF, Neall VE, Ronan KR, Paton D (2000) Impacts of the 1945 and 1995–1996 Ruapehu eruptions, New Zealand: an example of increasing societal vulnerability. Geological Society of America Bulletin 112:720–726

Jolly AD, Jousset P, Lyons JJ, Carniel R, Fournier N, Fry B, Miller C (2014a) Seismo-acoustic evidence for an avalanche driven phreatic eruption through a beheaded hydrothermal system: An example from the 2012 Tongariro eruption. Journal of Volcanology and Geothermal Research 286:331–347

Jolly GE, Keys HJR, Procter JN, Deligne NI (2014b) Overview of the co-ordinated risk-based approach to science and management response and recovery for the 2012 eruptions of Tongariro volcano, New Zealand. Journal of Volcanology and Geothermal Research 286:184–207

Kagoshima City (2010) Sakurajima Volcano Hazard Map. http://www.city.kagoshima.lg.jp/soumu/shichoshitu/kokusai/en/emergency/documents/sakurazimahm_eng.pdf. Accessed 19 October 2015

Kaneko T, Maeno F, Nakada S (2016) 2014 Mount Ontake eruption: characteristics of the phreatic eruption as inferred from aerial observations. Earth, Planets and Space 68:72-82

Keys HJR, Green PM (2010) Mitigation of volcanic risks at Mt Ruapehu, New Zealand. In: Malet J-P, Glade T, Casagli N (Eds.). Proceedings of the Mountain Risks International Conference, Firenze, Italy, 24–26 November 2010. CERG, Strasbourg, France, pp. 485–490

Keys H (2015) Tongariro Alpine Crossing visitors surveyed on effectiveness of new electronic light signs. Tongariro August 2015, p48-51. www.tongariro.org.nz/tongarirojournals. Accessed 18 October 2015

Kilgour G, Della Pasqua F, Hodgson KA, Jolly GE (2010) The 25 September 2007 eruption of Mount Ruapehu, New Zealand: Directed ballistics, surtseyan jets, and ice-slurry lahars. Journal of Volcanology and Geothermal Research 191(1-2):1–14

Leonard GS, Johnston DM, Paton D, Christianson A, Becker J, Keys H (2008) Developing effective warning systems: Ongoing research at Ruapehu volcano, New Zealand. Journal of Volcanology and Geothermal Research 172(3-4):199-215

Leonard GS, Stewart C, Wilson TM, Procter JN, Scott BJ, Keys HJ, Jolly GE, Wardman JB, Cronin SJ, McBride SK (2014) Integrating multidisciplinary science, modelling and impact data into evolving, syn-event volcanic hazard mapping and communication: A case

study from the 2012 Tongariro eruption crisis, New Zealand. Journal of Volcanology and Geothermal Research 286:208–232

Lindell MK (2013) Risk perception and communication. In: Bobrowsky PT (ed) Encyclopedia of Natural Hazards. Springer Netherlands pp.870-874

Lube G, Breard ECP, Cronin SJ, Procter JN, Brenna M, Moebis A, Pardo N, Stewart RB, Jolly A, Fournier N (2014) Dynamics of surges generated by hydrothermal blasts during the 6 August 2012 Te Maari eruption, Mt. Tongariro, New Zealand. Journal of Volcanology and Geothermal Research 286:348–366

Maeno F, Nakada S, Nagai M, Kozono T (2013) Ballistic ejecta and eruption condition of the vulcanian explosion of Shinmoedake volcano, Kyushu, Japan on 1 February, 2011. Earth, Planets and Space 65(6):609–621

Mainichi Shimbun 10/10/2014. Ballistic blocks killed 20 people instantly. http://mainichi.jp/select/news/20141010k0000m040138000c.html. Accessed 29 June 2016

Mileti D, Nathe S, Gori P, Greene M, Lemersal E (2004) Public Hazards Communication and Education: The State of the Art. Natural Hazards Informer, Issue 2. Boulder, p. 13

Minakami T (1942) 5. On the distribution of volcanic ejecta (Part I.): The distributions of volcanic bombs ejected by the recent explosions of Asama. Bulletin of Earthquake Research Institute 20:65 – 92

Mount Fuji Disaster Prevention Council (2004) Report of Mount Fuji Hazard Map Examination Committee (in Japanese). http://www.bousai.go.jp/kazan/fujisan-kyougikai/report/. Accessed 28 June 2016

Murphy PE, Bayley R (1989) Tourism and disaster planning. Geographical Review 79(1):36–46

Nadim F (2013) Hazard. In: Bobrowsky PT (ed) Encyclopedia of Natural Hazards, Springer, Netherlands, pp 425-426

Nairn IA, Self S (1978) Explosive eruptions and pyroclastic avalanches from Ngauruhoe in February 1975. Journal of Volcanology and Geothermal Research 3:36–60

Neal CA, McGimsey RG, Miller TP, Riehle JR, Waythomas CF (2001) Preliminary volcano-hazard assessment for Aniakchak Volcano, Alaska. United States Geological Survey Open File Report 00-519, Plate 1

NHK (Japan Broadcasting Corporation) (2015). Ontake: Eyewitnesses or eruption. http://www.nhk.or.jp/d-navi/link/ontake2014-en/index.html. Accessed July 21 2015

NIED (1980) Field report of the disaster from Ontake 1979 eruption. Natural Disaster Research Report 16, 41p

Odbert H, Hincks T, Aspinall W (2015) Combining volcano monitoring timeseries analysis with Bayesian Belief Networks to update hazard forecast estimates. EGU General Assembly 2015, 12-17 April 2015, Vienna, Austria

Oikawa T, Yoshimoto M, Nakada S, Maeno F, Komori J, Shimano T, Takeshita Y, Ishizuka Y, Ishimine Y (2016) Reconstruction of the 2014 eruption sequence of Ontake Volcano from recorded images and interviews. Earth, Planets and Space 68:79

Pardo N, Cronin SJ, Németh K, Brenna M, Schipper CI, Breard E, White JDL, Procter J, Stewart B, Agustin-Flores J, Moebis A, Zernack A, Kereszturi G, Lube G, Auer A, Wallace C (2014) Perils in distinguishing phreatic from phreatomagmatic ash; insights into the eruption mechanisms of the 6 August 2012 Mt. Tongariro eruption, New Zealand. Journal of Volcanology and Geothermal Research 286:397–414

Paton D, Millar M, Johnston DM (2001) Community resilience to volcanic hazard consequences. Natural Hazards 24:157–169

Paton D, Smith L, Daly M, Johnston D (2008) Risk perception and volcanic hazard mitigation: individual and social perspectives. Journal of Volcanology and Geothermal Research 172(3–4):179–188

Pistolesi M, Rosi M, Pioli L, Renzulli A, Bertagnini A, Andronico D (2008) The paroxysmal event and its deposits. The Stromboli Volcano: An Integrated Study of the 2002 - 2003 Eruption. Geophysica, 317–330

Pomonis A, Spence R, Baxter P (1999) Risk assessment of residential buildings for an eruption of Furnas Volcano, Sao Miguel, the Azores. J. Volcanol. Geotherm. Res. 92(1–2):107–131

Robertson R, Cole P, Sparks RSJ, Harford C, Lejeune AM, McGuire WJ, Miller AD, Murphy MD, Norton G, Stevens NF, Young SR (1998) The explosive eruption of Soufriere Hills Volcano, Montserrat, West Indies, 17 September, 1996. Geophysical Research Letters 25(18): 3429–3432

Scott BJ, Potter SH (2014) Aspects of historical eruptive activity and volcanic unrest at Mt. Tongariro, New Zealand: 1846–2013. Journal of Volcanology and Geothermal Research 286:263-276

Shinano Mainichi Shimbun (2015) Verification of Mount Ontake eruption—living with a volcano. What do we learn from 9.27?. The Shinano Mainichi Shimbun Press, Nagano (in Japanese)

Siegrist M, Cvetkovich G (2000) Perception of hazards: the role of social trust and knowledge. Risk Analysis 20(5):713–720

Sigurdsson H, Lopes-Gautier R (1999) Volcanoes and tourism. In: Sigurdsson H, Houghton B, McNutt SR, Rymer H, Stix J (ed) Encyclopedia of Volcanoes, Academic Press, pp 1283-1299

Slovic P (2000) Perception of risk. In: Slovic P (ed) The perception of risk. Earthscan, London, pp 220–231

Small C, Naumann T (2001) The global distribution of human population and recent volcanism. Environmental Hazards 3:93-109

Smithsonian Institution (2013) Ontakesan bulletin reports, Global Volcanism Program. http://www.volcano.si.edu/volcano.cfm?vn=283040. Accessed December 2014

Sorensen JH (2000) Hazard warning systems: review of 20 years of progress. Natural Hazards Review 1(2):119–125

Sorensen JH (2013) Communicating emergency information. In: Bobrowsky PT (ed) Encyclopedia of Natural Hazards, Springer, Netherlands, pp 110-112

Sparks RSJ, Aspinall WP, Crosweller HS, Hincks TK (2013) Risk and uncertainty assessment of volcanic hazards. In: Sparks RJS, Hill L (eds) Risk and uncertainty assessment for natural hazards, Cambridge University Press

Steinberg G, Lorenz V (1983) External ballistic of volcanic explosions. Bulletin Volcanologique 46(4):333-348

Swanson DA, Zolkos SP, Haravitch B (2012) Ballistic blocks around Kīlauea Caldera: Their vent locations and number of eruptions in the late 18th century. Journal of Volcanology and Geothermal Research 231-232:1-11

The Japan News 26/10/2014. Improved steps needed to inform volcano climbers in Japan. http://the-japan-news.com/news/article/0001671312. Accessed 28 October 2014

The Japan News 27/10/2014. Mt. Ontake risks reported in 1979. http://the-japan-news.com/news/article/0001673442. Accessed 28 October 2014

The Japan Times 27/9/2015. Families of Ontake victims mark first anniversary of deadly eruption. http://www.japantimes.co.jp/news/2015/09/27/national/familiesontakevictimsmarkfirstanniversarydeadlyeruption/#.VxRfHDB942w. Accessed 18 April 2016

Thompson MA, Lindsay JM, Gaillard JC (2015) The influence of probabilistic volcanic hazard map properties on hazard communication. Journal of Applied Volcanology 4:6

Thouret J-C, Lavigne F, Kelfoun K, Bronto S (2000) Toward a revised hazard assessment at Merapi volcano, Central Java. Journal of Volcanology and Geothermal Research 100(1-4):479–502

Tsunematsu K, Ishimine Y, Kaneko T, Yoshimoto M, Fujii T, Yamaoka K (2016) Estimation of ballistic block landing energy during 2014 Mount Ontake eruption. Earth, Planets and Space 68:88

Turtle EP, Lopes RMC, Lorenz RD, Radebaugh J, Howell RR (2016) Temporal behavior and temperatures of Yasur volcano, Vanuatu from field remote sensing observations, May 2014. Journal of Volcanology and Geothermal Research, doi:10.1016/j.jvolgeores.2016.02.030

Twigg J (2002) The human factor in early warnings: risk perception and appropriate communications. In: Zschau J, Kuppers AN (ed) Early warning systems for natural disaster reduction, Springer, Berlin, pp. 19–26

Ui T (2015) The difficulty of predicting volcanic eruptions and releasing information (In Japanese). Geography 60(5):43-49

UNISDR (2009) United Nations International Strategy for Disaster Risk Reduction: UNISDR Terminology on Disaster Risk Reduction (2009). http://www.unisdr.org/eng/terminology/terminology-2009-eng.html. Accessed June 2015

Vanuatu Geohazards Observatory (2009) Volcanic Alert Status. http://www.geohazards.gov.vu/index.php/hazards-updated-events/volcano-alert-status. Accessed March 2015

Vanuatu Geohazards Observatory (2014) Vanuatu Monitoring Network (2012-2014). http://www.geohazards.gov.vu/index.php/geophysical-monitoring-network/vanuatu-monitoring-network. Accessed April 2015

Wardman J, Sword-Daniels V, Stewart C, Wilson T (2012) Impact assessment of the May 2010 eruption of Pacaya volcano, Guatemala. GNS Science Report 2012/09, 90p

Williams KL, Keys HJR (2013) Reducing volcanic risk on the Tongariro Alpine Crossing. Report of a workshop 24 September 2013. Department of Conservation Tongariro District, 36p

Wilson L (1972) Explosive volcanic eruptions II. The atmospheric trajectories of pyroclasts. Geophysical Journal of the Royal Astronomical Society 30(1):381–392

Wilson TM, Stewart C, Wardman JB, Wilson G, Johnston DM, Hill D, Hampton SJ, Villemure M, McBride S, Leonard G, Daly M, Deligne N, Roberts L (2014) Volcanic ashfall preparedness poster series: a collaborative process for reducing the vulnerability of critical infrastructure. Journal of Applied Volcanology 3:10

Yamagishi H, Feebrey C (1994) Ballistic ejecta from the 1988–1989 andesitic Vulcanian eruptions of Tokachidake volcano, Japan: morphological features and genesis. Journal of Volcanology and Geothermal Research 59(4): 269–278

Preamble (Chapter 3)

The previous chapter highlighted the ways ballistic hazard has been managed and communicated around the world and recommended strategies to address ballistic hazard and risk in the future. It described how ballistic deposits had been mapped and assessed and used four case studies to investigate how ballistic hazard is managed and communicated at volcanoes with different eruption frequencies, styles and exposure.

Chapter 3 addresses the lack of spatial density, ballistic size and distribution data highlighted in Chapter 2 that limits our understanding of ballistic hazard and the effectiveness of DRR strategies. The ballistic field around Yasur Volcano, Vanuatu is mapped, and the spatial and temporal distribution of ballistics is analysed. Findings indicate that spatial density and ballistic size varies with distance and direction from the vents. Directionality in explosions is found in the ballistic distribution and explosion footage, however it changes over time. These characteristics are important when considering hazard assessments and DRR methods.

Chapter 3 has been submitted and is in review with the journal Volcanica

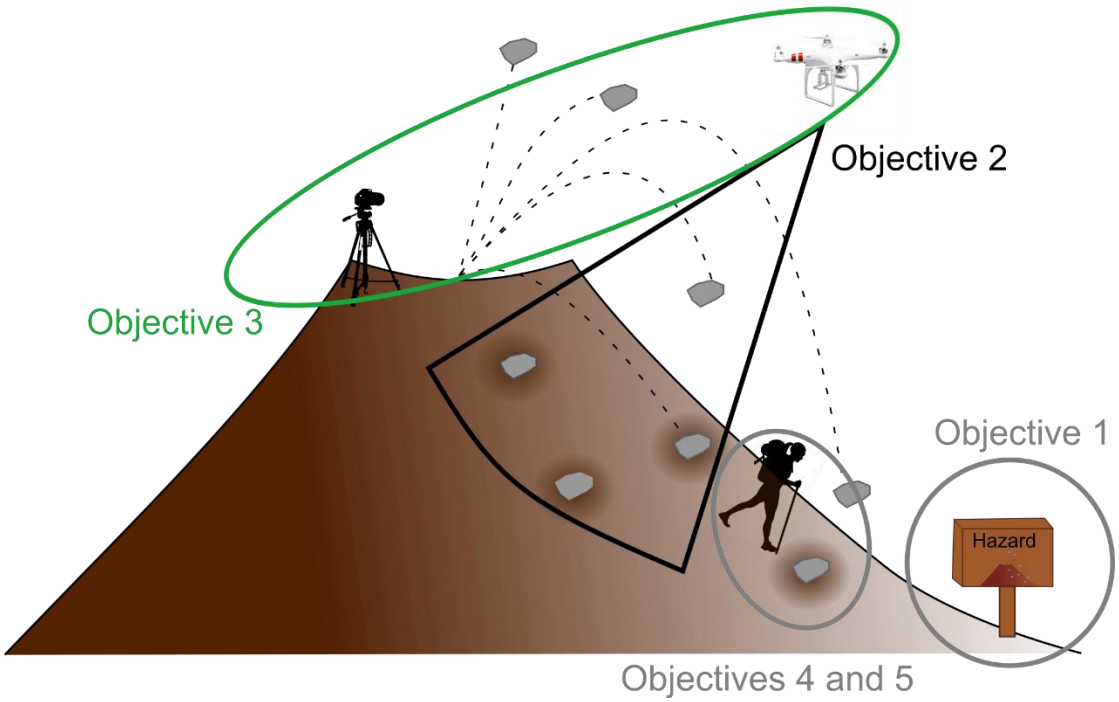

Conceptual diagram showing the objectives of the thesis with the objectives addressed in Chapter 3 in green and black.

Chapter Three – Volcanic ballistic projectile deposition from a continuously erupting volcano: Yasur Volcano, Vanuatu

3.1. Abstract

Volcanic ballistic projectiles are the main hazard to life and infrastructure from Strombolian eruptions. This eruption style is a tourist drawcard, exposing people to ballistic hazard. Most of the research on ballistics to date has been focussed on understanding how ballistics form and their trajectory. However, little focus has been placed on how ballistics are distributed within ballistic fields or the inclusion of this data into hazard and risk assessments. In this study we used a drone to image the ballistic field, and cameras to record explosions at Yasur Volcano, Vanuatu from 28 July to the 2 August and 17 to the 19 October 2016. We present the mapped distributions from the two trips, how the field changes with distance and direction from the vent, and how eruption dynamics influence these changes. Our evidence for directionality results in considerable variation in summit ballistic hazard and is an important consideration for ballistic hazard and risk assessments.

3.2. Introduction

Erupting volcanoes are increasingly frequented by tourists (Erfurt-Cooper, Sigurdsson and Lopes 2015). For example, Yasur volcano, on the SE of Tanna Island, Vanuatu, attracts ~50 tourists a day, who spend often two or more hours watching the frequent Strombolian explosions from the crater rim. Such proximity to the explosions exposes visitors and guides to multiple volcanic hazards, with volcanic ballistic projectiles (VBPs or ballistics) globally the most common cause of volcanic fatalities for tourists (Brown et al. 2017). Ballistics (bombs and blocks) can range from a few centimetres to tens of metres in diameter (Nairn and Self 1978; Bower and Woods 1996; Gurioli et al. 2013; Andronico et al. 2015; Tsunematsu et al. 2016), can travel tens to hundreds of metres per second (Fudali and Melson 1972; Yamagishi

and Feebrey 1994; Pioli et al. 2008; Taddeucci et al. 2012) and up to ~10 km from vent, although they are usually limited to within 5 km (Minakami 1942; Blong 1984; Kilgour et al. 2010; Alatorre-Ibargüengoitia et al. 2012; Gurioli et al. 2013). Their high impact and thermal energies make them a potentially lethal hazard (Blong 1984; Baxter and Gresham 1997; Alatorre-Ibargüengoitia et al. 2012; Wardman et al. 2012; Tsunematsu et al. 2016), capable of damaging exposed vehicles (Global Volcanism Program 2001; Wardman et al. 2012; Andronico et al. 2015), buildings (Booth 1979; Pistolesi et al. 2008; Jenkins et al. 2014; Williams et al. 2017), infrastructure (Pistolesi et al. 2008; Wardman et al. 2012; Andronico et al. 2015) and agriculture (Stern et al. 2007; Wardman et al. 2012). Three of the 367 globally recorded fatalities from ballistic strike have occurred at Yasur (Brown et al. 2017).

Risk reduction and mitigation measures (such as land use planning, exclusion zones, protective-wear, shelters, communication and education products) are key to reducing risk to visitors, though to be most effective they must be supported by robust hazard and risk assessment (Fitzgerald et al. 2017). Ballistic hazard assessments determine the likelihood of ballistic-producing eruptions and the likely affected areas (Thouret et al. 2000; Alatorre-Ibargüengoitia et al. 2012). Ballistic risk assessments go one step further and determine the likelihood of specific consequences occurring (e.g. fatalities, casualties, damage) due to the exposure to ballistics (Blong 1996). A common ballistic risk management approach has been to simply 'avoid' being exposed to ballistic hazard through use of exclusion and/or restricted-access zones (Fitzgerald et al. 2017). However, increasing tourism and other activities on active summit areas leads to greater exposure to the hazard, and there are increasing regulatory requirements and societal expectations to inform users about the risk to which they may be exposed (Jolly et al. 2014; Deligne et al. 2018). These have driven the requirement to more accurately assess risk so that it may be evaluated and treated within a risk management framework. Yet, our understanding of ballistic hazard is relatively limited. A lack of empirical mapping of how ballistics are distributed in space (ballistic fields) during explosive eruptions is notable with only a few fully mapped ballistic fields reported (e.g. Swanson et al. 2012; Gurioli et al. 2013; Fitzgerald et al. 2014). The main reasons for this are field time constraints (mapping every individual ballistic on foot is time-consuming), the high risk involved in mapping proximal vent areas especially during unrest or eruption phases, the resolution limitations of readily available remote sensing imagery, and the limited geological preservation

of ballistic fields due to cover from ash and lapilli and subsequent erosion. Instead, published ballistic distribution maps often only show the maximum travel distance or extent of the field (Minakami 1942; Nairn and Self 1978; Yamagishi and Feebrey 1994; Robertson et al. 1998). This does not give a complete understanding of the hazard and can lead to inaccurate estimations of risk, particularly without the knowledge of spatial density. Sufficiently high-resolution aerial photos help get a wider understanding of field characteristics, making mapping the field possible and allowing for targeted field investigations (to supplement and check the accuracy of photo mapped data, maintain detail and reduce uncertainty in identifying ballistics) and have been used to map ballistic fields (Breard et al. 2014; Fitzgerald et al. 2014; Kaneko et al. 2016). Previously this has been accomplished using planes and helicopters. However, the use of these aircraft is expensive and can be a limitation for scientists with limited resources.

Drones are a tool that can be used to assess geological hazards (Gomez and Purdie 2016) while reducing the risk to scientists. They offer particular capabilities that lend themselves to volcano observation and monitoring. This includes: (1) access to dangerous or hard to reach areas while keeping scientists at a safer distance from the hazard; (2) portability; (3) ability to produce higher resolution outputs compared with those taken by larger aircraft such as helicopters, by being able to get closer to features; and (4) relatively low cost. For example, drones have been used in volcanic research to thermally map a geothermal valley (Harvey et al. 2016), observe crater activities in active volcanoes (Patterson et al. 2005; Jordan 2015), map active lava flows and model future flow paths (Turner et al. 2017), determine the likely location of magma and dykes using aeromagnetic surveys (Kaneko et al. 2011), measure the gas composition (Shinohara 2013) and flux from a volcanic plume (McGonigle et al. 2008), 3D image a volcanic plume (Gomez and Kennedy 2017), and survey land changes after volcanic eruptions (Nakano et al. 2014). To the best of our knowledge, no-one has utilised a drone to map ballistic fields.

In this paper we present the results of two field campaigns from 28 July to the 2 August and 17 to the 19 October 2016 to map the ballistic field and understand the ballistic hazard at Yasur. The study objectives were to: (1) use drones and photogrammetry to determine the distribution and varying spatial intensity of the hazard (both the number and size of ballistics) constrained between the two flights; and (2) evaluate explosion frequency and dynamics from video footage to understand how this influences the ballistic hazard distribution at Yasur. The results

presented here will add to the limited data available on ballistic distributions from Strombolian eruptions, improve our knowledge of how ballistic fields vary with distance and direction from vent and over time, and improve understanding on the causes of heterogeneity around a vent as well as in a field. The paper is structured into four main sections. We describe our methodology, followed by results which are subdivided into Section 3.4.1 Spatial Distribution containing mapping results and Section 3.4.2 Eruption Dynamics containing video and observation derived results. We discuss the relationship between ballistic size and distance from vent, how spatial density changes with direction around the vents, differences between the two data sets, and finally, we describe the hazard/risk implications of our results.

3.2.1. Eruptive History

Yasur is a basaltic trachy-andesite scoria cone 361 m a.s.l. (at the summit), situated within the >20 ka Siwi caldera at the north-western edge of the Yenkahe resurgent dome (Métrich et al. 2011; Merle et al. 2013; Gaudin et al. 2014; Brothelande et al. 2015; Battaglia et al. 2016). Present-day Yasur is composed of a 660 m diameter crater subdivided into two sub-craters with three main vent areas (A and B in the southern sub-crater, and C in the northern sub-crater) (Nabyl et al. 1997; Oppenheimer et al. 2006; Kremers et al. 2012; Meier et al. 2015; Spina et al. 2015; Battaglia et al. 2016; Figure 3.1). It is evident that the positions of the vents migrate over time and the two southern vent areas (A and B) are alternately named by different authors. Drone footage from this study revealed a change in the number and position daily of vents in both the North and South craters. Thus, we have decided to adopt the Jolly et al. 2017 naming convention of simply North and South Crater.

Firth et al. (2014) identified 3 stages of eruption from tephra stratigraphy and literature review: pre-700 AD, a variable frequency and intensity eruptive episode; from ~700 AD to 1270 AD a higher magnitude lower frequency episode; and from 1270 AD to the present a persistently active low magnitude high frequency episode. This most recent eruptive stage has been predominantly Strombolian with intermittent Vulcanian activity (Nabyl et al. 1997; Bani and Lardy 2007; Firth et al. 2014). Explosion frequency has been variable over the current high frequency stage. Meier et al. (2015) reported explosions several times a minute while Marchetti

et al. (2013) and Battaglia et al. (2016) reported a frequency of at least one explosion per minute. Kremers et al. (2013) report similar results of explosion recurrence under one minute (from Crater A). However, Vent Area B frequency ranged from minutes to days and Vent Area C had strong explosions every 10 minutes. Vent Area B explosion recurrence was reported to be on the minutes end of the range by Oppenheimer et al. (2006) with 13 explosions occurring over a 15-minute period. Over a two-hour period, Bani et al. (2013) recorded 200 explosions from Vent Area B using a thermal infrared thermometer. Infrasound recordings reported by Le Pichon et al. (2005) showed 20-1300 explosions per day.

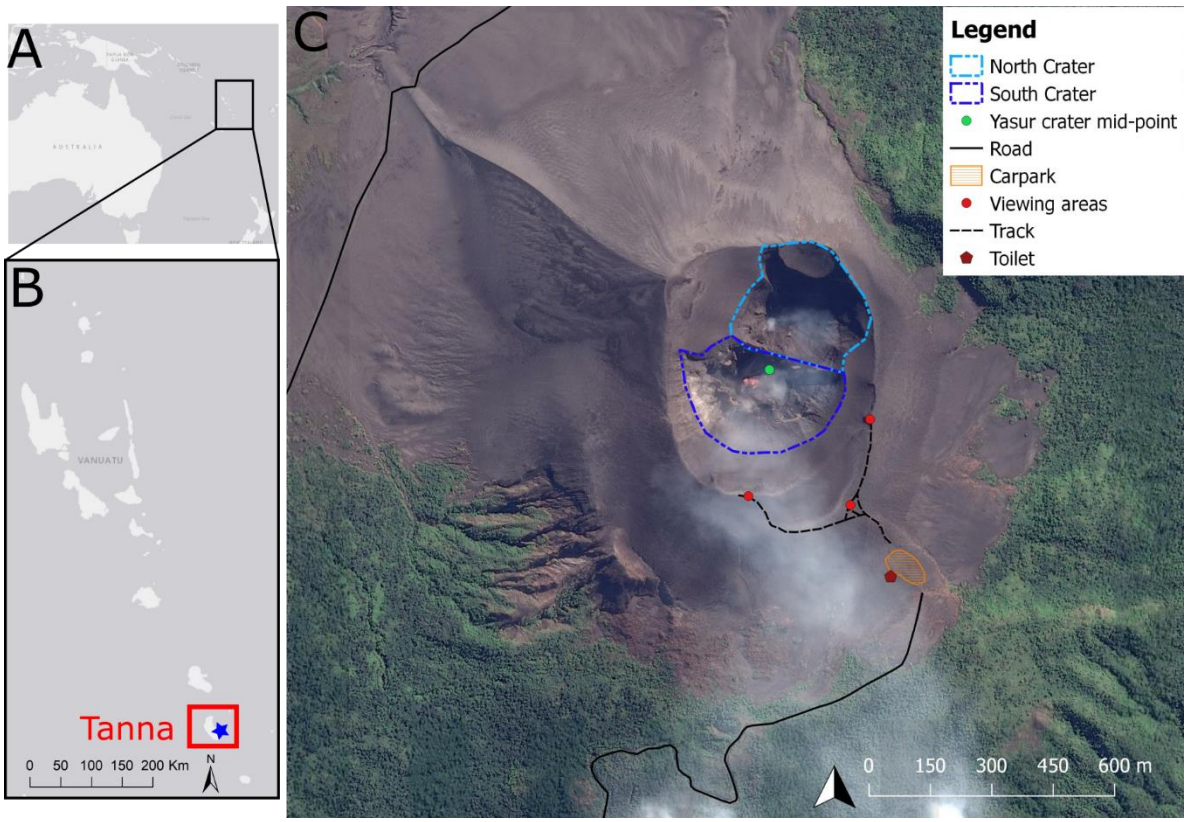

Figure 3.1: Location maps of Vanuatu (A) and the island of Tanna (B) with a blue star indicating where Yasur is. Yasur Volcano, the two sub-craters and the location of infrastructure are shown in C

3.3. Methodology

Ballistic fields can cover large areas (Fudali and Melson 1972; Fitzgerald et al. 2014), making them difficult to map in detail due to the time needed to record all pertinent information from each ballistic (e.g. dimensions, lithology, crater formation, impact angle) and the sheer number of ballistics that are contained in the field (Fitzgerald et al. 2014). Aerial photography and photogrammetry allow for mapping to be done remotely, in detail over the whole area and in a much shorter time frame. In our study, a DJI Phantom 3 drone was flown over the crater and flanks of Yasur Volcano, capturing 3,863 images and covering an 0.82 km^2 area from NE to S (Figure 3.2) at heights above the ground up to 60 m with a 12-megapixel camera. Time and equipment restrictions meant limiting flying to a 135° swath of the volcano, with the NE-S area chosen due to it encompassing the viewing areas, track, and carpark. Eight orthophotographs and accompanying DEMs were created from these images using Structure from Motion (SfM) software (PhotoScan) in high enough resolution to map individual ballistics. Flights were flown on autopilot (using the Map Pilot application) with flight paths created on an iPad in the field. Using Map Pilot ensured that photos were taken with sufficient overlap for SfM to be used and that no areas were missed. However, some flights were switched to manual towards the path end where there was a possibility of collision with the volcano flank (take off generally occurred at a lower elevation than the landing point and the DJI does not have the capability to adjust elevation mid-flight with changing topography).

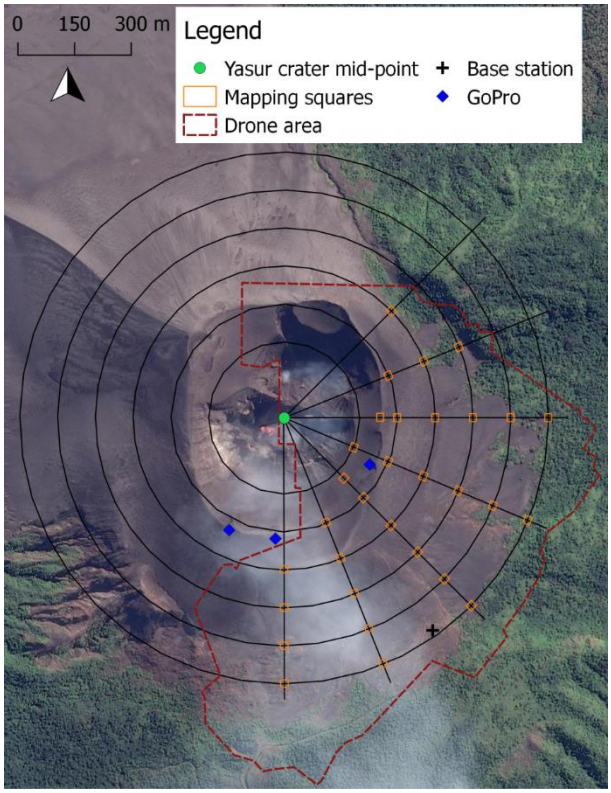

Figure 3.2: The crater mid-point, 100 m radii and transects used to create the mapping squares. Also shown is the area that the drone imaged

Geospatial data was collected using a Trimble R8 Real-time Kinematic Global Navigation Satellite System (RTK GNSS), with a base station set up at the edge of the car park (Figure 3.2) and linked to the drone imagery through ground control points taken at ground targets visible in the aerial images.

Although RTK GNSS produces a typical location error in X, Y < 2-5 cm and < 10 cm in Z compared to single GNSS and GPS units, the SfM photogrammetric method relies on statistical approximation of the camera characteristics (Westoby et al. 2012) and on the resolution of the imagery (Gomez 2014). Therefore, even with GNSS RTK tie points, error can spread in between the ground control points and precisely aligning the produced orthophotographs and DEMs from the two trips can be challenging once imported into the ArcGIS environment. To make visual comparisons between the two orthophoto datasets easier and rectify the misalignment, the orthophotos and DEM sets were stacked in the GIS software ENVI and

exported as combined TIFFs. The stacks were then imported into ArcGIS where they were split into smaller areas (between 4 and 20 depending on the size of the area the original orthophoto covered) and georeferenced to each other. Splitting the layers resulted in more accurate georeferencing as it reduced the warping produced when the larger datasets were used.

As the area captured in the orthophotos was too large to map all ballistics in the available timeframe, twenty-three 20 x 20 m squares (an area of 400 m^2 for each square) were visually mapped from the orthophotos from the July/August trip and thirty from the October trip (as the latter covered a larger area). The squares were positioned at 100 m increments and along transects 22.5° apart radiating from a central point (hereafter called the crater mid-point) between the two craters to capture as much of the orthophoto area and variation in ballistic distribution around the volcano as possible (Figure 3.2). A central point between the two craters was chosen as it was not possible to distinguish which ballistic came from which vent. Spatial density contours were then applied to the mapped distributions using the spline tool in ArcGIS and best fit estimates. In addition to the location being recorded, ballistic dimension (taken from the largest axis) and whether an impact crater has been produced and its dimensions was also noted. Identification of ballistics was based on multiple factors though not all were required for identification. Factors included (1) morphology (sitting on the surface, distinct ballistic rounding or angularity), (2) colour differences (darker or lighter clasts compared to the ground surface), (3) round depressions around or near a ballistic indicating impact with the ground, and (4) disturbed material around a ballistic indicating an impact. Figure 3.3 illustrates this process, showing a mapping square pre- and post-ballistic identification. Comparison of the July/August and October orthophotos helped to identify new ballistics that had landed post July/August data collection and also confirmed if something was a ballistic (i.e. seeing it in a slightly different light or angle in a different orthophoto could help to confirm it was a ballistic and not a lighter patch of ground or autobreccia from the old lava flows on the flanks). Unfortunately due to time constraints in the field, we could not ground-truth the mapping squares to validate our mapping methodology and assess for resolution error.

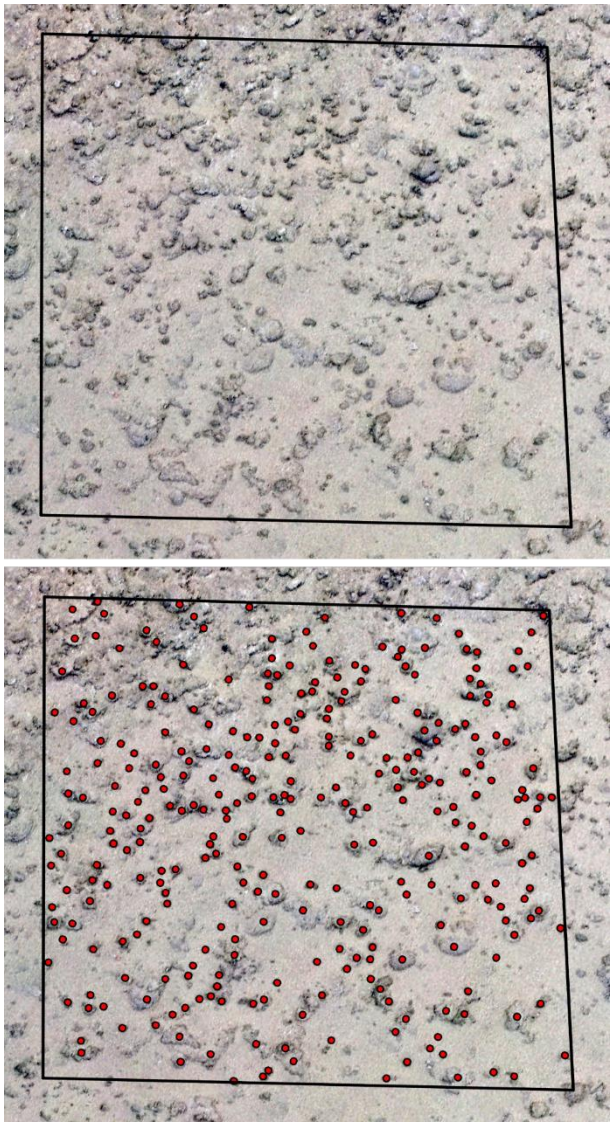

Figure 3.3 Mapping square pre- and post-ballistic identification

In addition to the drone flights, three GoPro Hero 3+ cameras with non-fish-eye lenses were set up around the crater rim to record eruption dynamics and frequency for 10 hours over 30 July to 1 August 2016. Each camera could see into the crater though not to the vents as crater walls blocked these from view. Where possible, we assessed the size and directionality of the explosions from the GoPro video footage. Multiple locations around the crater and concurrent filming from the cameras meant that directionality could be checked at another angle. Directionality was classified on the angle of the eruption jet in relation to landmarks around the crater (i.e. the viewing areas to the east and south). Explosions were sized based on the height that ballistics or a sustained tephra plume reached (small: a third of the way up the crater;

moderate: between a third of the crater height and the crater rim; large: above the crater rim). An anemometer (Kestrel 5500 L) was also assembled at the southern viewing area (Figure 3.1c) to record wind speed and direction every 1 to 5 minutes over 29 July to 1 August. Additionally, systematic observational logs were collected for one hour each day from the seating/viewing area in the SSE from 5 September to 16 October 2016 in between the two imaging trips. This record provided the source crater that any bombs were coming from, which direction they were landing and if they landed outside the crater rim.

As part of concurrent studies (Jolly et al. 2017), temporary infrasound and seismic networks were set up around the cone. Two stations from these arrays (YIB22 and YS01), located ~700 m from the vent area, are used in this paper to support changes in eruptive activity observed in video footage from the same time period. Peak event amplitudes for unfiltered infrasound data are analysed from YIB22 in a time-window from -5 to +10 s around an automatic network-coincident STA/LTA trigger. We define triggers with 0.1–50 Hz filtered data using an STA length of 0.5 s, an LTA length of 40 s, and a coincident STA/LTA threshold of 3 on at least 2 stations of a 3-element array. Real-Time Infrasonic Amplitude (RIAM) and Real-Time Seismic Amplitude (RSAM) were also recorded and calculated as the 10-minute mean of absolute amplitude of 0.1–50 Hz filtered data (Endo and Murray, 1991).

3.4. Results and Analysis

This section is divided into two subsections: 3.4.1 Spatial Distribution, which reports results from the aerial mapping; and 3.4.2 Eruption Dynamics which conveys the results from the GoPro footage and visual observations.

3.4.1. Spatial distribution

We present two ballistic distributions from Yasur volcano. The first is of ballistics deposited between 28 July and 19 October 2016 (hereafter referred to as the two-month distribution), by mapping ballistics that appear only in the October images and that are not present in the July/August images. The second was the distribution of all observable ballistics in October,

which includes the longer-term distribution of ballistics deposited potentially over months to years.

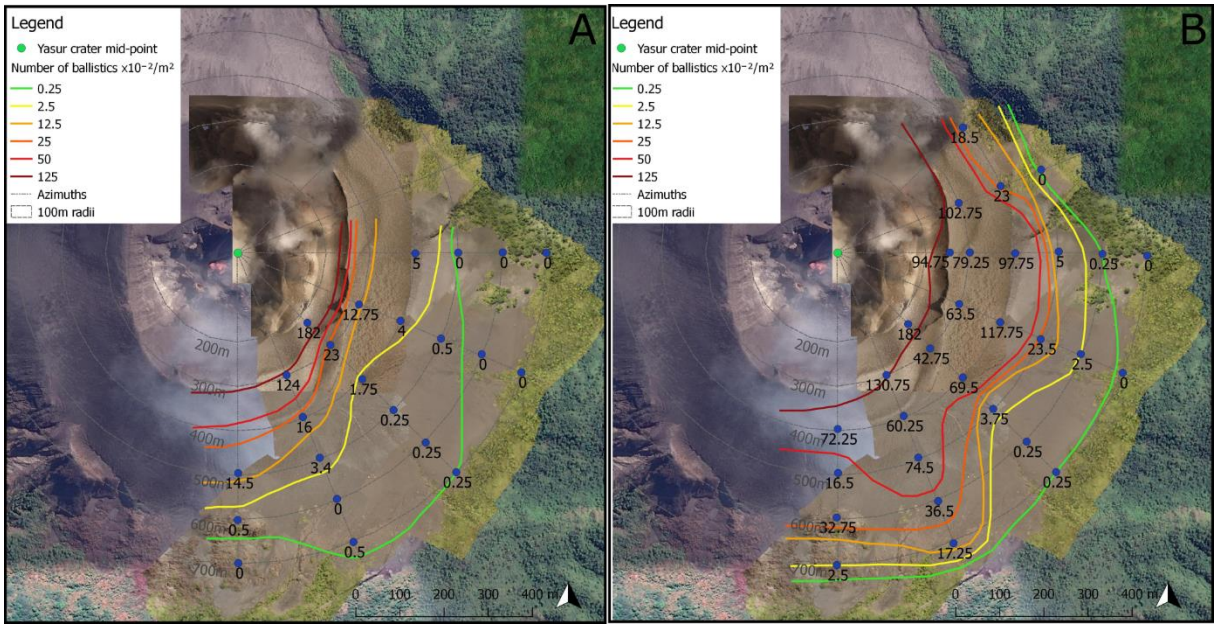

Figure 3.4: Ballistic spatial density (number of ballistics x 10^{-2} per m^2) from the deposition over two months (A) and everything on the ground in the later October images (B). The aerial imagery captured from the two trips is layered beneath the map contours

From the two-month distribution, 1,550 ballistics were identified from 23 mapping squares (each square 400 m^2 in area). Ballistic diameters ranged from 5 (the minimum size that could be distinguished) to 304 cm with a mean of 43 cm. The number of ballistics per m^2 drops rapidly as distance from the crater increases, from 182 x $10^{-2}/m^2$ at 200 m from the crater mid-point (defined in section 2) to an average of 6.69 x$10^{-2}/m^2$ at a distance of 400 m (Figure 3.4a). Greater than 500 m from the crater mid-point the number of ballistics decreases to between 0 and 0.5 x10^{-2} ballistics per m^2 in most azimuths. The distribution of ballistics also shows a directionality in the S and SSE azimuths where a greater number of ballistics exist between 300 and 500 m from the crater mid-point than in other azimuths (ballistic numbers ranging 124 – 3.4 x$10^{-2}/m^2$ compared to 23 – 0 x$10^{-2}/m^2$, respectively) (Figure 3.4a). The E and ESE azimuth also have more ballistics at 400 m from the crater mid-point than the SE. However, Figure 3.5a shows the SE having the largest median ballistic diameter at 300 m that decreases away towards the ESE and SSE, creating a lobe that might indicate directionality. Median diameter was used as there

are large ballistic outliers that skew the mean value. Analysis of the size distribution also revealed an increase in median diameter at 500 m following a trend of decreasing size in the SSE azimuth.

The total October distribution shows similar patterns as the two-month distribution. From 30 mapping squares (400 m^2 areas) 5481 ballistics were mapped. Ballistics ranged from 3 to 353 cm in diameter with an average of 34 cm. Ballistic density decreases with distance from the crater from an average of 138.5 $x10^{-2}/m^2$ at 200 m from the crater mid-point to 4 $x10^{-2}/m^2$ at 700 m, though not as rapidly as seen in the two-month distribution (Figures 3.4b and 3.5d). When analysed in azimuths we see a general decrease in density along all azimuths though at some point along all but the E and ENE azimuths, an increase in density is observed. For example, in the S azimuth, density decreases from 72.25 $x10^{-2}/m^2$ at 400 m from the crater mid-point to 16.5 $x10^{-2}/m^2$ at 500 m distance. Density then increases to 32.75 $x10^{-2}/m^2$ at 600 m from mid-point and then decreases again with distance. Similar to the two-month distribution, ballistic deposition is greater towards the S-SSE and E-ESE in contrast to the SE at most distances except at 400 m from mid-point where it is at similar densities to the S and SSE (Figure 3.4b).

Analysing the size distribution at varying distances and azimuths from the crater shows higher median ballistic diameters to the SE at 200, 300 and 500 m from crater mid-point that decrease away towards the ESE and SSE (Figure 3.5b). At 400 m from the crater mid-point, the ENE has the largest median diameter that decreases towards the E and NE, potentially indicating two lobes towards the SE and ENE (Figure 3.5b). The October distribution shows a general decrease of median ballistic size with distance from crater mid-point until 600 m where ballistic size begins to increase (Figure 3.5c). Increasing diameters following a general decreasing trend is also seen in the SSE, SE and ESE azimuths (Figure 3.5b).

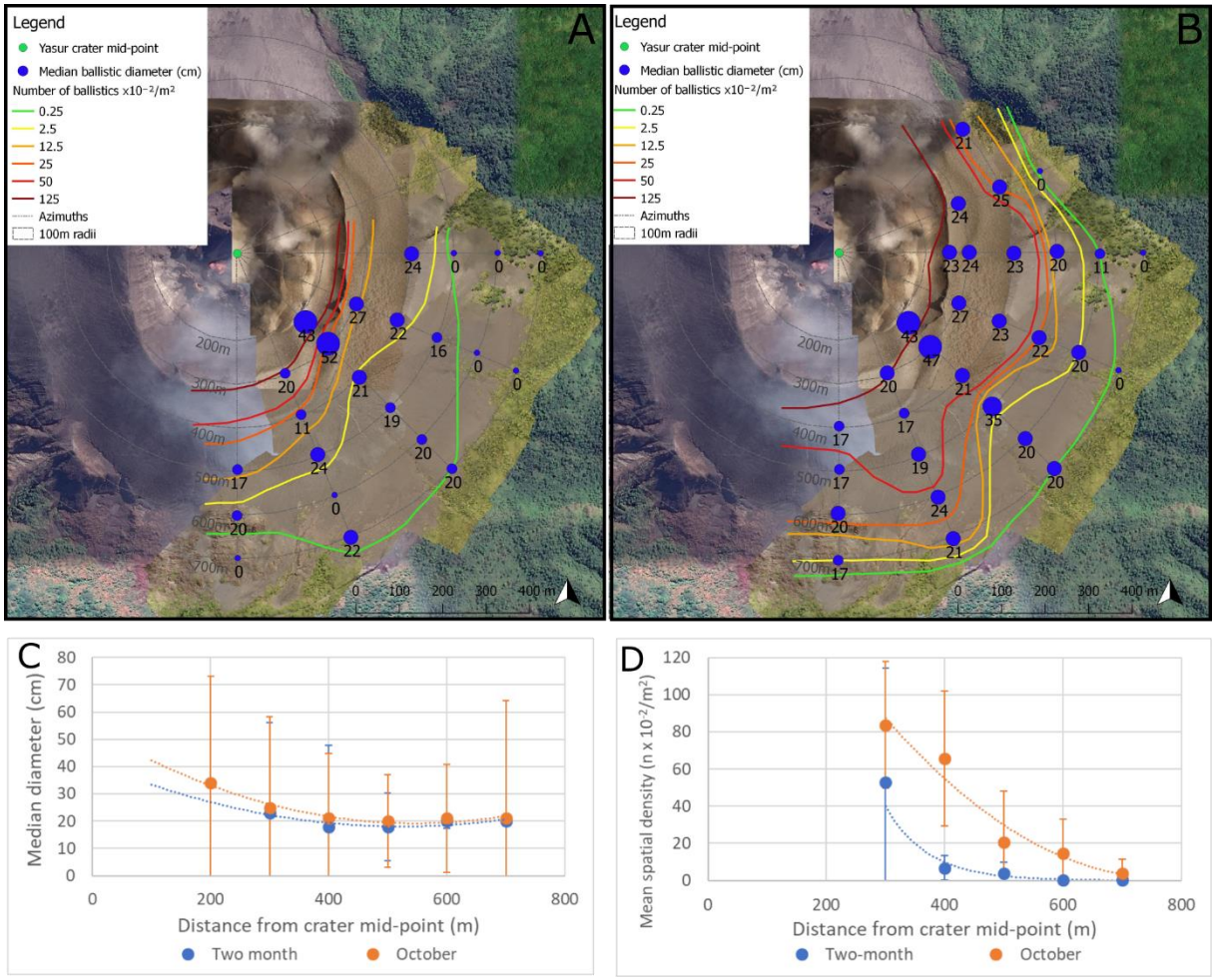

Figure 3.5: Relationship between median ballistic size and spatial density with distance and direction from crater mid-point from the two-month (A) and October (B) distributions. C and D show the median diameter and mean spatial density with distance from crater mid-point for both distributions, irrespective of azimuth (with standard deviation error bars).

3.4.2. Eruption dynamics

Over 10 hours (between 30 July and 1 August) of GoPro footage was collected, capturing 758 explosions. On average, 68 explosions occurred per hour, with 42/hr from South Crater and 27/hour from North Crater. Each explosion was classified small, moderate or large, the vent origin noted (Table 3.1), and what style of eruption it was. As described earlier, the larger the explosion, the higher the ballistics are ejected. Subsequently, a larger explosion has the ability to eject ballistics further from the vent area. Styles included ballistic, ballistic with a tephra plume, tephra plume, and gas. A marked increase in the proportion of large events is noted on

the 1 August (52%) compared to the previous days (12% on the 30 July and 18% on the 31 July). Additionally, an increase in the number of explosions from the south crater vs the northern crater was noted. The proportion increased from 52% (30 July) and 53% (31 July) to 80% on the 1 August. Seismic and infrasound data over this time also show an increase in explosivity (Figure 3.6). This can be more clearly seen in the infrasound record (Figure 3.6A and B) where on day 5 (1 August) there is a noticeable increase in peak event and total amplitude. Highlighted in blue in Figure 3.6A are the video observed explosions from Table 3.1. On average small explosions produce a peak pressure of 6.71 Pa, increasing to 13.6 Pa for moderate explosions and 27.7 Pa for large explosions. Eruptive activity therefore is not steady and can fluctuate over hours.

Table 3.1: Number and proportion of small, moderate and large events, and the proportion of explosions from each crater recorded on GoPros between 30 July and 1 August. Peak pressure recorded on infrasound station YIB22 was found for each video recorded explosion and the average and standard deviation of all explosions categorised into small, moderate or large was calculated

	30/07/2016		31/07/2016		1/08/2016		Peak pressure (Pa) at YIB22	
	No.	%	No.	%	No.	%	Average	SD
Small	153	55	223	49	2	8	6.71	7.28
Moderate	90	33	146	32	10	40	13.6	14.6
Large	32	12	83	19	13	52	27.7	20.6
North	131	48	212	47	5	20		
South	143	52	241	53	20	80		
Total	274		453		25			

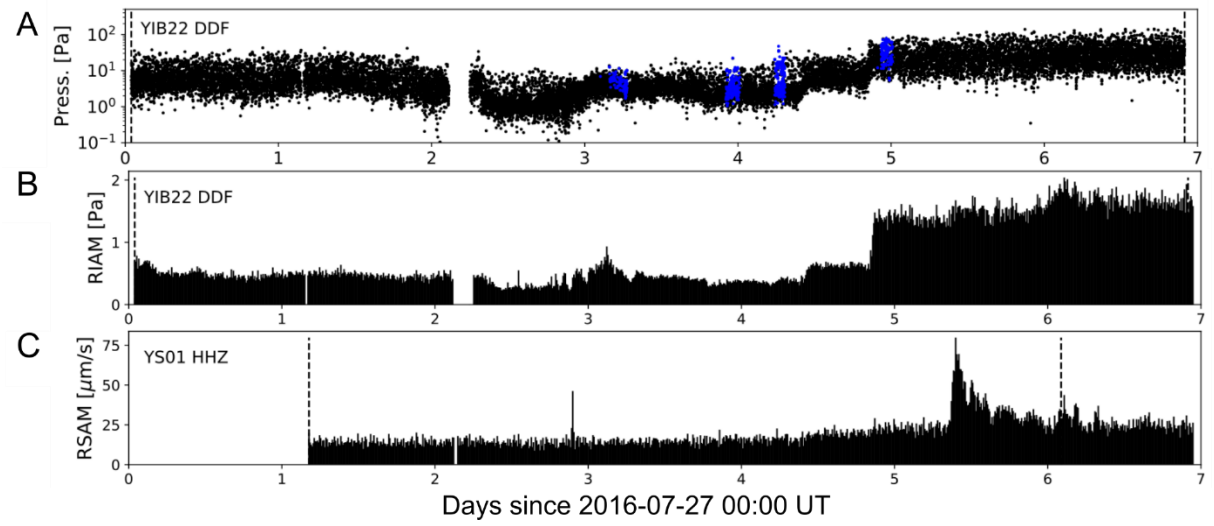

Figure 3.6: Infrasound and seismic amplitude metrics from a temporary co-located infrasound station (YIB22) and broadband seismometer (YS01) approximately 700 m from the summit vents. A shows peak event amplitudes for unfiltered infrasound data at YIB22. Blue symbols in A show infrasound amplitudes at YIB22 corresponding to the explosions analysed in video data in this study (see Table 1). Vertical dashed lines represent times of network completion for coincident triggers. B shows 10-minute Real-Time Infrasonic Amplitude (RIAM) and C shows Real-Time Seismic Amplitude (RSAM) values at YIB22 and YS01, respectively.

From our analysis of the GoPro footage over 30 July to 1 August period, most explosions were vertically directed (40%). However, when the jet was angled, a SE directionality was the favoured direction from South Crater and S from North Crater (Figure 3.7). Between the two trips from 5 September to the 16 October, observations were made daily for 1 hour a day of where bombs were landing (rather than orientation of the jet as for the GoPro footage), indicating directionality favouring the south. Figure 3.7c shows the azimuths where bombs ejected from South Crater landed, with 39% landing to the south. Only two observations were made of bomb directionality from North Crater. On both occasions they were directed to the south. During the second trip from 16 – 20 October, general visual observations of eruption dynamics showed directionality to the south and east from South Crater and to the east from North Crater (Gomez and Kennedy 2017).

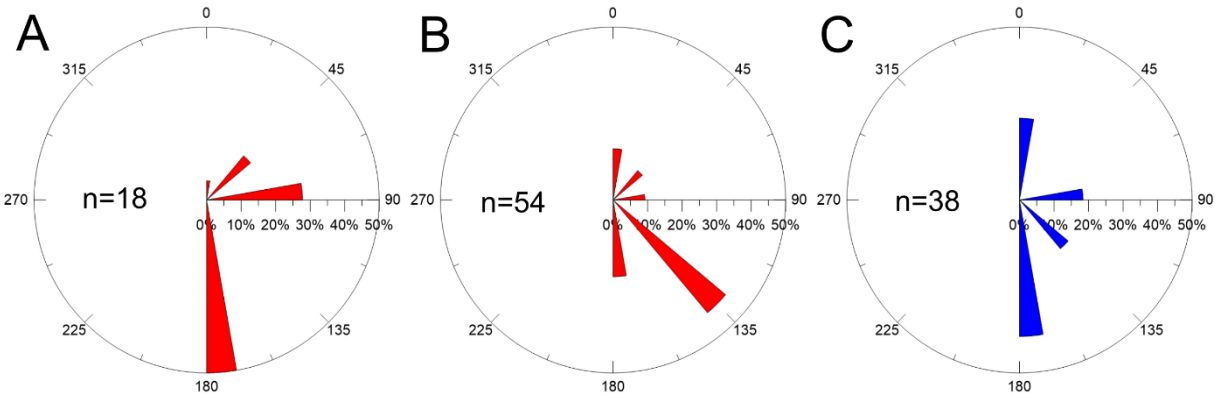

Figure 3.7: Directionality of explosion pulses. A and B show the percentages of individual explosions that are directed in varying directions from North Crater (A) and South Crater (B) recorded on the GoPros over three days. C shows the directionality from South Crater seen from the observational logs from 5 September – 20 October 2016

We also noted a changing directionality throughout individual eruption events on some occasions. For example, ballistics would be ejected toward the north at the start of the explosion and subsequently move towards the south in a spraying motion. This was also noted by Gaudin et al. (2014) in Strombolian explosions, where the mean ejection angle shifted up to 40° in a single explosion. They theorise that this is due to the changing location of the bubble rupture point as the rupture area continues to open and increase in size. These instances have not been included in the directionality data presented here for simplicity, however, it is important to recognise that directionality is not fixed and can change even during one eruption event.

Not all explosions at Yasur have a ballistic component, with 18% of the explosions recorded on the GoPro videos having no observable ballistic component at all. This is an important consideration when using eruption frequency to assess ballistic hazard.

Summarising our key results, we find that spatial density of ballistics decreases with distance from the crater, with this occurring more sharply in the two-month distribution than the October distribution, and that median ballistic diameter decreases with distance from crater. Directionality is evident in the spatial density mapping (S-SSE with a minor increase in density to the E), ballistic size distribution analysis (SE and minor ENE) and video analysis (SE from South Crater and S from North Crater) and the daily visual observations, though they do not all agree. Video footage showed an increase in the proportion of large explosions from the 30 July to the 1 August, with large explosions capable of ejecting ballistics above the crater rim and

creating a hazard for visitors. This is also seen in the infrasound and seismic record where amplitude increased on the 1 August.

3.5. Discussion

The ballistic distributions mapped from the aerial photos are the products of both the North and South Craters. The frequency of explosions from both craters, the lack of temporal sampling and the varying explosion directionalities make it difficult to assign specific vents to a distribution. However, it is likely that the higher densities in the S-SSE come from South Crater and those in the E from the North Crater. This deduction is based on the dominant explosion directionalities observed from video records and the observational logs and the greater distance ballistics from North Crater need to travel when directed toward the S-SSE.

3.5.1. Decreasing median ballistic size with distance from the crater

The relationship between ballistic size and distance travelled from source has been discussed in the literature with both increasing and decreasing size with distance observed. Taddeucci et al. (2017) summarise this literature to say that an increase in ballistic size with distance is observed in many ash and block rich Vulcanian eruptions (Minakami et al. 1969; Steinberg 1974, 1976; Self et al. 1980; Druitt et al. 2002; Fitzgerald et al. 2014) and a decrease in size with distance is usually observed in phreatomagmatic eruptions (Lorenz 1970; Self et al. 1980; Waitt et al. 1995; De Novellis and Luongo 2006). The former is hypothesised to be because all ballistics exit the vent at similar velocities and due to inertia, larger ballistics travel further while smaller ballistics are more greatly affected by drag and land closer to the vent (Fagents and Wilson 1993; De Novellis and Luongo 2006; Bertin 2017; Taddeucci et al. 2017). For the latter, ballistics ejected in a gas stream may decrease the effects of drag on particles allowing smaller ones to travel higher than larger ones before dropping out of the stream and therefore travelling further than their larger counterparts (Lorenz, 1970; Self et al. 1980; De Novellis and Luongo 2006; Taddeucci et al. 2017; Kilgour et al. 2019). For clarity, we term the increase in ballistic size with distance as a normal distribution, and a decrease in ballistic size with distance, a reverse distribution. Ballistic fields can also show no evident size trend (Mastin 1991;

Taddeucci et al. 2017). Taddeucci et al. (2017) attribute this to three reasons: not all ballistics are ejected with the same velocity in an eruption; overlapping ballistics distributions either from multiple eruptions or multiple vents; and ballistic collisions.

However, ballistic size-distance relationships have not been discussed in relation to Strombolian eruptions. As Strombolian explosions tend to be frequent (up to 9/hour at Stromboli (Harris and Ripepe 2007)) and typically deposit bombs closer to the vent, the risk of being impacted while conducting fieldwork is high and is likely the main reason the size-distance relationship has not been investigated. A literature search resulted in two references where a relationship was found. Gurioli et al. (2013) note that in the 21 January 2010 eruption at Stromboli, thermal video shows 'a leading spray of smaller bombs, quickly followed by an emission of larger bombs that attained lower heights and fell closer to the vent than those of the first spray'. Andronico and Pistolesi (2010) report pumiceous clast sizes between 7 and 20 cm in the summit area of Stromboli (~790 m.a.s.l.) that reduce to an average long axis of the five largest clasts of 11 cm at 650 m.a.s.l. from the 24th November 2009 eruption. Both papers show a reverse distribution. Bombrun et al. (2015) also recorded lower initial ejection velocities of larger projectiles compared to smaller projectiles at Stromboli volcano. Similar to the phreatomagmatic eruptions, Strombolian eruptions are driven by gas slugs, providing the gas stream needed to reduce drag on smaller projectiles (Harris et al. 2012; Taddeucci et al. 2015). This is likely the reason for the reverse distribution described in this paper and seen in the aforementioned publications.

3.5.2. Changing spatial density with direction around the crater

We see a change in spatial density from the south to the east, with higher densities in the S-SSE and ESE-E than the SE. Three main factors might influence where ballistics cluster or appear to cluster: (1) topography (Kilgour et al. 2019), (2) preservation of the deposit and (3) eruption directionality (Kilgour et al. 2010; Gurioli et al., 2013). A topographic high or steep sided crater wall may block ballistic deposition as ballistics may not be able to reach heights capable of landing on the other side of the topography or angled ballistics may get blocked by steep sided crater walls. There does not appear to be any topographic shadowing affecting ballistic deposition in the SE from South Crater or North Crater. The height of the crater rim is the same

in the SE as the ESE (~320m), though is 10 m and 35 m higher in the SSE and S respectively when measured from the crater mid-point. Therefore, if the SE were shadowed we should see similar densities to the SE in the ESE and lower densities in the SSE and S. Analysing the ability of ballistics to be ejected from the vents uninhibited by crater walls reveals that ballistics ejected at angles ≥34° from horizontal could escape the crater from the ESE to the SSE (Figure 3.8). The angles were measured from the middle of the North and South Craters respectively, rather than the all-encompassing crater mid-point to be as accurate as possible. In Strombolian explosions ejection angles are typically close to vertical (within 5° from vertical at Stromboli – Chouet et al. 1974; around 72° at Mt Etna - Gouhier and Donnadieu 2011; 70-85° at Stromboli - Pistolesi et al. 2008) with 80 – 90% of particles ejected within 20° of the ejection axis (Chouet et al. 1974; Gouhier and Donnadieu 2010). If we use the lower end of the reported average ejection angles (72°) and add on 20° for the dispersion cone, all ballistics would successfully clear the ESE – SSE crater walls.

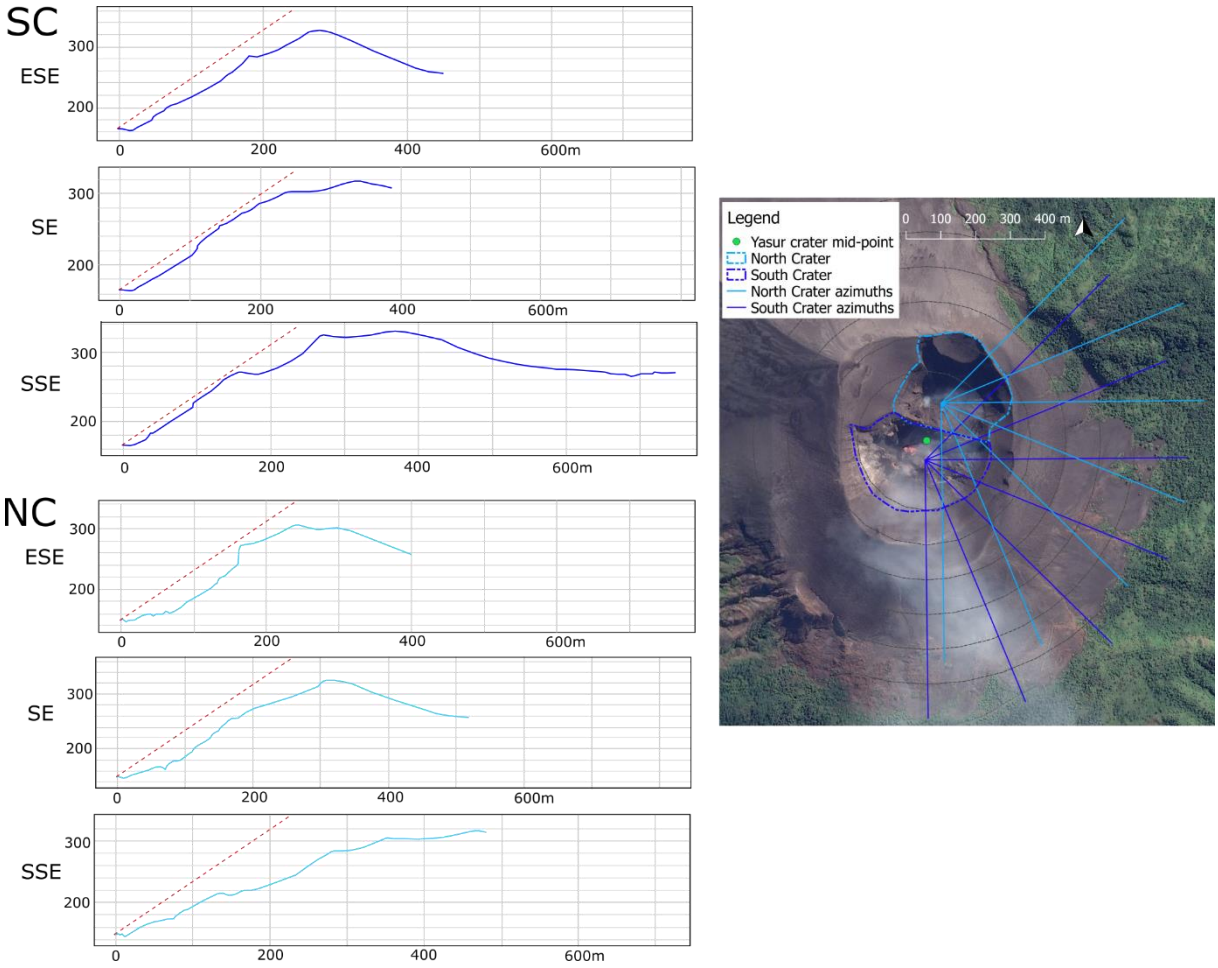

Figure 3.8 Topographic profiles of the crater rim and walls measured from the centre points of North Crater (NC) and South Crater (SC) along azimuths illustrated on the map, created from combining DEMs from the two trips. The red hatched line indicates 34°, the minimum angle that ballistics would clear the crater walls.

Topography may also impact the preservation of the original spatial density (landing positions). We see a lower spatial density in the SE at 300 m from the crater mid-point compared to the same distance in the ESE and SSE (Figure 3.4b). This area is on the lee side of the crater rim dipping toward the vents (Figure 3.9). Landing on the lee side might explain lower densities in the SE at 300 m as the ballistics might land and then either roll back into crater or stop on lower part of the inner crater rim. None of the other mapping squares at a 300 m distance are on a lee slope towards the crater – the others either at the base of the inner rim or on the crater rim where it is flatter. We see three examples of empty impact craters with similar sized ballistics downhill (toward the crater) in the mapping square, as well as multiple cases of ballistics being on the crater edge of their impact craters (Figure 3.9).

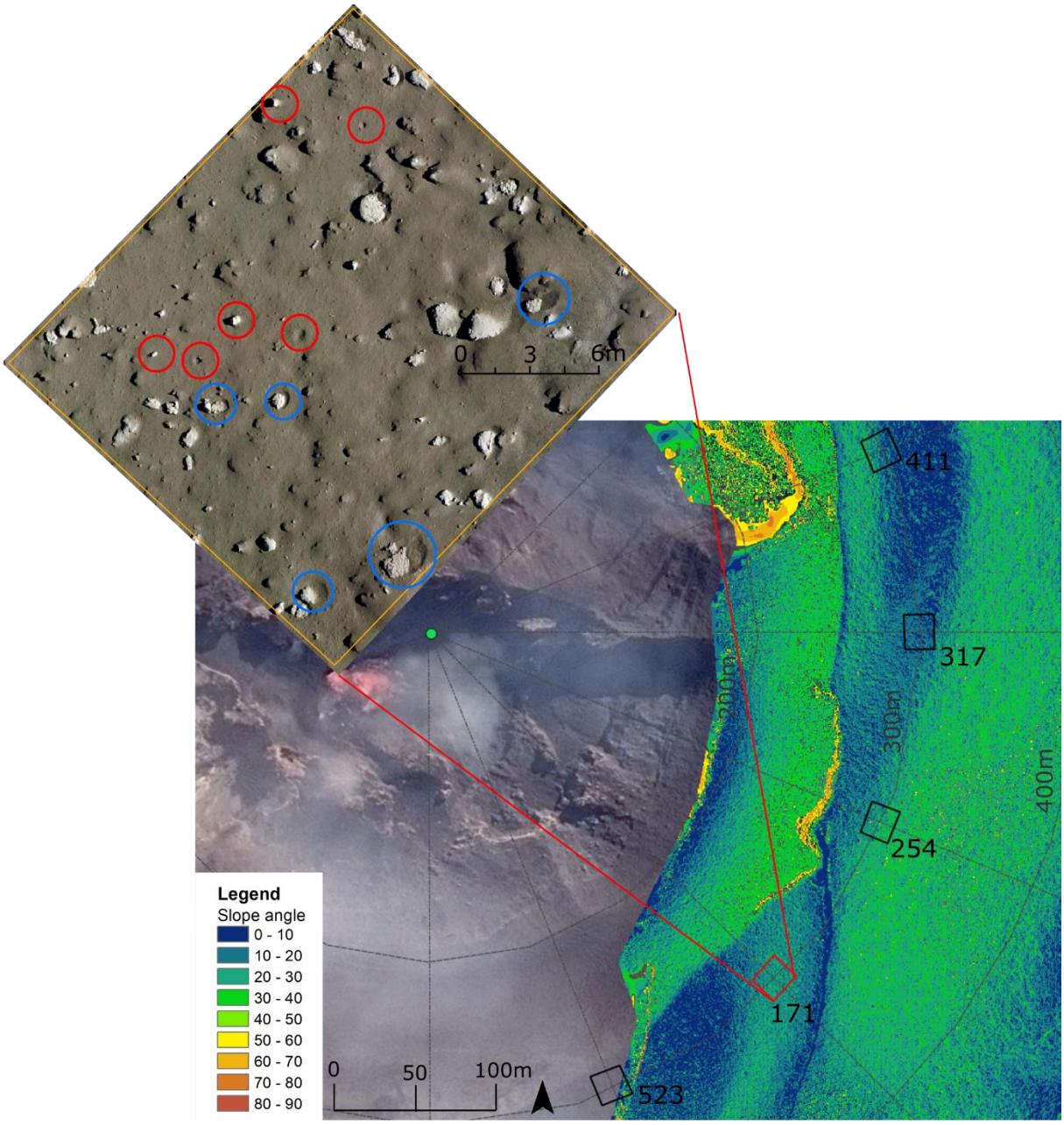

Figure 3.9: Slope angles of the areas mapped 300 m from crater mid-point, highlighting the location of a mapping square on the lee side of the crater dipping towards the vents. Ballistics in the mapping square have bounced out of their craters (red circles show the crater and the likely ballistic) or have slumped to the edge of their crater closest to the vent (blue circles)

The deposition of tephra fall has the ability to impede preservation of the ballistic field and can affect the estimations of hazard and risk. Yasur not only erupts ballistics but also tephra fall (ash and lapilli). We see a complete burial of the ballistics in the July images and deposition of new ballistics by the two-month distribution in the SE 200 m from the crater mid-point. Tephra deposition could also contribute to the lower spatial densities seen in the SE where windblown

tephra fall may have been deposited. To assess this possibility, we looked at the number of ballistics that were mapped in the July images but were no longer visible in the October images (Figure 3.10) and the wind directionality over the mapping period. Of the ballistics mapped in the July orthophotos, 50% were not visible in the October orthophotos. When divided into distance and azimuth from vent area, it is apparent that the SE does not have an increased percentage of missing ballistics compared to other azimuths and so rejects the hypothesis of SE ash and lapilli tephra fall directionality or preservation issues. Additionally, the prevailing wind direction for Tanna is from the E to SE which deposits tephra fall in the opposite direction to the W to NW. The anemometer deployed on the south rim of the crater recorded N-SE winds throughout the July/August trip, though predominantly E-SE (see Jolly et al. 2017), that again would not be responsible for depositing tephra fall preferentially to the SE. However, deposition of tephra fall in proximal areas of the cone is still likely, especially when wind speeds are low and this along with ballistic deposition would explain the 50% of ballistics that could not be identified in the second survey in October.

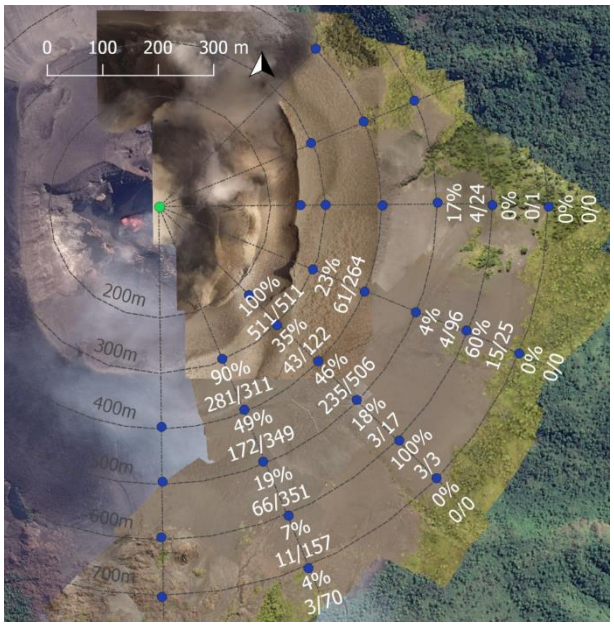

Figure 3.10: Number and percentage of ballistics missing from the October images that were mapped in the July/August images out of the total mapped from the July/August images. Five sites were excluded (500 – 700 m in the south azimuth and 400 m in the ESE and E) as photo resolution inhibited determining whether tephra fall did cover previously mapped areas.

Directed eruptions can produce asymmetric ballistic fields (Kilgour et al. 2010; Houghton et al. 2011; Gurioli et al. 2013; Fitzgerald et al. 2014). We observed from the video footage a

predominantly SE directionality from South Crater and a predominantly S directionality from North Crater. From the observational logs taken over the two-month period, more bombs were reported landing to the south of the vents in South Crater (i.e. both on the southern crater wall and outside the crater rim to the south). The longer observations of directionality over two months from the observational logs and those from the North Crater would explain the increased spatial density in the S and SSE in the mapped distribution. However, the dominant SE directionality from South Crater recorded on video during the July/August fieldwork is not supported in the mapped distributions (we would see an increased spatial density in the SE). This could be due to the short timeframe of recorded video (3 days) not representing the longer-term directionality. The E-ESE increase in spatial density seen in the mapped distribution can also be explained by explosion directionality, with 27% of the directed explosions recorded on video from North Crater going to the east. Higher spatial density in the SSE and E are also noted in maps produced following increased activity in 1994 (Global Volcanism Program 1995). Salvatore et al. (2018) recorded variations in jet directionality over short timescales of hours to days at Stromboli from a four-year record and that this was the result of changes to vent size and morphology. Over longer timescales (months to years) vents were observed to migrate and merge. Both of these factors could cause the asymmetry seen in our mapping.

In summary, ballistic spatial density changes with direction from the crater. This is caused by explosion directionality and minimally by slope changes. Topographic shadowing was not observed from the NE to S (though may affect the unmapped western side which is higher than the east and south), and tephra fall and ballistic burial of the ballistic field does not explain the observed changes in spatial density with direction but does explain the lack of preservation of many ballistics.

3.5.3. Contrasting size, density and directionality data

A larger median ballistic diameter is observed at each of 200, 300 and 500 m distance in the SE compared to other azimuths. In the SE azimuth, we also observe the lowest ballistic spatial density and highest proportion of explosion directionality from the GoPro videos. The contradicting GoPro explosion directionality and spatial density, as explained earlier, is due to

the GoPro footage representing a small timeframe and not the longer-term preferential directionality. However, this does not explain the large clast size anomaly in the SE. We suggest this is the result of larger less frequent eruptions ejecting larger ballistics further and wider, depositing large clasts in the SE as well as in all other directions. The more common smaller explosions are directed in other directions, depositing smaller ballistics in these areas (with larger ballistics landing closer to the vents) and decreasing the median clast size of the azimuths. Figure 3.11 supports this idea, showing fewer ballistics 10-20 cm in size in the SE than the other azimuths in both distributions. In the October distribution (Figure 3.11b) we also observe fewer 20-40 cm size ballistics in the SE than other azimuths. From 50 cm+ similar numbers of ballistics are seen in all azimuths.

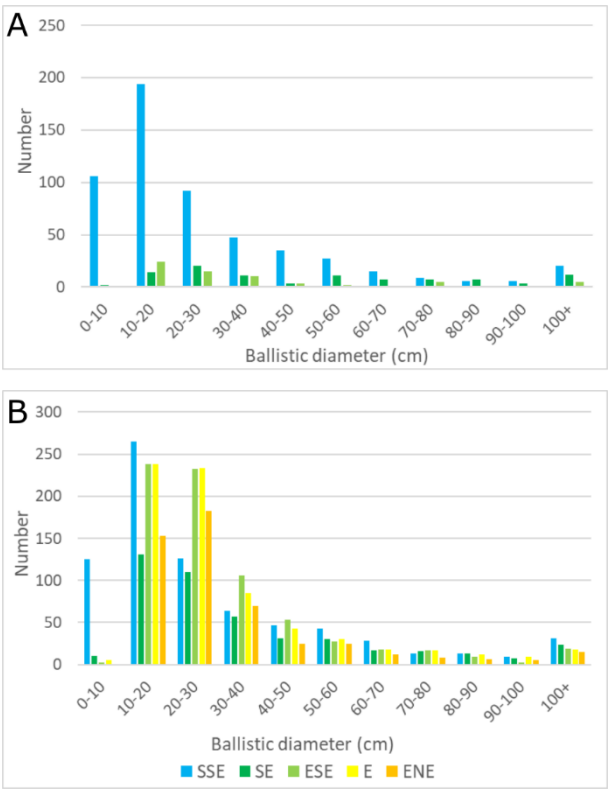

Figure 3.11: Size distribution of ballistics in each azimuth between 300 and 500 m from the crater mid-point. A: Two-month distribution. B: October distribution

3.5.4. Differences in the density with distance trend between the two-month and October distributions

A decrease in the ballistic spatial density with increasing distance from the vent area is evident in both the two-month and October distributions, though they do not follow the same trend. A steeper decrease is seen in the two-month distribution. The October distribution covers a longer time period where larger eruptions likely occurred over months to years prior to the survey date, ejecting a greater number of ballistics further than in the two-month period.

3.6. Hazard/risk implications

Our results have implications for risk management. Understanding which areas have higher densities of ballistic impact and how the spatial density decreases with distance can be used to determine where transient visitors may be safer to visit or where infrastructure is sited.

The spatial density of ballistics reported here should be considered conservative due to burial of proximal deposits by subsequent tephra fall, masking the true deposition; hence the hazard to visitors may be underestimated. Preservation issues with ballistic deposits (e.g. burial of deposits as witnessed here, but also erosion of craters by weather and other factors) show how time sensitive ballistic mapping is to capture the true distribution from an eruption.

This ballistic hazard research does not encompass the hazard from larger eruptions which would likely produce a larger ballistic field that may extend into the jungle at Yasur. Reports from a more explosive eruption period in June-July 1999 describe ejected ballistics reaching as far as 600 m from the nearest edge of the crater (Global Volcanism Program 1999). This would require fieldwork at greater distances from the crater and modelling to understand the potential distributions. Further assessment would also be beneficial over a longer time period (e.g. 12-24 months), like that performed by Salvatore et al. (2018), to capture any temporal variability in eruption directionality and potentially eruption size, which may reduce the spatial variability seen in this study. We note the Vanuatu National Disaster Management Office (NDMO), the government agency responsible for disaster risk reduction, have a permanent exclusion zone that includes the crater and the top of the flanks extending around from the viewing points.

Additional 'zones' are restricted during periods of elevated seismic activity (monitored by Vanuatu Meteorology and Geohazards Department (VMGD)) associated with larger or more frequent explosions (Table 3.1 and Figure 3.6 show the correlation between elevated seismo-acoustic activity and an observed increase in the proportion of larger explosions). Danger Zone A includes the cone and volcano viewing is only allowed from the carpark. Danger Zone B is an ~500 m radius from the edge of the crater rim that includes the car park and parts of the ash plain (Vanuatu Meteorology and Geohazards Department 2019). As shown in Figure 3.6 and Table 3.1, acoustic sensors are highly complementary to the seismic and visual observations with regards to energy dynamics of eruptions and ballistic hazard. Acoustic monitoring at the sole seismic station monitored by VMGD may add value to monitoring and risk decision making, though further investigation of its limitations is needed which is outside the scope of this study.

As well-known with volcanoes, past behaviour does not necessarily dictate future behaviour. This needs to be considered when using eruption directionality to assess potential ballistic hazard areas (i.e. areas exposed to volcanic ballistic deposition), which could then be used to inform where access on the volcano may be tolerable within risk management decision making. Our data shows that the ballistic hazard is highly spatially variable, in part due to explosion directionality, but that directionality may vary significantly temporally. Therefore directionality results from this study alone should not be used as the basis for hazard and risk decisions. Longitudinal studies on directionality patterns are needed to determine the stability, usefulness and representativeness of directionality in ballistic hazard and risk decision-making. It may be more pragmatic to use spatial density and how this changes with distance from the vent to describe the hazard intensity and for a radius of a certain distance around the vent based on spatial density to be used to define 'hazard areas' so that any future change in directionality is accounted for. In the past hazard areas have been defined by the maximum travel distance of a specific diameter ballistic. However, as discussed earlier, eruptions can produce normal and reverse ballistic distributions and thus setting a high or low diameter threshold could mean over or underestimating travel distance depending on the eruption style. Combining these two approaches where spatial density of ballistic deposition above a dangerous diameter is used as a measure to define hazard areas could also be considered in the future. Further investigation is needed to determine what measure is best to apply to characterise ballistic hazard.

The ballistic hazard mapping and analysis presented in this paper is intended to improve our understanding of the extent and distribution of ballistic hazard from Strombolian eruptions. This study should not be used in isolation to guide or inform risk management decisions at Yasur or any other volcano necessarily. Rather this study provides data and analysis for one step (of many) in the process of assessing risk to visitors and infrastructure, which can contribute to informing decisions as to how the risk should be managed.

3.7. Conclusions

Understanding where ballistics land, their spatial density and size, and how this changes with distance and direction from the vent can inform more effective risk management. This is especially important on volcanoes that are frequently visited such as Yasur Volcano, Vanuatu. We used a drone to image part of the ballistic field around Yasur and GoPro cameras and daily observations to record explosions. Mapping and analysis of the images and video taken revealed:

1) The spatial density of the ballistics decreased with increasing distance away from the crater
2) The median ballistic diameter decreased with distance from the crater, similar to that seen from Strombolian eruption deposits at Stromboli and also from phreatomagmatic eruptions around the world. This is likely due to the presence of a gas jet decreasing drag on particles, allowing smaller ones to travel higher and further than larger ones.
3) Higher spatial densities of ballistics are seen in the S-SSE than in other directions. We attribute this to directionality and angularity in the blasts and not to topographic shadowing.
4) A different directionality was observed in the GoPro videos than in the daily observations and ballistics mapped from aerial photos. The mapping represents a longer time frame than the observations or videos and likely represents the longer-term directionality trend.
5) Field preservation issues are apparent, with the burial of ballistics by further deposition of tephra fall. Therefore, ballistic mapping is time sensitive after an eruption and delays

in mapping will likely be accompanied by decrease in field preservation and result in an underestimation of ballistic hazard.

When creating ballistic hazard and risk maps or making risk management decisions at continuously erupting volcanoes it is important to remember that the hazard can vary over relatively small areas and over different time frames. Assessing the hazard over as much of the volcano as possible and over as long a time frame as possible will produce more effective results to subsequently base successful risk management decisions from.

3.8. Acknowledgements

This work was supported by a biennial grant (16/727) from the New Zealand Earthquake Commission (EQC). RHF was funded by a Ngāi Tahu Research Centre Doctoral Scholarship. RSM was partially supported by NSF grant EAR-1620576. We thank Nick Key, Matt Cockcroft, Adrien Teissier, Janvion Cevuard, Athanase Worwor and Julius Mala for invaluable field assistance, and Sandrine Cevuard at VMGD for monitoring support. Seismic and infrasonic data analysis included the use of ObsPy (Beyreuther et al., 2010).

3.9. References

Alatorre-Ibargüengoitia MA, Delgado-Granados H, Dingwell DB (2012). Hazard map for volcanic ballistic impacts at Popocatépetl volcano (Mexico). Bulletin of Volcanology 74(9), 2155–2169.

Andronico D, Pistolesi M (2010). The November 2009 paroxysmal explosions at Stromboli. Journal of Volcanology and Geothermal Research, 196(1–2), 120–125. https://doi.org/10.1016/j.jvolgeores.2010.06.005.

Andronico D, Scollo S, Cristaldi A (2015). Unexpected hazards from tephra fallouts at Mt Etna: The 23 November 2013 lava fountain. Journal of Volcanology and Geothermal Research, 304, 118-125.

Bani P, Harris AJL, Shinohara H, Donnadieu F (2013). Magma dynamics feeding Yasur's explosive activity observed using thermal infrared remote sensing. Geophysical Research Letters, 40(15), 3830-3835.

Bani P, Lardy M (2007). Sulphur dioxide emission rates from Yasur volcano, Vanuatu archipelago. Geophysical Research Letters 34, L20309.

Battaglia J, Métaxian J-P, Garaebiti E (2016). Families ofsimilar events andmodes ofoscillation ofthe conduit at Yasur volcano (Vanuatu). Journal of Volcanology and Geothermal Research, 322, 196 – 211.

Baxter P, Gresham A (1997). Deaths and injuries in the eruption of Galeras Volcano, Colombia, 14 January 1993. Journal of Volcanology and Geothermal Research 77, 325–338.

Bertin D (2017). 3-D ballistic transport of ellipsoidal volcanic projectiles considering horizontal wind field and variable shape-dependent drag coefficients. Journal of Geophysical Research: Solid Earth, 122(2), 1126–1151. https://doi.org/10.1002/2016JB013320.

Beyreuther M, Barsch R, Krischer L, Megies T, Behr Y, Wassermann J (2010). ObsPy: A Python toolbox for seismology. Seismological Research Letters, 81(3), 530–533. https://doi.org/10.1785/gssrl.81.3.530.

Blong RJ (1984). Volcanic hazards: A sourcebook on the effects of eruptions. Orlando: Academic Press.

Blong RJ (1996). Volcanic hazards risk assessment. In: Scarpa R, Tilling RI (ed) Monitoring and Mitigation of Volcanic Hazards, Springer, Berlin, 675–698.

Bombrun M, Harris A, Gurioli L, Battaglia J, Barra V (2015). Anatomy of a Strombolian eruption: Inferences from particle data recorded with thermal video. Journal of Geophysical Research: Solid Earth, 120(4), 2367-2387. DOI: 10.1002/2014JB011556

Booth B (1979). Assessing volcanic risk. Journal of the Geological Society 136(3), 331–340.

Bower S, Woods A (1996). On the dispersal of clasts from volcanic craters during small explosive eruptions. Journal of Volcanology and Geothermal Research 73, 19–32.

Breard ECP, Lube G, Cronin SJ, Fitzgerald R, Kennedy B, Scheu B, Montanaro C, White JDL, Tost M, Procter JN, Moebis A (2014). Using the spatial distribution and lithology of ballistic blocks to interpret eruption sequence and dynamics: August 6 2012 Upper Te Maari eruption, New Zealand. Journal of Volcanology and Geothermal Research, 286, 373–386.

Brothelande E, Lénat J-F, Chaput M, Gailler L, Finizola A, Dumont S, Peltier A, Bachèlery P, Barde-Cabusson S, Byrdina S, Menny P, Colonge J, Douillet GA, Letort J, Letourneur L, Merle O, Di Gangi F, Nakedau D, Garaebiti E (2015). Structure and evolution of an active resurgent dome evidenced by geophysical investigations: The Yenkahe dome-Yasur volcano system (Siwi caldera, Vanuatu). Journal of Volcanology and Geothermal Research, 322, 241 – 262.

Brown SK, Jenkins SF, Sparks RSJ, Odbert H, Auker MR (2017). Volcanic fatalities database: analysis of volcanic threat with distance and victim classification. Journal of Applied Volcanology, 6, 15.

Chouet B, Hamisevicz N, McGetchin TR (1974). Photoballistics of volcanic jet activity at Stromboli, Italy. Journal of Geophysical Research, 79(32), 4961–4976. https://doi.org/10.1029/JB079i032p04961.

Deligne NI, Jolly GE, Taig T, Webb TH (2018). Evaluating life-safety risk for fieldwork on active volcanoes: the volcano life risk estimator (VoLREst), a volcano observatory's decision-support tool. Journal of Applied Volcanology 7, 7.

De Novellis V, Luongo G (2006). Chapter 5 ballistics shower during Plinian scenario at Vesuvius. In: Dobran F (ed) Vesuvius: Education, Security and Prosperity, Elsevier, 432p.

Druitt TH, Young SR, Baptie B, Bonadonna C, Calder ES, Clarke AB, Cole PD, Harford CL, Herd RA, Luckett R, Ryan G, Voight B (2002). Episodes of cyclic Vulcanian explosive activity with fountain collapse at Soufriere Hills Volcano, Montserrat. In: Druitt TH,

Kokelaar P (Eds). The eruption of Soufriere Hills Volcano, Montserrat, from 1995-1999. Geological Society of London, 645p.

Endo ET, Murray T (1991). Real-time seismic amplitude measurement (RSAM): a volcano monitoring and prediction tool. Bulletin of Volcanology, 53(7), 533-545.

Erfurt-Cooper P, Sigurdsson H, Lopes RMC (2015). Volcanoes and Tourism. In: Sigurdsson H (ed), The Encyclopedia of Volcanoes, Academic Press, 1295-1311.

Fagents S, Wilson L (1993). Explosive volcanic eruptions—VII. The ranges of pyroclasts ejected in transient volcanic explosions. Geophysical Journal International, 113, 359–370.

Firth CW, Handley HK, Cronin SJ, Turner SP (2014). The eruptive history and chemical stratigraphy of a post-caldera, steady-state volcano: Yasur, Vanuatu. Bulletin of Volcanology 76(7), 837.

Fitzgerald RH, Kennedy BM, Wilson TM, Leonard GS, Tsunematsu K and Keys H (2017). The communication and risk management of volcanic ballistic hazards. In: Fearnley C, Bird D, Jolly G, Haynes K and McGuire B (Eds) Observing the Volcano World: Volcano Crisis Communication, Advances in Volcanology, Springer International Publishing, ISBN 978-3-319-44095-8.

Fitzgerald RH, Tsunematsu K, Kennedy BM, Breard ECP, Lube G, Wilson TM, Jolly AD, Pawson J, Rosenberg MD, Cronin SJ (2014). The application of a calibrated 3D ballistic trajectory model to ballistic hazard assessments at Upper Te Maari, Tongariro. Journal of Volcanology and Geothermal Research, 286, 248–262.

Fudali R, Melson W (1972). Ejecta velocities, magma chamber pressure and kinetic energy associated with the 1968 eruption of Arenal volcano. Bulletin of Volcanology 35, 383 – 401

Gaudin D, Taddeucci J, Scarlato P, Moroni M, Freda C, Gaeta M, Palladino DM (2014). Pyroclast Tracking Velocimetry illuminates bomb ejection and explosion dynamics at Stromboli (Italy) and Yasur (Vanuatu) volcanoes. Journal of Geophysical Research: Solid Earth, 119, 5384 – 5397.

Global Volcanism Program (1995). Report on Yasur (Vanuatu). In: Wunderman R (ed.), Bulletin of the Global Volcanism Network, 20:8. Smithsonian Institution. https://doi.org/10.5479/si.GVP.BGVN199508-257100.

Global Volcanism Program (1999). Report on Yasur (Vanuatu). In: Wunderman R (ed.), Bulletin of the Global Volcanism Network, 24:7. Smithsonian Institution. https://doi.org/10.5479/si.GVP.BGVN199907-257100.

Global Volcanism Program (2001). Report on Masaya (Nicaragua). In: Wunderman R (ed.), Bulletin of the Global Volcanism Network, 26:4. Smithsonian Institution. https://doi.org/10.5479/si.GVP.BGVN200104-344100.

Gomez C (2014). Digital photogrammetry and GIS-based analysis of the biogeomorphological evolution of Sakurajima Volcano. Diachronic analysis from 1947 to 2006. Journal of Volcanology and Geothermal Research 280, 1-13.

Gomez C, Kennedy B (2017). Capturing volcanic plumes in 3D with UAV-based photogrammetry at Yasur Volcano – Vanuatu. Journal of Volcanology and Geothermal Research 350, 84-88.

Gomez C, Purdie H (2016). UAV- based Photogrammetry and Geocomputing for Hazards and Disaster Risk Monitoring – A Review. Geoenvironmental Disasters, 3, 23.

Gouhier M, Donnadieu F (2010). The geometry of Strombolian explosions: insights from Doppler radar measurements. Geophysical Journal International, 183(3), 1376–1391. https://doi.org/10.1111/j.1365-246X.2010.04829.x.

Gouhier M, Donnadieu F (2011). Systematic retrieval of ejecta velocities and gas fluxes at Etna volcano using L-Band Doppler radar. Bulletin of Volcanology, 73(9), 1139–1145. https://doi.org/10.1007/s00445-011-0500-1.

Gurioli L, Harris AJL, Colo L, Bernard J, Favalli M, Ripepe M, Andronico D (2013). Classification, landing distribution, and associated flight parameters for a bomb field emplaced during a single major explosion at Stromboli, Italy. Geology 41(5), 559–562.

Harris A, Ripepe M (2007). Temperature and dynamics of degassing at Stromboli, Journal of Geophysical Research, 112, B03205.

Harris AJL, Ripepe M, Hughes EA (2012). Detailed analysis of particle launch velocities, size distributions and gas densities during normal explosions at Stromboli. Journal of Volcanology and Geothermal Research, 231–232, 109–131. https://doi.org/10.1016/j.jvolgeores.2012.02.012.

Harvey MC, Rowland JV, Luketina KM (2016). Drone with thermal infrared camera provides high resolution georeferenced imagery of the Waikite geothermal area, New Zealand. Journal of Volcanology and Geothermal Research, 325, 61 – 69.

Houghton BF, Swanson DA, Carey RJ, Rausch J, Sutton AJ (2011). Pigeonholing pyroclasts: Insights from the 19 March 2008 explosive eruption of Kilauea volcano. Geology, 39(3), 263–266. https://doi.org/10.1130/G31509.1.

Jenkins SF, Spence RJS, Fonseca JFBD, Solidum RU, Wilson TM (2014). Volcanic risk assessment: Quantifying physical vulnerability in the built environment. Journal of Volcanology and Geothermal Research 276, 105–120.

Jolly AD, Matoza RS, Fee D, Kennedy BM, Iezzi AM, Fitzgerald RH, Austin AC, Johnson R (2017). Capturing the Acoustic Radiation Pattern of Strombolian Eruptions using Infrasound Sensors Aboard a Tethered Aerostat, Yasur Volcano, Vanuatu. Geophysical Research Letters, 44(19), 9672-9680.

Jolly GE, Keys HJR, Procter JN, Deligne NI (2014). Overview of the co-ordinated risk-based approach to science and management response and recovery for the 2012 eruptions of Tongariro volcano, New Zealand. Journal of Volcanology and Geothermal Research 286, 184–207.

Jordan BR (2015). A bird's-eye view of geology: The use of micro drones/UAVs in geologic fieldwork and education. GSA Today, 25(7), 50 – 52.

Kaneko T, Koyama T, Yasuda A, Takeo M, Yanagisawa T, Kajiwara K, Honda Y (2011). Low-altitude remote sensing of volcanoes using an unmanned autonomous helicopter: an

example of aeromagnetic observation at Izu-Oshima volcano, Japan. International Journal of Remote Sensing, 32(5), 1491-1504.

Kaneko T, Maeno F, Nakada S (2016). 2014 Mount Ontake eruption: characteristics of the phreatic eruption as inferred from aerial observations. Earth, Planets and Space 68, 72-82.

Kilgour G, Della Pasqua F, Hodgson KA, Jolly GE (2010). The 25 September 2007 eruption of Mount Ruapehu, New Zealand: Directed ballistics, surtseyan jets, and ice-slurry lahars. Journal of Volcanology and Geothermal Research 191(1-2), 1–14.

Kilgour G, Gates S, Kennedy BM, Farquhar A, McSporran A, Asher C (2019). Phreatic eruption dynamics derived from deposit analysis: A case study from a small, phreatic eruption from Whakāri/White Island, New Zealand. Earth Planets and Space, Accepted manuscript.

Kremers S, Lavallée Y, Hanson J, Hess K-U, Chevrel MO, Wassermann J, Dingwell DB (2012). Shallow magma-mingling-driven Strombolian eruptions at Mt. Yasur volcano, Vanuatu. Geophysical Research Letters, 39, L21304.

Kremers S, Wassermann J, Meier K, Pelties C, van Driel M, Vasseur J, Hort M (2013). Inverting the source mechanism of Strombolian explosions at Mt. Yasur, Vanuatu, using a multi-parameter dataset. Journal of Volcanology and Geothermal Research, 262, 104-122.

Le Pichon A, Blanc E, Drob D, Lambotte S, Dessa JX, Lardy M, Bani P, Vergniolle S (2005). Infrasound monitoring of volcanoes to probe high-altitude winds. Journal Geophysical Research, 110, D13106.

Lorenz V (1970). Some Aspects of the Eruption Mechanism of the Big Hole Maar, Central Oregon. Geological Society of America Bulletin 81, 1823-1830.

Marchetti E, Ripepe M, Delle Donne D, Genco R, Finizola A, Garaebiti E (2013). Blast waves from violent explosive activity at Yasur Volcano, Vanuatu. Geophysical Research Letters, 40, 5838-5843.

Mastin LG (1991). The roles of magma and groundwater in the phreatic eruptions at Inyo Craters, Long Valley Caldera, California. Bulletin of Volcanology, 53, 579–596.

McGonigle AJS, Aiuppa A, Giudice G, Tamburello G, Hodson AJ, Gurrieri S (2008). Unmanned aerial vehicle measurements of volcanic carbon dioxide fluxes. Geophysical Research Letters, 35, L06303.

Meier K, Hort M, Wassermann J, Garaebiti E (2015). Strombolian surface activity regimes at Yasur volcano, Vanuatu, as observed by Doppler radar, infrared camera and infrasound. Journal of Volcanology and Geothermal Research, 322, 184-195.

Merle O, Brothelande E, Lénat J-F, Bachèlery P, Garabéiti E (2013). A structural outline of the Yenkahe volcanic resurgent dome (Tanna Island, Vanuatu Arc, South Pacific). Journal of Volcanology and Geothermal Research, 268, 64–72.

Métrich N, Allard P, Aiuppa A, Bani P, Bertagnini A, Shinohara H, Parello F, Dimuro A, Garaebiti E, Belhadj O, Massare D (2011). Magma and volatile supply to post- collapse volcanism and block resurgence in Siwi caldera (Tanna island, Vanuatu arc). Journal of Petrology, 52, 1077–1105.

Minakami T (1942). 5. On the distribution of volcanic ejecta (Part I.): The distributions of volcanic bombs ejected by the recent explosions of Asama. Bulletin of Earthquake Research Institute, 20, 65 – 92.

Minakami T, Utibori S, Hiraga S (1969). The 1968 eruption of volcano Arenal, Costa Rica. Bulletin of the Earthquake Research Institute, Tokyo University, 47, 783–802.

Nabyl A, Dorel J, Lardy M (1997). A comparative study of low-frequency seismic signals recorded at Stromboli volcano, Italy, and at Yasur volcano, Vanuatu, New Zealand Journal of Geology and Geophysics, 40(4), 549-558.

Nairn IA, Self S (1978). Explosive eruptions and pyroclastic avalanches from Ngauruhoe in February 1975. Journal of Volcanology and Geothermal Research 3, 36–60.

Nakano T, Kamiya I, Tobita M, Iwahashi J, Nakajima H (2014). Landform monitoring in active volcano by UAV and SfM-MVS Technique. The International Archives of the Photogrammetry, Remote Sensing and Spatial Information Sciences, Volume XL-8.

Oppenheimer C, Bani P, Calkins JA, Burton MR, Sawyer GM (2006). Rapid FTIR sensing of volcanic gases released by Strombolian explosions at Yasur volcano, Vanuatu. Applied Physics B: Lasers and Optics, 85, 453-460.

Patterson MCL, Mulligan A, Douglas J, Robinson J, Wardell L (2005). Volcano Surveillance by ACR Silver Fox. American Institute of Aeronautics and Astronautics conference, 6954, DOI: 10.2514/6.2005-6954.

Pioli L, Erlund E, Johnson E, Cashman K, Wallace P, Rosi M, Delgado Granados H (2008). Explosive dynamics of violent Strombolian eruptions: The eruption of Parícutin Volcano 1943–1952 (Mexico). Earth and Planetary Science Letters 271, 359-368.

Pistolesi M, Rosi M, Pioli L, Renzulli A, Bertagnini A, Andronico D (2008). The paroxysmal event and its deposits. The Stromboli Volcano: An Integrated Study of the 2002 - 2003 Eruption. Geophysica, 317–330.

Ripepe M, Ciliberto S, Schiava D (2001). Time constraints for modeling source dynamics of volcanic explosions at Stromboli. Journal of Geophysical Research 106 (B5), 8713–8727.

Robertson R, Cole P, Sparks RSJ, Harford C, Lejeune AM, McGuire WJ, Miller AD, Murphy MD, Norton G, Stevens NF, Young SR (1998). The explosive eruption of Soufriere Hills Volcano, Montserrat, West Indies, 17 September, 1996. Geophysical Research Letters, 25(18), 3429–3432.

Self S, Kienle J, Huot J (1980). Ukinrek Maars, Alaska, II. Deposits and formation of the 1977 craters. Journal of Volcanology and Geothermal Research, 7, 39–65.

Shinohara H (2013). Composition of volcanic gases emitted during repeating Vulcanian eruption stage of Shinmoedake, Kirishima volcano, Japan. Earth Planets Space, 65, 667-675.

Spina L, Taddeucci J, Cannata A, Gresta S, Lodato L, Privitera E, Scarlato P, Gaeta M, Gaudin D, Palladino DM (2015). Explosive volcanic activity at Mt. Yasur: A characterization of the acoustic events (9–12th July 2011). Journal of Volcanology and Geothermal Research, 322, 175-183.

Steinberg GS (1974). On explosive caldera formation. Modern Geology, 5, 27–30.

Steinberg GS (1976). On the determination of the energy and depth of volcanic explosions. Bulletin of Volcanology, 40, 116–120.

Steinberg GS, Babenko JL (1978). Gas velocity and density determination by filming gas discharges. Journal of Volcanology and Geothermal Research 3, 89–98.

Stern CR, Moreno H, Lopez-Escobar L, Clavero JE, Lara LE, Naranjo JA, Parada MA, Skewes MA (2007). Chilean Volcanoes. In: Moreno T and Gibbons W (eds), The Geology of Chile. Geological Society of London, UK.

Swanson DA, Zolkos SP, Haravitch B (2012). Ballistic blocks around Kīlauea Caldera: Their vent locations and number of eruptions in the late 18th century. Journal of Volcanology and Geothermal Research, 231-232, 1-11.

Taddeucci J, Alatorre-Ibargüengoitia MA, Palladino DM, Scarlato P, Camaldo C (2015). High-speed imaging of Strombolian eruptions: Gas-pyroclast dynamics in initial volcanic jets. Geophysical Research Letters, 42, 6253–6260, DOI:10.1002/2015GL064874

Taddeucci J, Alatorre-Ibargüengoitia MA, Cruz-Vázquez O, Del Bello E, Scarlato P, Ricci T (2017). In-flight dynamics of volcanic ballistic projectiles. Reviews of Geophysics, 55(3), 675–718. https://doi.org/10.1002/2017RG000564.

Taddeucci J, Scarlato P, Capponi A, Del Bello E, Cimarelli C, Palladino DM, Kueppers U (2012). High-speed imaging of Strombolian explosions: The ejection velocity of pyroclasts. Geophysical Research Letters 39, L02301.

Thouret J-C, Lavigne F, Kelfoun K, Bronto S (2000). Toward a revised hazard assessment at Merapi volcano, Central Java. Journal of Volcanology and Geothermal Research, 100(1-4), 479–502.

Tsunematsu K, Ishimine Y, Kaneko T, Yoshimoto M, Fujii T, Yamaoka K (2016). Estimation of ballistic block landing energy during 2014 Mount Ontake eruption. Earth, Planets and Space, 68, 88.

Turner NR, Perroy RL, Hon K (2017). Lava flow hazard prediction and monitoring with UAS: a case study from the 2014–2015 Pāhoa lava flow crisis, Hawai‘i. Journal of Applied Volcanology, 6, 17.

Vanuatu Meteorology and Geohazards Department (2019). Yasur Visitor Fact Sheet. Retrieved February 12, 2019 from https://www.vmgd.gov.vu/vmgd/index.php/geohazards/volcano/volcano-info/resources.

Waitt RB, Mastin LG, Miller TP (1995). Ballistic showers during crater peak eruptions of Mount Spurr volcano, summer 1992. USGS Bulletin, 2139.

Wardman J, Sword-Daniels V, Stewart C, Wilson T (2012). Impact assessment of the May 2010 eruption of Pacaya volcano, Guatemala. GNS Science Report 2012/09, 90p.

Westoby M, Brasington J, Glasser NF, Hambrey MJ, Reynolds J (2012). ‘Structure from Motion’ photogrammetry: A low-cost effective tool for geoscience applications. Geomorphology 179, 300-314.

Williams GT, Kennedy BM, Wilson TM, Fitzgerald RH, Tsunematsu K, Teissier A (2017). Buildings vs. ballistics: Quantifying the vulnerability of buildings to volcanic ballistic impacts using field studies and pneumatic cannon experiments. Journal of Volcanology and Geothermal Research 343, 171-180.

Yamagishi H, Feebrey C (1994). Ballistic ejecta from the 1988–1989 andesitic Vulcanian eruptions of Tokachidake volcano, Japan: morphological features and genesis. Journal of Volcanology and Geothermal Research, 59(4), 269–278.

Preamble (Chapter 4)

Chapter 3 described the spatial and temporal distribution of ballistics from Yasur Volcano, Vanuatu. Chapter 4 builds on Chapters 2 and 3 by investigating the hazard footprint from an individual ballistic and the hazard intensity within this area. Understanding the hazard intensity within the ballistic field and also within the individual ballistic hazard footprint allows for more precise assessment of exposure and vulnerability, and thus more effective risk management decisions. Findings from this chapter suggest that ballistic size, crater size, ejecta apron size, impact angle, ballistic kinetic energy, ballistic density and surface hardness can all influence the size of the individual ballistic hazard footprint. A pneumatic cannon is used to assess the kinetic energy (the hazard intensity metric) and travel distance from ejecta produced on impact from ballistics of different densities fired at different strength surfaces.

Chapter 4 is to be submitted to the Journal of Applied Volcanology.

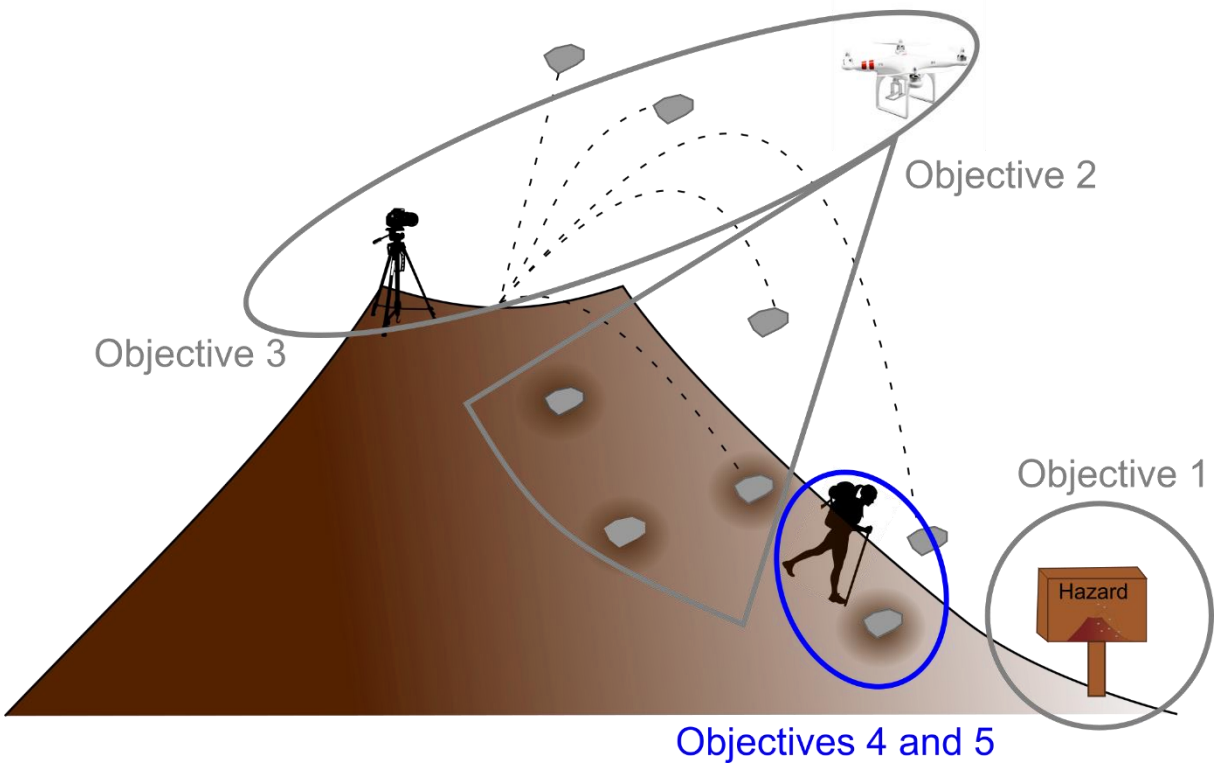

Conceptual diagram showing the objectives of the thesis with the objectives addressed in Chapter 4 in blue.

Chapter Four – Using pneumatic cannon experiments to understand ballistic hazard footprints

4.1. Abstract

Ballistic projectiles from explosive volcanic eruptions can have sufficient kinetic energy to cause injury or death to exposed people. An increasing number of visitors to volcanoes and an increasing global population means increased exposure to volcanic hazards. This has driven the need for a more complete understanding of volcanic ballistic phenomena, the hazard they pose, human vulnerability, and risk management strategies. Previous volcanic ballistic research has focused predominantly on spatial distribution, formation and transport mechanisms, complemented by records of the injuries that ballistics can inflict. But an important knowledge gap is the hazard footprint from an individual ballistic impact – what aspects contribute to it and its size, and the quantification of injury severity with respect to ballistic kinetic energy. In this study we review the variables that influence the hazard footprint and the literature on kinetic energy thresholds for injury and death from this and other hazards. We then focus on the contribution of impact ejecta on the hazard footprint using a pneumatic cannon to fire volcanic rocks towards a range of substrates and recording the tests with a high-speed camera. We found that ballistic impacts can produce ejecta with enough kinetic energy to injure, implying hazard footprint estimates should be substantially larger than ballistic diameter. More porous ballistics (1.43 and 2.13 g/cm^3) were more likely to produce ejecta from fragmentation than higher density ballistics (2.89 g/cm^3) and harder, more cohesive substrates produced higher kinetic energy/velocity ejecta than looser substrates. From the injury data we propose energy thresholds for minor and serious injury and death. The thresholds were then applied to two ejecta scenarios and each hazard footprint zoned by damage state to understand how the hazard intensity and injury severity changed with distance from impact. Our experiments improve our understanding of the hazard to people on volcanoes from ballistics and provide important data to inform risk assessments and mitigation measures in areas exposed to ballistic hazard.

4.2. Introduction

Ballistics, fragments of molten lava or solid rock ejected from explosive volcanic eruptions, can travel up to hundreds of metres per second and range between centimetres to tens of metres in diameter. They can have sufficient kinetic energy to cause injury or death to exposed people (e.g. Baxter and Gresham 1997; Shiroko 2016). Increasing visitor numbers to volcanoes, recent fatal ballistic incidents, and an increasing global need for disaster risk reduction is driving the need for a more complete understanding of the spatial and temporal distribution and intensity of ballistic hazard, what societal elements (e.g. people) may be exposed to the hazard, and how vulnerable those elements are to the hazard to enable more robust assessment of risk (Fitzgerald et al. 2017).

Research has been focused on improving understanding of extent and frequency of ballistic hazard (e.g. Alatorre-Ibargüengoitia et al. 2012, 2016; Gurioli et al. 2013; Fitzgerald et al. 2019). However, little work has been undertaken on the individual ballistic hazard footprint, consequences from ballistics and how this is linked to hazard intensity (e.g. kinetic energy of the ballistic). Field observations have shown that factors that can influence the hazard footprint include volcano slope, substrate hardness, and ejecta from the substrate or ballistic (Pistolesi et al. 2008; Maeno et al. 2013; Taddeucci et al. 2017). For example, a ballistic impacting a hard surface may break, ejecting shrapnel metres away, therefore increasing the area affected by hazard. Whereas an impact onto a softer surface may not cause the ballistic to break and as such the hazard footprint would be smaller as there is no shrapnel produced (Rosi et al. 2006; Pistolesi et al. 2008; Taddeucci et al. 2017). A number of studies have considerably improved our understanding of building vulnerability to ballistics (Blong 1984; Pomonis et al. 1999; Jenkins et al. 2014; Biass et al. 2016; Williams et al. 2017/Appendix D), yet there is a lack of equivalent attention to human vulnerability. Three studies have included human vulnerability in their ballistic assessments (Jolly et al. 2014; Deligne et al. 2018; Fitzgerald et al. 2014), but only consider block size, crater size and impact angle as factors that can influence the hazard footprint (the area the hazard affects), and do not link the intensity of the hazard to the intensity of the consequence. Rather they take a simple precautionary approach assuming only direct interaction with the ballistic and crater, and that any interaction will cause casualty (therefore considered a binary hazard). These assumptions are made with no investigation into the intensity of the hazard (kinetic energies of the ballistic and ejecta) at which these might occur.

Improved understanding of the hazard footprint, hazard intensity within the footprint, and injury severity will allow for more accurate vulnerability and risk assessments to be completed and more effective risk management strategies applied.

We present an overview of the factors that may influence the ballistic hazard footprint and the range of injuries that can occur. We use experimental data and a trajectory model to investigate the impact energies and travel distances of ballistic impact ejecta and their contributions to the hazard footprint. Using the collected injury data, we create damage states, hazard intensity metrics and fragility functions, and apply these to our experimental data to understand how hazard intensity and injury severity changes with distance.

4.2.1. Hazard footprint

One of the fundamental elements of natural hazard risk assessment is defining the spatial (and often temporal) domain that will be affected by the hazard (Smith 2013) – the hazard footprint. When a measure of hazard intensity (HIM) (e.g. thickness of tephra fall, density of ballistics, etc) is distributed across the hazard footprint then the potential consequences of the hazard may be analysed when combined with exposed elements and their associated vulnerability characteristics.

Jolly et al. (2014) estimated a hazard footprint that assumes fatality of $7m^2$ per ballistic impact from the August 2012 eruption of Upper Te Maari, Tongariro, New Zealand. This was based on the diameter of a person, the size of the ballistic, and a direct impact from vertical. Deligne et al. (2018) took a similar approach, though included an option for a side impact (a lower impact angle) in VoLREst (used by GNS Science to assess life safety for staff conducting fieldwork on active volcanoes). Instead of fatality, Fitzgerald et al. (2014) estimated the likelihood of casualty (injury or death) from the 2012 eruptions of Upper Te Maari, Tongariro and two eruption scenarios. They used the crater diameter and the block diameter, the diameter of a person and the impact angle/flight path in their hazard footprint and vulnerability calculations. They also placed the person outside of the crater in their model to allow for vulnerability to ejecta. However, a number of factors have been identified as potentially influencing the risk to humans from ballistic hazards, including: ballistic kinetic energy (a

function of ballistic mass and velocity), ballistic size, crater size, ejecta apron size, ejecta velocity, impact angle, slope, substrate hardness, and ballistic lithology/density (Figure 4.1). In the following sections we review relationships found in the literature for each variable to help refine models for estimating ballistic hazard footprint.

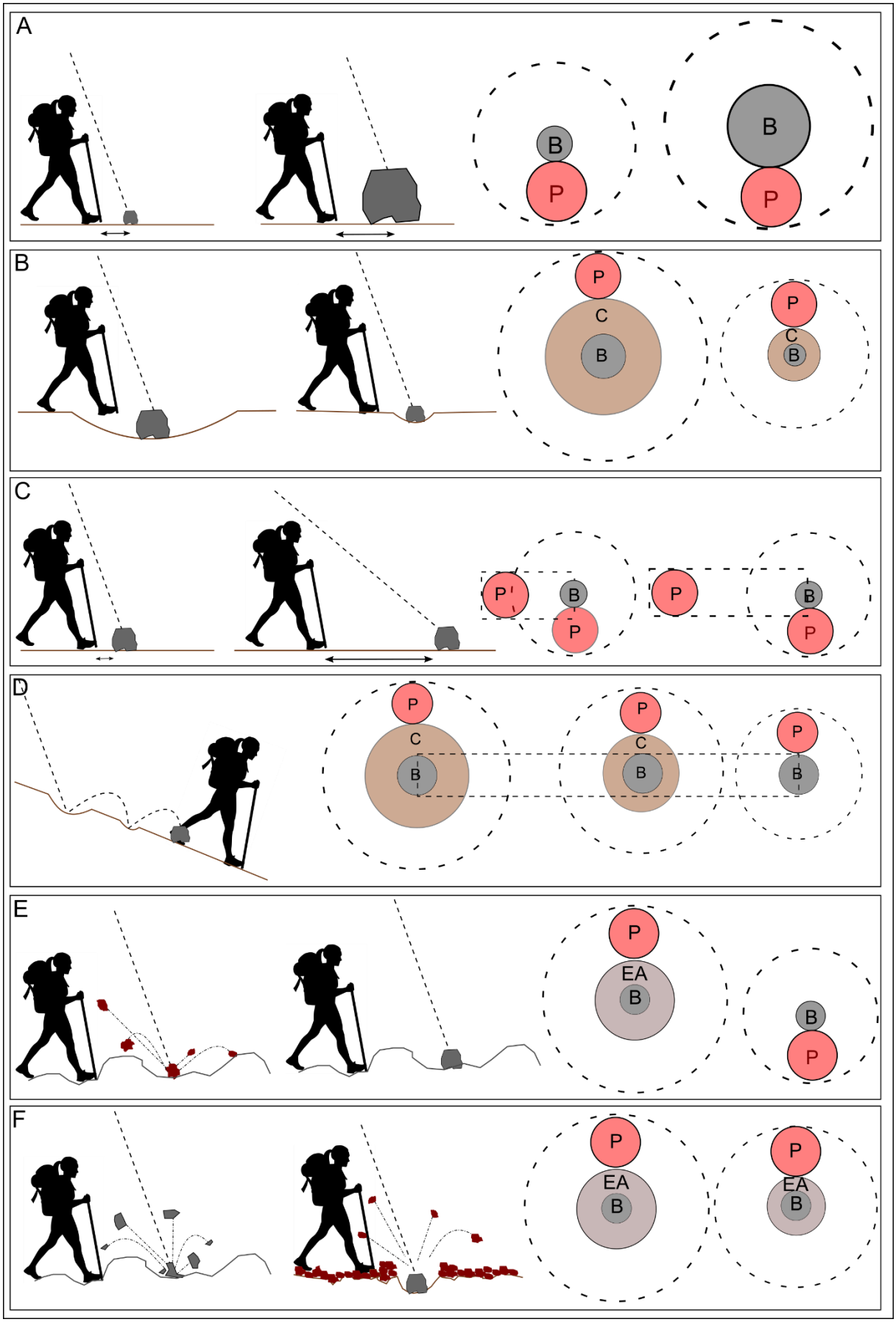
A
B
P
B
P
B
P
C
B
P
C
B
C
P
B
P
P
B
P
D
P
C
B
P
C
B
P
B
E
P
EA
B
B
P
F
P
EA
B
P
EA
B

Figure 4.1 Ballistic hazard footprint size is influenced by many factors. A) Ballistic size, B) Crater size, C) Impact angle, D) Slope, E) Ballistic density/lithology, F) Substrate hardness. Initials: P= person, C= crater, B= ballistic, EA= ejecta apron

4.2.1.1. Kinetic energy of the ballistic

The ballistic itself is the main hazard, capable of killing or injuring a person by direct impact (Baxter and Gresham 1997; Shiroko 2016) depending on the kinetic energy of the ballistic. A faster and larger/heavier ballistic will do more damage than a slower and smaller/lighter ballistic. Ballistics can range in size from several centimetres to tens of metres in diameter (Table 4.1). Jolly et al. (2014) and Deligne et al. (2018) use ballistic size in their vulnerability calculations, applying values of 1 m and 20 cm respectively. The amount of kinetic energy also influences whether a crater is formed and its size (Dufresne et al. 2013), as well as the size and velocity of impact crater ejecta (Hartmann 1985). Kinetic energy (*KE*) is the product of the mass (*m*) and velocity (*v*) of the ballistic, expressed as:

$$KE = \frac{1}{2}mv^2 \quad (1)$$

Many studies report measured or modelled initial ballistic velocities (Minakami 1942; Gouhier and Donnadieu 2011; Harris et al. 2012; Taddeucci et al. 2012) but very few state impact velocities. Using trajectory modelling Maeno et al. (2013) found impact velocities of 120 – 160 m/s for two large blocks 1 – 3 tonnes in size. Taddeucci et al. (2017) reported impact velocities of 10 – 30 m/s with kinetic energies of 10^2 – 10^5 J. Tsunematsu et al. (2016) model the ballistics ejected in the 2014 eruption of Mt Ontake, Japan. They found mean impact velocities of 83 – 85 m/s and mean landing energies of 10^4 J.

Table 4.1 Measurements of ballistic diameters from various eruptions and volcanoes around the world

Ballistic diameter	Volcano	Reference
Average of three axes 0.2-0.6m	Popocatepetl, Mexico	Alatorre-Ibargüengoitia et al. 2012
Average of three axes 0.12-0.26m	El Chichon, Mexico	Alatorre-Ibargüengoitia et al. 2016
0.15 – 0.20 m	Mt Etna, Italy	Andronico et al. 2015
0.07 – 4.59 m	Stromboli, Italy	Gurioli et al. 2013

0.08 – 2 m	Mt Spurr, USA	Waitt et al. 1992
0.2 – 20 m	Tokachidake, Japan	Yamagishi and Feebrey 1994
Maximum 20 m	Ngauruhoe, New Zealand	Nairn and Self 1978
Median 0.1 – 0.3 m. Largest 1m	Mt Etna	McGetchin et al. 1974
0.05 – 3.04 m	Yasur, Vanuatu	Chapter 3
0.25 – 2.01 m	Kilauea, USA	Swanson et al. 2012
0.1 – 1 m	Mt Ontake, Japan	Kaneko et al. 2016
2 – 25 m	Ukinrek Maars, USA	Self et al. 1980
0.1 – 1 m	Stromboli, Italy	Pistolesi et al. 2008

4.2.1.2. Ballistic size, crater size and the relationship between the two

Ballistic size affects the width of the flight path (trajectory prior to impact that poses a hazard to a person) (Figure 4.1A). In this way, a larger diameter ballistic creates a larger area where a person could be impacted, as well as a larger proportion of the person's body which could be impacted, likely causing greater injury than a smaller ballistic.

Ballistic size also has a considerable influence on crater size. For any given impact velocity, a larger size ballistic will generally have more mass and thus impact with more kinetic energy creating a larger crater (Figure 4.1B). Field measurements of ballistic craters range from tens of centimetres to tens of metres in size. Kaneko et al. (2016) and Swanson et al. (2012) reported craters of tens of centimetres to 1 m at Mt Ontake and 3 – 4 m at Kilauea, respectively. On the larger end, Fudali and Melson (1972) measured craters up to 30 m in diameter at Arenal Volcano, Costa Rica and Self et al. (1980) measured craters up to 25 m at Ukinrek Maars. Fitzgerald et al. (2014) used an average crater size of 1.2 m at Upper Te Maari in their hazard footprint.

On the occasion that only ballistic diameter or crater diameter is known, it may be possible to use a scaling relationship to calculate the unknown variable to use in hazard and vulnerability calculations. Alatorre-Ibargüengoitia et al. (2012) found that impact craters at Popocatepetl were on average 4 – 5 times the diameter of the corresponding ballistics. This relationship was found to be greater (1:10) by Breard et al. (2014) at Upper Te Maari due to soft substrates. Experimental work by Uehara et al. (2003) concluded that crater diameter scales at ¼ power of the energy of the projectile at impact in loose granular substrates.

Despite creating a large physical change to the surface, it is unclear whether crater formation would harm a person within the cratering area (i.e. by shockwave). It may be that the ejecta is the hazard and therefore the ejecta apron size, not crater size, needs to be considered in the hazard footprint.

4.2.1.3. Ejecta travel distance

On impact with the ground, a ballistic may eject material either from fragmentation of the ballistic (shrapnel) or from excavation of the ground/crater formation (debris) (Figure 4.2). It is possible that material may be ejected with sufficient kinetic energy or thermal energy to cause injury or death. The distance that ejecta travels can therefore define the hazard footprint beyond the impact crater. Two to four rays of ejecta extending up to 5 m surrounded craters larger than 3 m formed in the 1992 Mt Spurr eruption (Waitt et al. 1992). Ballistics with impact velocities of 10 – 30 m/s and kinetic energies of 102 – 105 J were found by Taddeucci et al. (2017) to fragment and travel in excess of 5 m from the impact. Following the 5 April 2003 eruption of Stromboli, Pistolesi et al. (2008) and Rosi et al. (2006) noted ballistic impacts ejected material up to tens of metres from the impact. Similar distances were recorded at Shinmoedake Volcano after the 2011 eruption. Maeno et al. (2013) found two impact craters 7 m in diameter that ejected soil debris and lava fragments up to 15 m and 28 m from the crater. Even greater distances were reached in the 1974-75 eruption of Ngauruhoe, New Zealand. Nairn and Self (1978) found many impact craters near walking tracks ~ 2 – 3 km from the crater were surrounded by rays of ejecta that reached up to 100 m from the crater.

Figure 4.2 Bomb impact at Yasur Volcano, Vanuatu that produced an impact crater and debris rays (darker material)

Relationships between the size of the ejecta apron and crater size have been found by Fitzgerald et al. (2014) and Gault and Greeley (1978). Ejecta aprons measured following the August 2012 Upper Te Maari eruption were on average 110% greater in diameter than the crater diameter (Fitzgerald et al. 2014). The mechanism has also been observed in planetary impact studies. Analysis of Martian impact craters by Gault and Greeley (1978) found ejecta deposits up to two crater diameters away from the crater rim. However, care must be taken when applying the planetary results to volcanic examples as they are hypervelocity impacts and occur in much lower gravity. The reports mentioned above illustrate that ejecta travel distance is an understudied but important dimension of a ballistic hazard footprint.

4.2.1.4. Ejecta velocity

The velocity at which material is ejected is also an important variable in the hazard footprint. If ejecta are not travelling fast enough to cause injury, then the entire travel distance does not need to be included in the footprint, e.g. ejecta may have fast enough velocity over the first metre but slow down past this distance so that the rest of its travel distance is not relevant in the footprint. Only studies on extra-terrestrial impacts could be found with ejecta velocities. Experiments in these publications were done in near-vacuum or vacuum conditions at very high speed. Hartmann (1985) describe increasing ejecta velocities with increasing impact energy and

crater size from near-vacuum experiments. Holsapple et al. (2002) reported on experiments of high-speed impacts onto rock targets and found that ejecta velocities were typically between 0.1 and 0.5% of the impactor velocity. They also found that fine dust is usually the fastest ejecta produced near the impact, travelling an order of magnitude faster than larger ejecta. Results reported by Hartmann (1985) contradict this finding. In near-vacuum experiments finer powder targets ejected particles with lower velocities than coarser powder targets. Oberbeck (1975) and Braslau (1970) conclude that ejecta launched later in the cratering process is slower than ejecta launched earlier in the process. Braslau (1970) recorded ejecta velocities of ~4000 m/s in the early stages reducing to a few metres per second in the late stages of cratering. Air densities and velocities used in these experiments would likely influence the applicability of these results to a terrestrial volcano.

4.2.1.5. Impact angle

The impact angle of a ballistic can increase the hazard footprint, as illustrated in Figure 4.1C, because the flight path distance below the height of a person is longer with lower impact angles. It is therefore important to use the impact angle to calculate the length of this critical flight path. Fitzgerald et al. (2014) found the average impact angle of blocks from the August 2012 eruption of Upper Te Maari to be 59°. Similarly, Maeno et al. (2013) found impact angles of 50 - 60° from broken trees at two craters from the 2011 eruption of Shinmoedake; and Minakami (1942) reported 57 – 61° impact angles from the 16 April 1937 and 7 June 1938 eruptions at Asama.
The impact angle can also change the size and shape of the crater and ejecta apron. Hypervelocity impacts with impact angles between 0 - 30° produced elongated craters in experiments performed by Gault and Wedekind (1978). At angles < 70°, Manga et al. (2012) reported projectiles did not remain in their impact crater in low velocity experiments, bouncing out and becoming hazardous again. Pierazzo and Melosh (2000) found that decreasing impact angles below 45° produced asymmetric ejecta aprons. Butterfly wing patterns of ejecta were also noted in very oblique impacts (< 5°) where ejecta is distributed perpendicular to the path of the projectile rather than up or down range.

4.2.1.6. Slope

Similarly to the impact angle, the slope angle of the plane that the ballistic impacts can cause bouncing or rolling of the ballistic outside of its crater or original landing position (Figure 4.1D). Bouncing, rolling and sliding post-impact has been observed on Tungurahua (Bernard 2018), on the north-western slope of Ngauruhoe in 1948 eruption (Allen 1948/Hobden et al. 2002), at Kilauea (Swanson et al. 2012), and at Stromboli, Etna, Fuego, Yasur, Batu Tara and Sakurajima (Taddeucci et al. 2017). Steinberg and Lorenz (1983) observed bouncing and landing outside impact craters on steep slopes > 15 - 20° at Alaid Volcano following the 1972 eruption. Rolling was noted at Etna on slopes between 31° and 38° (McGetchin et al. 1974). Blocks ejected in the 5th April 2003 eruption of Stromboli slipped downslope for tens of metres when impacting soft soil or vegetation (Pistolesi et al. 2008). Rosi et al. (2006) report that a large block from the same eruption slid downslope and created an elongated 18 x 8 m crater. Gault and Wedekind (1978) concluded from hypervelocity experiments that a specific critical angle of impact for causing ricochet (bouncing) did not exist as it depended on multiple variables. Slope can also lower impact angles, increasing the flight path, as well as creating elongated craters and ejecta aprons, and subsequently changing the hazard footprint. Breard et al. (2014) concluded that slope had an important influence on crater elongation by decreasing or increasing the local impact angle of the ballistic to the surface, with 30% of craters on the stoss side of ridges at Upper Te Maari and 70% on the lee side elongated. Asymmetric aprons were also noted by Krohn et al. (2014) on an asteroid (Vesta). Ejected material was prevented from depositing uphill on slopes > 20°.

4.2.1.7. Substrate effects on impacts

Substrate strength can influence the size of the hazard footprint (Figure 4.1F). Impacts into harder substrates are more likely to result in fragmentation of the ballistic, producing shrapnel but less likely to create craters or produce debris. Rosi et al. (2006) and Taddeucci et al. (2017) have observed ballistics impacting hard substrates, such as lava flows, and shattering. While ballistics impacting soft substrates such as vegetation have been observed to stay intact (Andronico et al. 2015; Pistolesi et al. 2008). Manga et al. (2012) found water saturation of the substrate also influenced crater size and the amount of material ejected from the crater. Less material was ejected in experiments on water saturated sand and a shallower crater produced

compared to dry sand. Cintala et al. (1977) also found that substrate affected crater morphology and size, analysing extra-terrestrial impact craters.

Impacts into harder substrates can also produce faster ejecta than that from softer substrates. Experiments performed by Michikami et al. (2001) found that as porosity increased in their targets, ejecta velocity decreased. They found that velocities were more than two magnitudes lower from glass bead targets of 60-80% than rock targets.

4.2.1.8. Ballistic density/strength

The density or lithology of the ballistic can change crater depth, as this reduces the relative mass and energy of the impactor. Shallower craters were recorded from lower density impactors in hypervelocity experiments by Dufresne et al. (2013). Additionally, lower density ballistics are more likely to shatter on impact than higher density ballistics (Figure 4.1E). Yamagishi and Feebrey (1994) observed that most vesiculated bombs broke on impact with the ground. Ductile bombs, which can continue to vesiculate during flight and are usually associated with low densities, have also been observed to tear and break on impact, producing ejecta (Kimura 2016; Taddeucci et al. 2017).

4.2.2. Human vulnerability to ballistic hazards

Contemporary risk-to-life ballistic risk assessments consider human vulnerability in a relatively simple manner as a binary hazard, with the lack of clear empirical evidence necessitating a precautionary approach (Fitzgerald et al. 2014; Jolly et al. 2014; Deligne et al. 2018). Specifically, none of the three approaches relate kinetic energy (hazard intensity) to the potential consequences to people. So as our understanding of ballistic phenomena and hazard assessment technique improve (as outlined above and in earlier components of the thesis), there is now a growing need to better constrain and consider vulnerability within risk assessment approaches. In particular, the knowledge gaps of insufficient (if any) human fragility to ballistic impacts and the potential hazard footprint of ballistics. This necessitated a wider search for human vulnerability estimates from other similar hazards. Three risk assessments of landslides, rockfall and large clast fallout were found that included human vulnerability to projectile

hazards. Finlay et al. (1988) attribute a probability of 0.5 to a person being struck by rockfall and it causing death based on fatalities from landslides in Hong Kong. Massey et al. (2012) combine the probability given by Finlay et al. (1988) and research on the rockfalls generated in the 22 February 2011 'Christchurch' earthquake in New Zealand to also use a probability of 0.5 for a person being hit by rockfall causing death. Neither of these studies provided kinetic energy estimates, simply assuming any interaction with a ballistics will cause harm. In a risk assessment of the fallout of large clasts from an eruption at Mt Etna, Osman et al. (2019) modelled the kinetic energy of 5 cm clasts on impact. Energies ranged from 6 – 46 J and thus they defined this size of clast as hazardous, supported by a medical study that showed skull fracture could occur at approximately 28 J (Yoganandan et al. 1995). This was the only assessment that could be found that provided kinetic energy thresholds for consequences.

Before we apply kinetic energy thresholds to consequences of ballistic impacts, we must explore the range of consequences that could and have occurred. Impact from ballistics have caused 367 fatalities globally and many more injuries, from a range of eruption sizes (VEI 1 – 4) (Brown et al. 2017). They are the most common cause of fatality for both tourists and scientists on volcanoes (Brown et al. 2017). In-depth analysis of causes and types of injury from two incidents with fatalities and casualties have been conducted by Baxter and Gresham (1997) and Shiroko (2016). Five people were killed by ballistics in the 1993 eruption of Galeras, Colombia. Baxter and Gresham (1997) reported that most fatalities were due to impacts to the head causing destruction of the skull, exposure of the brain and brain injuries. However, spinal and internal rupture injuries from being thrown forward on impact, full thickness burns from contact with hot ballistics, and severing of the upper and lower body by a large ballistic were also noted. Survivors suffered from burns, fractures of the skull, leg and hand, sprains, concussion, contusions and lacerations. Shiroko (2016) reported ballistic injuries from three survivors of the 2014 Mt Ontake, Japan eruption. Injuries included fractures of the shoulder, ribs, upper arm and thumb, extensive contusions, and burns. The severity of bone destruction in one case is compared to that seen in gunshot victims or blast injuries seen in war.

To assess whether and what aspects of ballistic impact could cause injury or death it is important to know the kinetic energy thresholds responsible for each. Two reports of contrasting outcomes highlight the importance of using kinetic energy as a hazard intensity metric rather than solely

size, mass or velocity. Fragments 9 cm in diameter caused no discomfort on impact in the 1973 Eldjfell eruption, though fibreglass helmets and padded clothing were worn (Booth 1979). However, scoria fragments less than 8 cm in diameter caused severe scalp lacerations in the 1974 eruption of Etna, and 5cm dense fragments from an eruption at Etna in 1971 penetrated a fibreglass helmet left outside overnight (Booth 1979).

Studies of blunt force trauma and penetration wounds (e.g. gunshot) have based their evaluation of potential injury on this equation while others have used kinetic energy density which additionally considers the size of the impactor. Larger objects have a greater surface area to transfer energy which means that the kinetic energy from the impactor is spread over a larger area. Whereas a smaller impactor has less area to do this and thus the kinetic energy is more concentrated. Energy density is calculated using:

$$e = \frac{KE}{A} = \frac{2mv^2}{\pi d^2} \quad (2)$$

Where *A* is the impactor area, calculated using the diameter *d* of the impactor. Results are given as J/cm^2. Others (Lyon et al. 1999; Sturdivan et al. 2004; Raymond et al. 2009; Radi 2013) have used the blunt criterion (BC) model which considers the ability of the body to tolerate/absorb the impact by including the target mass *M* and the thickness of the body wall of the target *T:*

$$BC = ln\left[\frac{\frac{1}{2}mv^2}{M^{1/3}Td}\right] \quad (3)$$

The BC model is typically plotted against the Abbreviated Injury Scale (AIS) created by the American Association of Automotive Medicine to assess the relative severity of motor vehicle related injury (Petrucelli et al. 1981). It scales injury severity from minor (1) to maximum (6) and allocates a probability of fatality to each level. AIS 1 is a minor injury with a probability of death of 0%, AIS 6 is a maximum injury with a probability of 100%. Anything above AIS 3 is considered life threatening (Radi 2013).

Baxter and Gresham (1997) report the threshold for fatality as 80 J. Radi (2013) estimate a similar value for skull fracture (76 J or 1.6 J/cm^2) from a ≥30 cm impactor but attribute a probability of fatality to <10% (AIS 3). Skull fracture occurred at lower KE (28 J and 19.6 - 63.8 J respectively) in biomechanical experiments performed by Yoganandan et al. (1995) and Raymond et al. (2009). Smedra-Kazmirska et al. (2013) found pellets < 1 cm length fired at 13 J at 1 m distance from the cadaver can cause lung and heart membrane, liver, spleen, kidney, femoral artery and aorta injuries. They found the minimum initial KE from an airgun pellet that can result in lung or liver injury is 1.7 J when fired from 1 m. The KE required to cause bruising onto the lower leg was found to by 6.5 J from a 6 cm impactor by Desmoulin and Anderson (2011), with an energy density of 3.8 J/cm^2. Skin penetration or laceration thresholds have also been investigated. At 23.99 J/cm^2 the probability of skin penetration on the torso is 50%, with the required energy density increasing to 33.3 J/cm^2 in areas without underlying bone (Bir et al. 2012). Di Maio et al. (1982) found a lower energy density threshold of 12.8 - 18.9 J/cm^2 when testing with lead air gun pellets, depending on the size of the pellet used. Koene and Papy (2011) report skin penetration can occur at > 10 J/cm^2. This is also supported by Warlow et al. (2005) who found penetration occurred at 9.7 J/cm^2. Lacerations occurred in 67% of the tests performed by Whittle et al. (2008) at 9.02 J. Eye injuries occur at much lower thresholds than other parts of the body. There is a 50% probability of corneal abrasion occurring at 0.184 J, retinal damage at 1.09 J, and globe rupture at 4 J (Duma 2005). In energy density thresholds, Sellier and Kneubuehl (1994) report 6J/cm^2 needed for cornea perforation, and Koene and Papy (2011) report irreversible eye damage occurring at 2.5 J/cm^2. These reports present a wide range of injuries with different kinetic energy thresholds, enforcing the need for better vulnerability assessment.

The hazard footprint from an individual ballistic and the hazard intensity within it can be influenced by a variety of factors. These include crater size, ballistic size, ballistic kinetic energy, impact angle, slope, ballistic density, substrate hardness, ejecta travel distance and ejecta velocity. We now focus on ballistic kinetic energy, ballistic density, substrate hardness, ejecta travel distance and ejecta velocity which are suitable to investigate using the University of Canterbury's pneumatic cannon.

4.3. Methodology

4.3.1. Cannon experiments

A pneumatic cannon was used to conduct impact ejecta experiments (Figure 4.3). Compressed air is used to build pressure in the barrel and release the trigger, allowing the piston to push the attached rock toward the ground. Only vertical tests could be completed due to the cannon being fixed to shipping containers in a vertical position. A container filled with different substrates was placed directly beneath the cannon. Each test was recorded by a Sony DSLR camera at 1000 fps oriented perpendicular to the container, and three GoPro Hero 3+ and 4 cameras looking down onto the filled container, and across areas where ejecta would travel.

In total 48 tests were completed, 24 onto a 1600 x 700 mm circular container filled with crusher dust (silt to pebble pieces of greywacke) to simulate ash and lapilli substrate, and 24 onto a 1400 x 500 mm container filled with large basalt boulders to simulate lava flows and ballistics (Figure 4.3B). To keep substrate strength as constant as possible, the crusher dust was dug up after each test, recompacted and its strength measured twice using a Dynamic Cone Penetrometer (DCP).

The ballistics used in these tests (Figure 4.3E, F and G) were dense basalt (~2.8 g/cm^3), vesicular basalt (~2.13 g/cm^3) and scoria (~1.43 g/cm^3). All ballistics used measured between 15 and 19 cm on their longest axis and each was weighed prior to testing. The dense and vesicular basalt ballistics were subrounded due to the coastal location we collected them from. The scoria was subangular to subrounded. To test the ballistic lithology, three tests of each lithology at 4 bar were conducted onto both substrates.

In addition to substrate and lithology/density, velocity of the block was also varied, controlled by the pre-firing pressure reached in the barrel. Three tests at each pressure (1, 2, 3, 4, 5, and 6 bar) were completed using the dense basalt blocks onto each substrate (18 tests for each).

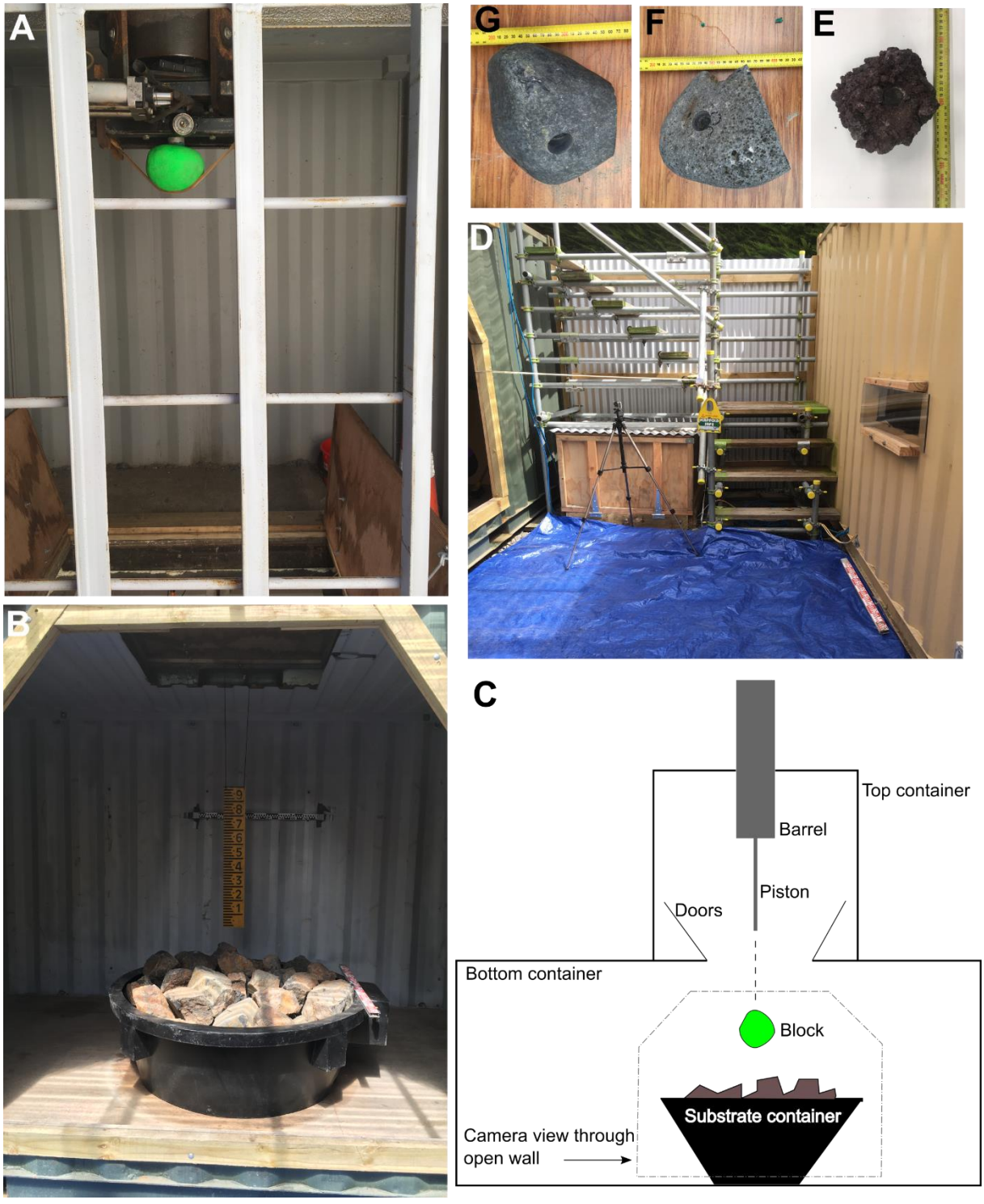

Figure 4.3 Pneumatic cannon setup. Anticlockwise from top left: A) Barrel and piston with ballistic attached, B) Substrate container holding basalt boulders, C) Profile view of cannon containers with top container holding the barrel and piston and the bottom container holding the substrate container and deposition area, D) Area between cannon containers and control container with window for high-speed camera, laid with a tarpaulin to identify ejecta deposition, E) Scoria used as a ballistic, F) Vesicular basalt used as a ballistic, drilled partially to attach to piston, F) Dense basalt used as a ballistic, drilled partially to attach to piston

The maximum travel distance of the ejecta was recorded immediately after each test. Travel distance was, however, limited by the shipping container walls providing us with only a minimum travel distance for most tests. Additionally recorded was the size of the ejecta that travelled the maximum distance, the largest fragment ejected from the impact and its distance from impact, whether ejecta was from the substrate or the ballistic (ballistics were painted a bright colour in each of the basalt substrate tests), and the state of the ballistic post impact (e.g. whether it was intact, had shattered, left the substrate container).

4.3.2. Video analysis

High-speed videos were converted into stills of each frame using FFmpeg and imported into ImageJ. Some videos were too dark, and, in these instances, stills were imported into FastStone and the gamma changed to brighten the images and then imported into ImageJ. MtrackJ, an ImageJ plugin, was used to calculate velocity of the ejecta in each test. Five of the fastest moving particles (~1 cm in length) were tracked in each test along with one large fragment if present (from either the ballistic or the basalt substrate). Only those travelling perpendicular to the camera (i.e. left or right) were tracked to minimise error in velocity estimates due to the effects of tracking in 2D (Figure 4.4). Once velocity was calculated, kinetic energy was calculated for both the ballistic and the ejecta.

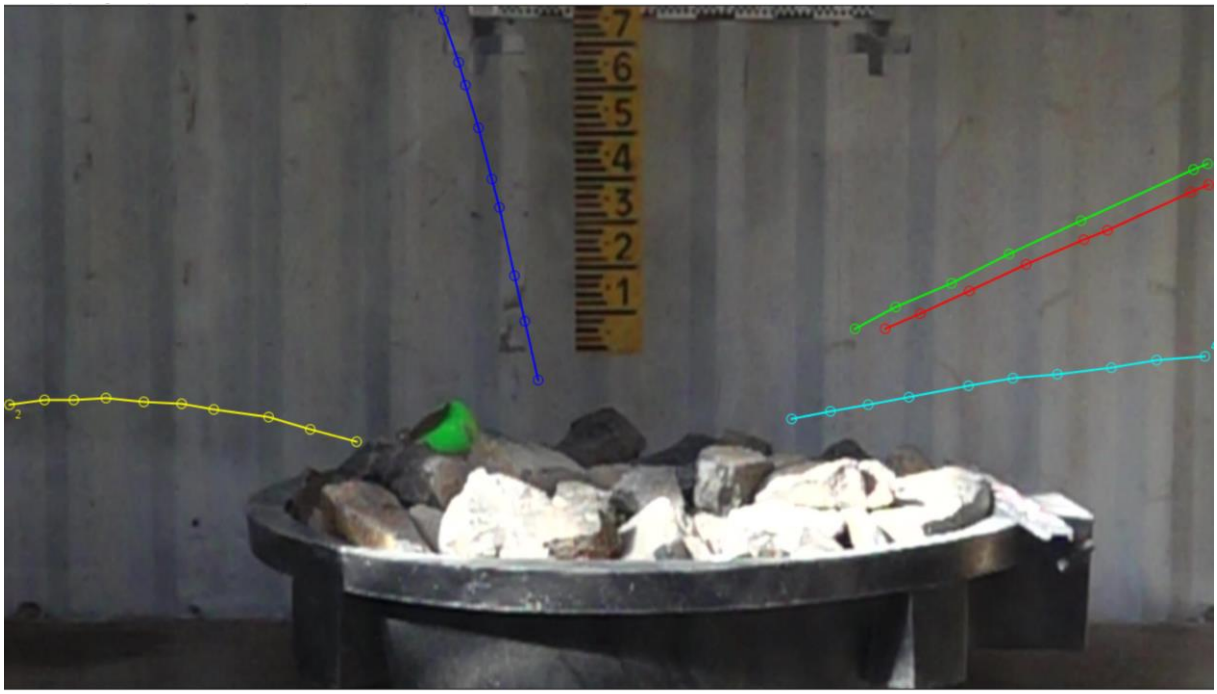

Track #	Points	Dur [sec]	Min v [m/s]	Max v [m/s]	Mean v [m/s]	SD v [m/s]	Min angle [deg]	Max angle [deg]	Mean angle [deg]	SD angle [deg]
1	8	0.057	13.54	14.506	14.151	0.356	-24.963	-21.448	-23.622	1.336
2	10	0.173	4.375	4.914	4.589	0.168	-177.455	180	-54.754	173.656
3	7	0.067	12.483	17.169	13.672	1.74	-27.512	-19.44	-24.414	2.773
4	10	0.1	8.706	10.238	9.462	0.57	-11.07	-4.927	-8.645	2.306
5	10	0.231	1.895	5.682	3.755	1.274	-111.038	-102.095	-105.803	3.138

Figure 4.4 Five fastest ejecta tracked using MTrackJ. Each piece of ejecta has a different coloured track

4.3.3. Ballistic trajectory modelling

As the high-speed video could not capture the full ejecta trajectories, a ballistic trajectory model was used to produce the missing parts of the trajectories. Eject! (Mastin 2001) was used for ease of use as particles could be modelled individually. Table 4.2 lists the input parameters required and the range of values that were used in our modelling. Eject! has the option of modelling particles as a cube, sphere or artillery shell. As most of the ejecta were more rectangular in shape, the volume of the measured ejecta was calculated, and the cube root of this value used as the diameter and modelled as a cube. Thus, the diameter range provided in Table 4.2 is representative of particles with longest axes of 1 – 19 cm.

Table 4.2 Eject! input parameters and values used in the modelling for this study

Parameter	Value	Justification
Drag coefficient	0.1 – 10.0, variable	Set to variable unless trend did not match, then adjusted so that the output matched the experimental results
Shape	Cube low	Ejecta were typically angular
Density	1430, 2800 and 2890 kg/m^3	Depended on whether modelling crusher dust, rock substrate or ballistic
Diameter	0.00464 – 0.088 m	0.00464m for small ejecta (cube root of 1 x 0.5 x 0.2cm) and > 0.00464 m for larger ejecta measured on the video
Tailwind	0 m/s	Tests performed inside containers
Initial ejection velocity	4 – 210 m/s	Depending on track modelled and MTrackJ velocity results
Reduced drag	0 m	No gas jet is present upon impact in contrast to an expanding column in an eruption
Ejection angle	1 – 88°	Based on angles found using MTrackJ and specific to each track
Distance of landing below take-off point	0 m	Experiments on flat ground
Elevation	20 m	Elevation of cannon setup
Temperature	25°C	Average temperature while conducting tests

4.4. Results

4.4.1. Experiments

Ballistics were fired between 12 and 70 m/s, impacting with kinetic energies between 275 and 12618 J. Based on the fatality threshold stated in Baxter and Gresham (1997), all ballistics had impact energies capable of causing fatality.

Substrate played a large part in whether the ballistic shattered on impact. Of the 24 tests onto crusher dust, none of the dense basalt ballistics broke on impact. In contrast 1 out of 3 and 2 out of 3 of vesicular basalt and scoria ballistics respectively broke on impact (Table 4.3). Shattering increased when the substrate was dense basalt blocks. Of the 23 tests 10 out of 17 dense basalt ballistics broke and 100% of the vesicular basalt and scoria ballistics fragmented (Table 4.3). The kinetic energy threshold for dense basalt to break on impact with the crusher dust was therefore > 12800 J, and < 5900 J for vesicular basalt and scoria. The energy threshold for breakage for all ballistic densities onto the dense basalt substrate was < 2800 J.

Table 4.3 Number of ballistics that broke on impact split into substrate, lithology and kinetic energy

	Crusher Dust			Basalt rock		
KE	**Dense basalt**	**Vesicular basalt**	**Scoria**	**Dense basalt**	**Vesicular basalt**	**Scoria**
<1000	0/2			3/5		
1000-2000	0/1		1/1			
2000-3000	0/2		1/2	1/1	1/1	3/3
3000-4000	0/4			0/2	1/1	
4000-5000	0/1	0/1		0/1	1/1	
5000-6000	0/1	1/2		1/1		
6000-7000	0/4					
7000-8000	0/1			3/4		
8000+	0/2			2/3		
Total	**0/18**	**1/3**	**2/3**	**10/17**	**3/3**	**3/3**

Small ejecta (~1 cm length) velocity ranged from 2 to 138 m/s. Larger shrapnel from the ballistics or ejecta from the basalt substrate (2 to 19.5 cm length) was generally slower and ranged from 2 to 30 m/s. Plotting the small ejecta kinetic energy against the ballistics kinetic energy of all the dense basalt tests onto rock shows that ejecta kinetic energy increases with the ballistics kinetic energy (Figure 4.5A). Comparing the dense basalt tests onto crusher dust with impacts onto dense basalt blocks, it is evident that impacts onto harder or more consolidated substrates produce ejecta with higher kinetic energies. A dense basalt ballistic impacting at 12618 J onto crusher dust produced 1 cm ejecta with 0.02 J of kinetic energy. A dense basalt ballistic with similar kinetic energy (12096 J) that impacted a basalt target produced 1 cm ejecta with 0.59 J – an order of magnitude more kinetic energy than the crusher dust test (Figure 4.5B).

Ballistic density also influenced the ejecta kinetic energy. Denser ballistics produced ejecta with higher kinetic energies than low density ballistics when fired at basalt targets. Figure 4.5C shows 1 cm ejecta from dense basalt ballistics with kinetic energies between 0.1 and 0.33 J compared with 0.04 J from vesicular basalt ballistics and 0.02 – 0.04 J from scoria ballistics. Additionally, the ejecta produced in the scoria and vesicular basalt tests is almost entirely shrapnel from the ballistics rather than any debris from the substrate (basalt). This differs from the dense basalt onto basalt block substrate tests where ejecta was a mix of both shrapnel and substrate debris.

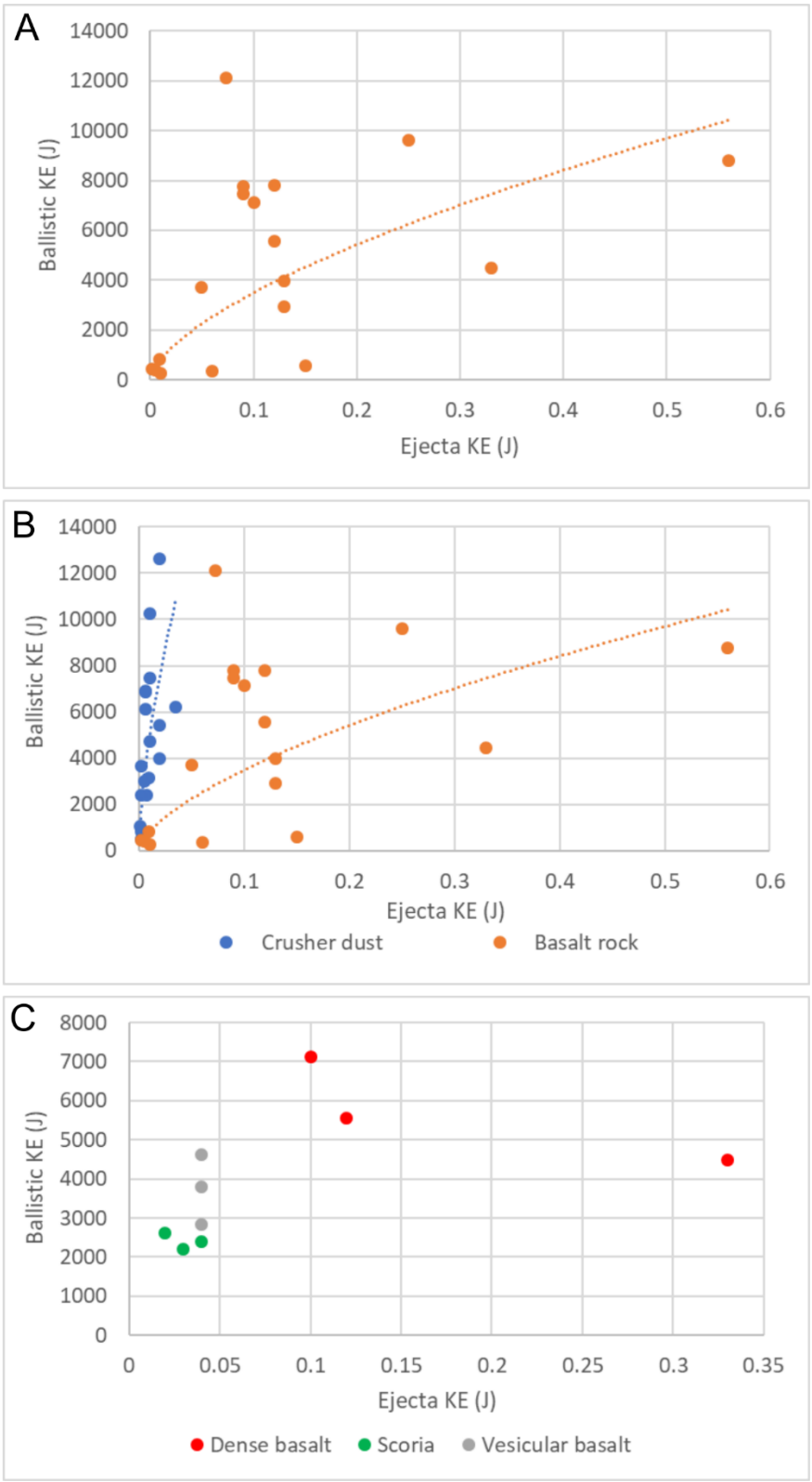

Figure 4.5 Ejecta kinetic energy (KE) plotted against the ballistic kinetic energy. A) Average small ejecta KE from each test from dense basalt ballistics impacting basalt rock surface, B) Average small ejecta KE from each test from dense basalt ballistics impacting crusher dust and basalt rock, C) Average small ejecta KE from each test of dense basalt, scoria and vesicular basalt ballistics fired at the same pressure impacting basalt rock

In 41 out of 44 of the tests, ejecta reached 2.95 m – to the confining walls of the cannon structure. As we could not measure the full distance that the ejecta reached, we used the trajectory model Eject! (Mastin 2001) to model how the kinetic energy would change over the full trajectory.

4.4.2. Experiments vs model

The kinetic energy of ejecta generally decreases with distance from impact which means that ejecta may not be hazardous over the entire trajectory or may decrease the resulting injury severity. High speed video of the impact tests allowed us to analyse the ejecta kinetic energy changes over the first 1.4 m from the impact site. However, over this short distance we noted a considerable variation in velocity (0.2 – 4 m/s) along each track. In Figure 4.6 ejecta kinetic energy is plotted against distance for 12 tracked particles from the cannon tests (labelled video).

To assess how kinetic energy changed with distances greater than 1.4 m, we used Eject! to model the full trajectories of ejecta. Firstly, we modelled our experimental ejecta tracks to validate Eject! against our results. To match our recorded tracks we adjusted the initial velocity (as due to the dust created on impact, tracks did not begin immediately at the impact site) and the drag coefficient (between 0.1 and 10 depending on the size and velocity of the ejecta) to get the best fit with the tracks. The other values were known from the video analysis or measurements taken at the site (Table 4.2). Modelling generally matched well to the video tracked ejecta as seen in Figure 4.6. However, in most of the tests performed in this study, a wobble in ejecta kinetic energy with distance is observed. Taddeucci et al. (2017) have observed wobbles in ballistic projectile trajectories and velocities, attributing this to rotation and spinning (among other factors) of the projectile. They observed decreasing acceleration of irregular shaped ballistics when the ballistic's frontal area (orthogonal to the trajectory) increases due to rotation and the subsequent changes to drag on the ballistic. Additionally, they observed centimetre to decimetre scale wobbling in some trajectories, especially those of irregular shaped ballistics. Video footage of the experiments reported here clearly show spinning and rotation, therefore it is likely that this is the mechanism causing the observed wobble in kinetic energy.

This phenomenon, however, is not observed in the modelled trajectories as Eject! ignores the effects of spinning and rotation (Mastin 2001).

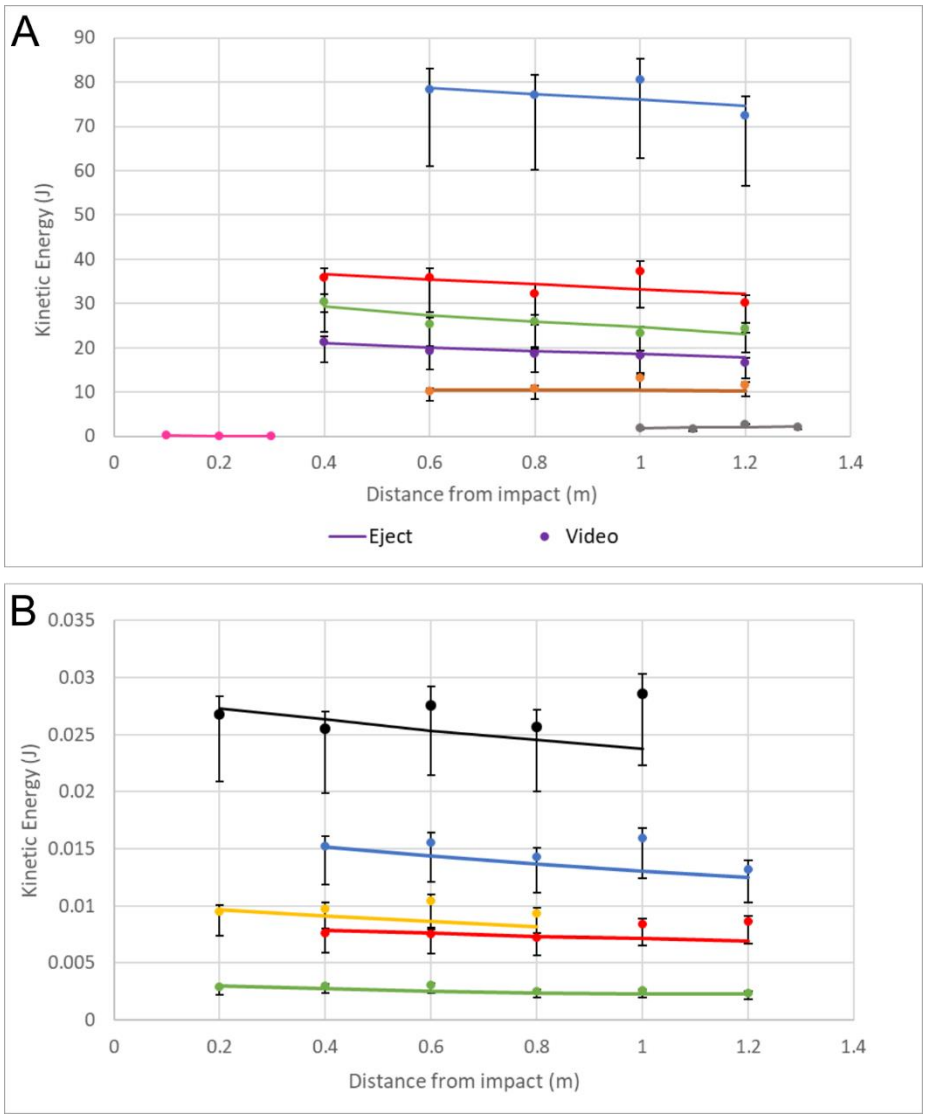

Figure 4.6 Tracked (shown as points) and modelled (presented as a line) ejecta kinetic energy plotted with distance from impact. A) large ejecta, B) small ejecta. Each colour represents one tracked ejecta. Error bars have been applied to the tracked ejecta for error in velocity from trajectories that may not be perpendicular to the camera (between 70 – 90°).

4.4.3. Modelled ejecta

Modelling ejecta trajectories allowed us to analyse changes in kinetic energy at greater distances than what could be observed in the cannon experiment footage, and to assess the full extent of the ejecta footprint. Additionally, as we could not model every particle in each test (only the five fastest and the largest) because of time limitations, we modelled what was theoretically possible based on the tracked ejecta and observations recorded from each test. This allowed us to see the range of ejecta hazard footprints that could be produced from ballistics with similar characteristics (e.g. size, velocity, lithology) to those used in the tests. Size, velocity and ejection angle were varied one at a time to see the influence of each variable separately. Based on the range of ejecta sizes produced in our tests, we modelled ejecta 1 cm to 19 cm in length (Figure 4.7A) at 9 m/s (the average speed of ejecta > 1 cm) and 45°. Initial kinetic energies ranged between 0.01 J and 78 J. Each trajectory was parabolic; kinetic energy declines with distance during the upward trajectory and then increases in kinetic energy again during the downward trajectory due to gravity. Ejecta travel distance ranged between 6.2 m and 8.1 m.

Velocity and ejection angle were modelled for two sizes (1 cm and 9 cm) as the smallest ejecta in our experiments were observed to travel much faster than the larger particles. Therefore, modelling at 1 cm and 9 cm better represents the commonly observed ejecta characteristics. Figure 4.7B and C show the results for a 1 cm ejecta. Velocities were modelled at 20 m/s increments up to 210 m/s – the fastest velocity measured in the cannon tests. Initial kinetic energies ranged between 0.01 J and 6.17 J and maximum travel distance between 7.2 and 52 m. Varying the ejection angle influenced the travel distance of the 1 cm ejecta (Figure 4.7C). A 1 cm particle ejected at 210 m/s could travel between 3 m when ejected at 88° and 60 m at 50°.

Figure 4.7D shows a 9 cm particle (the average size for large ejecta) ejected at 45° could have initial kinetic energies between 0.4 J and 92 J and a travel distance between 40 cm and 65 m when ejected at velocities between 2 and 30 m/s (the slowest and fastest velocities recorded for large ejecta). As with the 1 cm particle, when ejection angle of a 9 cm particle is varied, the maximum travel distance changes (Figure 4.7E). A 9 cm particle ejected at 9 m/s can travel between 0.6m when ejected at 88° and 7.8 m at 40°.

The hazard footprint for ejecta from ballistics impacting at 275 - 12618 J could therefore vary between 0.4 and 60 m radius, with ejecta kinetic energies between 0.01 and 92 J.

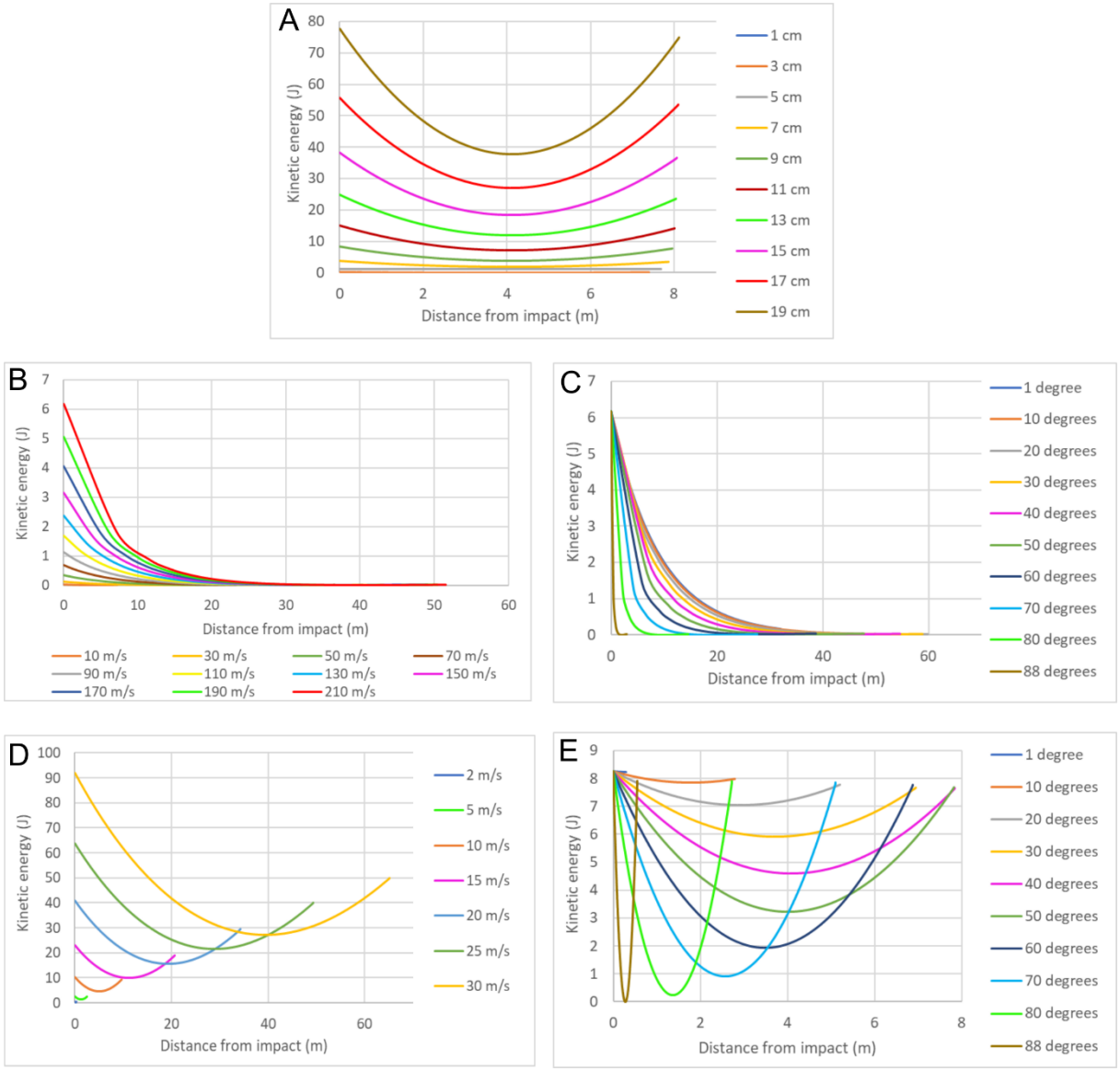

Figure 4.7 Modelled possibilities of ejecta trajectories and kinetic energies with distance from impact. Varying A) size keeping velocity set at 9 m/s and ejection angle at 45°, B) velocity of small ejecta (1 cm) with ejection angles of 45°, C) ejection angle of small ejecta (1 cm) at 210 m/s, D) velocity of average large ejecta (9 cm) at 45°, E) ejection angle of average large ejecta (9 cm) at 9 m/s

Pneumatic cannon experiments were used to investigate impact ejecta travel distances and impact energies to better constrain the role ejecta plays in the ballistic hazard footprint. We found that blocks impacting into harder/more consolidated substrate were more likely to

fragment on impact than into less consolidated substrate, and harder/denser blocks were less likely to fragment than lower density blocks. Additionally, substrate, block density and velocity all affected the kinetic energy of ejecta. Ejecta kinetic energy was found to increase as the impacting block kinetic energy increased. Furthermore, the kinetic energy of ejecta from dense block impacts onto hard substrates was higher than those from more porous blocks and softer substrates. As the full trajectory of ejecta could not be captured by the high-speed camera, Eject! ballistic trajectory model was used to assess the full travel distance and analyse how kinetic energy changes over the entire trajectory. Using the cannon experiment data to inform modelling parameters, we found that ejecta could produce hazard footprint radii between 0.4 m and 60 m, and kinetic energies between 0.1 and 92 J.

4.5. Discussion

Results from the cannon experiments show that substrate and ballistic density influenced whether the ballistic broke on impact and the kinetic energy of the ejecta produced. This is likely due to the varying rock properties and how energy is partitioned in an impact. Dense basalt has a higher Young's Modulus (11 - 73 GPa) than vesicular basalt (5 - 19 GPa), scoria (11.3 GPa) or sand (10 – 69 MPa), thus it needs greater stress before it will elastically deform (Shultz 1993; Kılıç et al. 2003; Zhu 2014; Schaefer et al. 2015). Additionally, dense basalt also has a higher uniaxial compressive strength (138 - 262 MPa) than scoria (0.24 - 28.3 MPa), vesicular basalt (38 - 106 MPa) or sand (<0.1 MPa) and needs greater stress applied to it before it will break (Schultz 1993; Kılıç et al. 2003; Schaefer et al. 2015; Juimo et al. 2017).

Braslau (1970) and Gault and Heitowit (1963) analysed the partitioning of energy from hypervelocity impacts into loose sand and basalt targets respectively. They found that ~53% of the ballistic's impact energy was transferred to the ejecta kinetic energy. For loose sand impacts, 8% went into comminution, 20% into compaction and 32% into waste heat. In the basalt target tests 10 – 24% of the impact energy went into comminution, < 1% into compaction and 23 – 35% into waste heat. Hartmann (1985) observed much lower partitioning of impact energy into ejecta kinetic energy, with around 0.1% for slow impacts (<1 km/s) to ~10% for fast impacts (up to 2.3 km/s). Other experiments of impacts into rock have found ejecta kinetic energy ranged from 10% of the initial impact energy (O'Keefe and Ahrens 1977) to 9 – 92% (Waza et

al. 1985). We do not have the data to analyse energy partitioning from our impact tests, however, we can compare our results and draw some conclusions.

We propose that dense basalt ballistics did not break when impacting crusher dust as more of the impact energy was transferred into the surface to compact the sand and eject debris to produce a crater than into breaking the rock. The dense basalt rebounded elastically and did not experience enough stress to fail and cause breakage (the stress on impact was less than the compressive strength of the dense basalt). Whereas for the scoria and vesicular basalt, their lower compressive strengths were overcome by the impact stress, and they failed. The greatest ejecta kinetic energies were produced from dense basalt impacts onto basalt rock. There was no loss in energy into compaction and crater production, instead most of the energy was partitioned into fragmentation and kinetic energy of the ejecta. The higher Young's Modulus of the dense basalt allowed for efficient elastic rebound and more of kinetic energy transferred into the ejecta. Because the scoria and vesicular basalt was weaker and had a lower Young's Modulus, more energy was lost during fragmentation which produced more ejecta but with less kinetic energy.

4.6. Application of results to ballistic hazard footprint

The experimental and modelling data presented in this paper can be used to better constrain the size of the individual ballistic hazard footprint and better understand the hazard intensity from ejecta and how this changes over the footprint. In addition, the injury data described in Section 4.2.2 can be used to create damage states, hazard intensity thresholds and fragility functions to understand potential injury severity from being within a ballistic hazard footprint. We apply the damage states, hazard intensity thresholds and fragility functions to two cannon experiments to show how these results could be used in future risk assessments.

4.6.1. Vulnerability model

A range of outcomes can occur from being impacted or being in the impact area of a ballistic, from no injury to death. These outcomes can be classified, categorised and assessed for their damage severity using an impact scale (Blong 2003; Wilson et al. 2014, 2017). The ideal scale

to use in this instance would be the Abbreviated Injury Scale (AIS). It is a numerical scale and is now widely used as a traumatic injury scoring system (Loftis et al. 2018). However, it does not link the damage severity to the hazard intensity (impact energy). Whether ballistics cause death or injury and the severity of that injury largely depends on their impact energy and where on the body they impact. We use impact energy as the measure of hazard intensity (Hazard Intensity Metric). As we do not have sufficient hazard intensity data to apply to every level of the AIS, we have created our own damage states (Table 4.4). Levels include 0 (no injury), 1 (minor injury), 2 (serious injury) and 3 (death). Minor injuries were considered non-life threatening and included lacerations, bruising and eye injuries. Serious injuries were those that could be life threatening, potentially causing internal bleeding and brain injury.

Table 4.4 Numerical damage state scale with associated damage descriptions

Damage State	Damage description
0	No injury
1	Minor injury
2	Serious injury
3	Death

The damage states were then applied to the damage data presented in Section 4.2.2, in Table 4.5.

Table 4.5 Ballistic damage descriptions and hazard intensity metrics from the medical literature with damage states applied

Study	Kinetic Energy (J)	Injury	DS	Reference
1	80	Death	3	Baxter and Gresham 1997
2	76	Skull fracture with 10% chance of fatality	2	Radi 2013
3	28	Skull fracture	2	Yoganandan et al. 1995
4	13	Lung membrane injury	2	Smedra-Kazmirska et al. 2013
4	13	Heart membrane injury	2	Smedra-Kazmirska et al. 2013
4	13	Liver injury	2	Smedra-Kazmirska et al. 2013
4	13	Spleen injury	2	Smedra-Kazmirska et al. 2013
4	13	Kidney injury	2	Smedra-Kazmirska et al. 2013
4	13	Femoral artery injury	2	Smedra-Kazmirska et al. 2013
4	13	Aorta injury	2	Smedra-Kazmirska et al. 2013
4	1.7	Lung injury	2	Smedra-Kazmirska et al. 2013
4	1.7	Liver injury	2	Smedra-Kazmirska et al. 2013

5	6.5	Bruising to lower leg	1	Desmoulin and Anderson 2011
6	23.99	50% probability of skin penetration of the torso	1	Bir et al. 2012
7	12.8	Skin penetration	1	Di Maio et al. 1982
8	10	Skin penetration	1	Koene and Papy 2011
9	9.7	Skin penetration	1	Warlow et al. 2005
10	9.02	Laceration	1	Whittle et al. 2008
11	0.184	Corneal abrasion	1	Duma 2005
11	1.09	Retinal damage	1	Duma 2005
11	4	Eye globe rupture	1	Duma 2005
12	6	Corneal perforation	1	Sellier and Kneubuehl 1994
8	2.5	Irreversible eye damage	1	Koene and Papy 2011
13	27.4	Skull fracture	2	Raymond et al. 2009
13	19.6	Skull fracture	2	Raymond et al. 2009
13	51.5	Skull fracture	2	Raymond et al. 2009
13	54.1	Skull fracture	2	Raymond et al. 2009
13	58.5	Skull fracture	2	Raymond et al. 2009
13	63.4	Skull fracture	2	Raymond et al. 2009
13	63.8	Skull fracture	2	Raymond et al. 2009

To relate hazard intensity (kinetic energy) to damage severity (damage state) fragility functions derived from our collated damage data (Table 4.5) were created. Fragility functions express the probability that a damage state will be reached or exceeded as a function of hazard intensity (Wilson et al. 2017). Following the methodology set out in Porter (2007) and Wilson et al. (2017), all damage data was ordered by increasing impact energy and binned, with each bin having approximately the same number of data points (Figure 4.8). The probability of reaching or exceeding each damage state was then calculated for each HIM bin by adding the number of data points that were equal or greater than the specific damage state and dividing that by the total number of data points in that bin. The probability for that damage state can then be plotted against the median impact energy of each bin (Figure 4.8). To assign a HIM for each damage state we use 50% probability, therefore DS1 will occur at or above 1.6 J, DS2 at or above 8.2 J, and DS3 at or above 66.8 J.

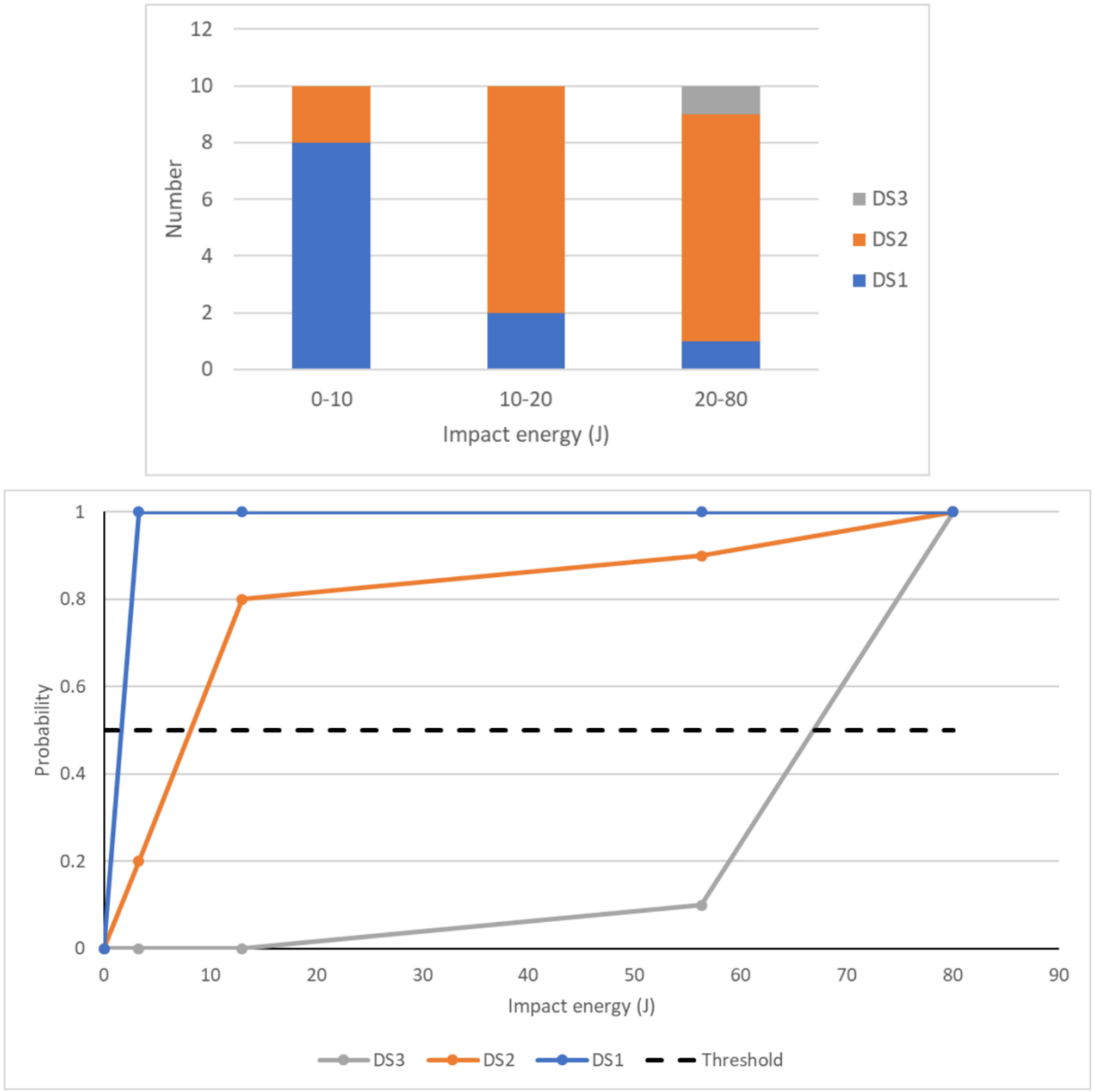

Figure 4.8 Ejecta damage histogram and fragility functions. A) Bar graph of literature derived damage data classified by damage state into three ejecta impact energy bins. B) Fragility functions derived from damage literature showing probability of reaching or exceeding each damage state vs ejecta impact energy

4.6.2. Hazard model

Damage states and hazard intensity metrics allow us to understand and explore the range of consequences to humans from ballistic impact and the hazard intensity at which these are likely to occur. As demonstrated in the preceding sections, the hazard intensity can vary across the

hazard footprint as impact energy usually decreases with distance from impact. Subsequently, the likely impact severity will also vary across the footprint and thus ballistics should not be considered binary hazards. To assess likely impact severity across the hazard footprint, we can apply our damage states and HIMs to the hazard footprint and zone the footprint depending on what DS is expected. This allows us to estimate areas and distances at which to expect certain consequences. We apply the damages states and HIMs produced in Section 4.6.1 to our cannon results to provide an example of this methodology.

As observed in Figure 4.7, the ejecta hazard footprint can change with changing velocity, size and ejection angle of the ejecta. Thus, two scenarios were chosen from the cannon results to illustrate how the vulnerability model can be applied to the hazard footprint to assess the changing hazard intensity: 1) A cannon test fired at 2 bar onto crusher dust using a dense basalt ballistic; and 2) a 5-bar test fired at basalt rock using a dense basalt ballistic. The tracked ejecta from the relevant test were modelled in Eject! to ascertain the full trajectories of the ejecta. The hazard footprint radius is based on the maximum travel distance as ejecta cannot travel further than this. Therefore, the hazard footprint for scenario 1 has a radius of 8 m and is 201 m^2 (Figure 4.9A), and scenario 2 has a radius of 29 m and an area of 2642 m^2 (Figure 4.9B).

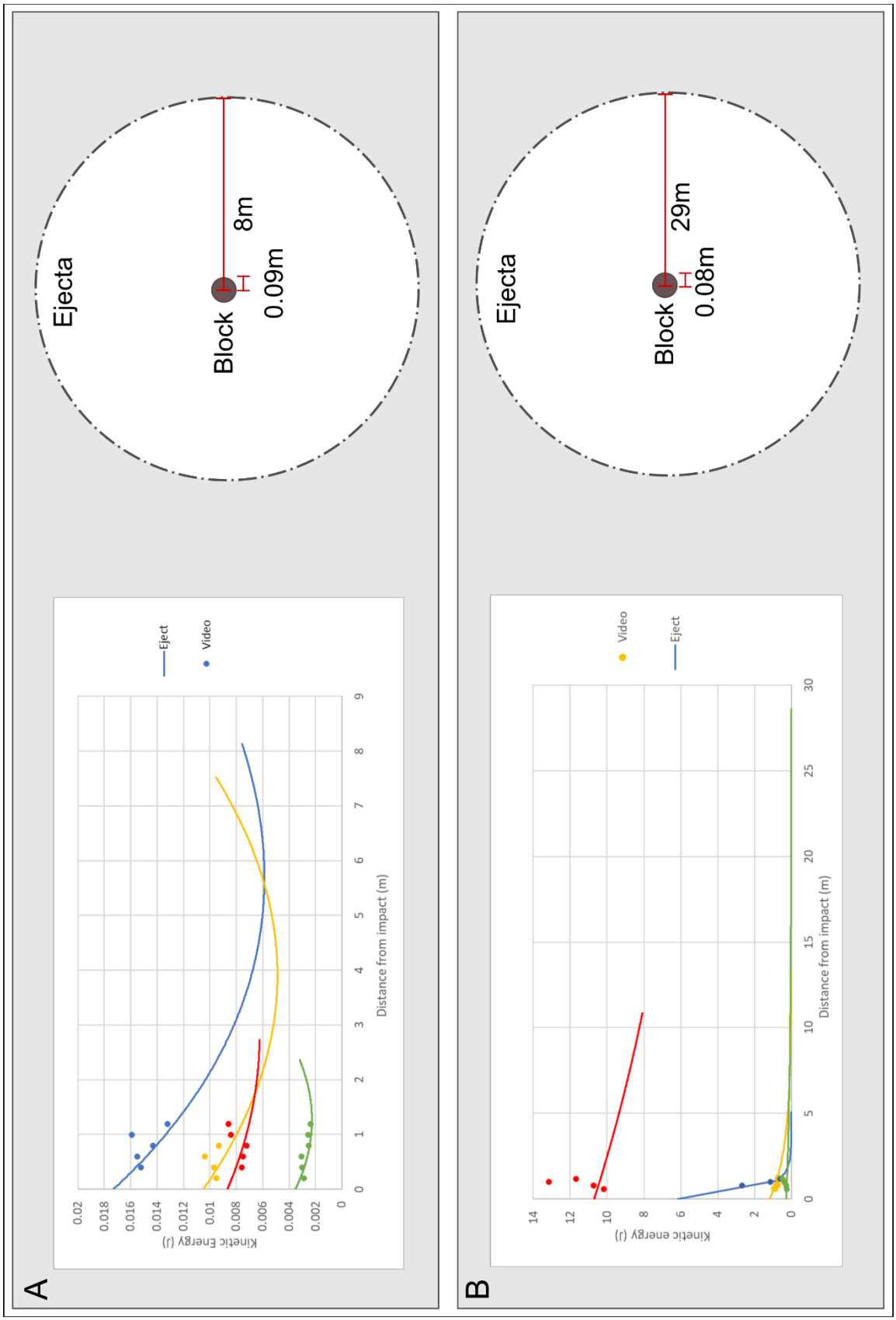

Figure 4.9 Hazard footprints from two tests based on modelled maximum ejecta travel distance. A) 2 bar test onto crusher dust using a dense basalt ballistic, and B) a 5-bar test fired at basalt rock using a dense basalt ballistic. Each colour represents a piece of ejecta

All ejecta from scenario 1 fall within DS0 as none have kinetic energies ≥ 1.6 J. However, we do know the kinetic energy of the ballistic (2403 J) which is above the DS3 threshold therefore the first 9 cm is classified as DS3 (Figure 4.10A).

Scenario 2 can be divided up into three damage states. As with scenario 1, the ballistic impacts above the threshold of DS 3 at 8784 J, thus the first 8 cm are zoned DS3. Four ejecta were tracked and range in their kinetic energies and travel distances. Taking a precautionary/conservative approach as it is a potential life safety issue, we use the highest kinetic energy and greatest travel distance to set damage zones. Figure 4.10B shows that the highest ejecta KE is above the DS2 threshold until 10 m at which point it drops below this threshold to DS1 until it lands at 11 m. The highest kinetic energy from here is well below the DS1 threshold with ejecta landing until 29 m distance from the ballistic impact. Thus, we have zoned DS2 until 10 m, DS1 until 11 m and DS0 until 29 m where the hazard footprint ends. However, the kinetic energies of the tracks could also be averaged, and the average trajectory used to set damage zones.

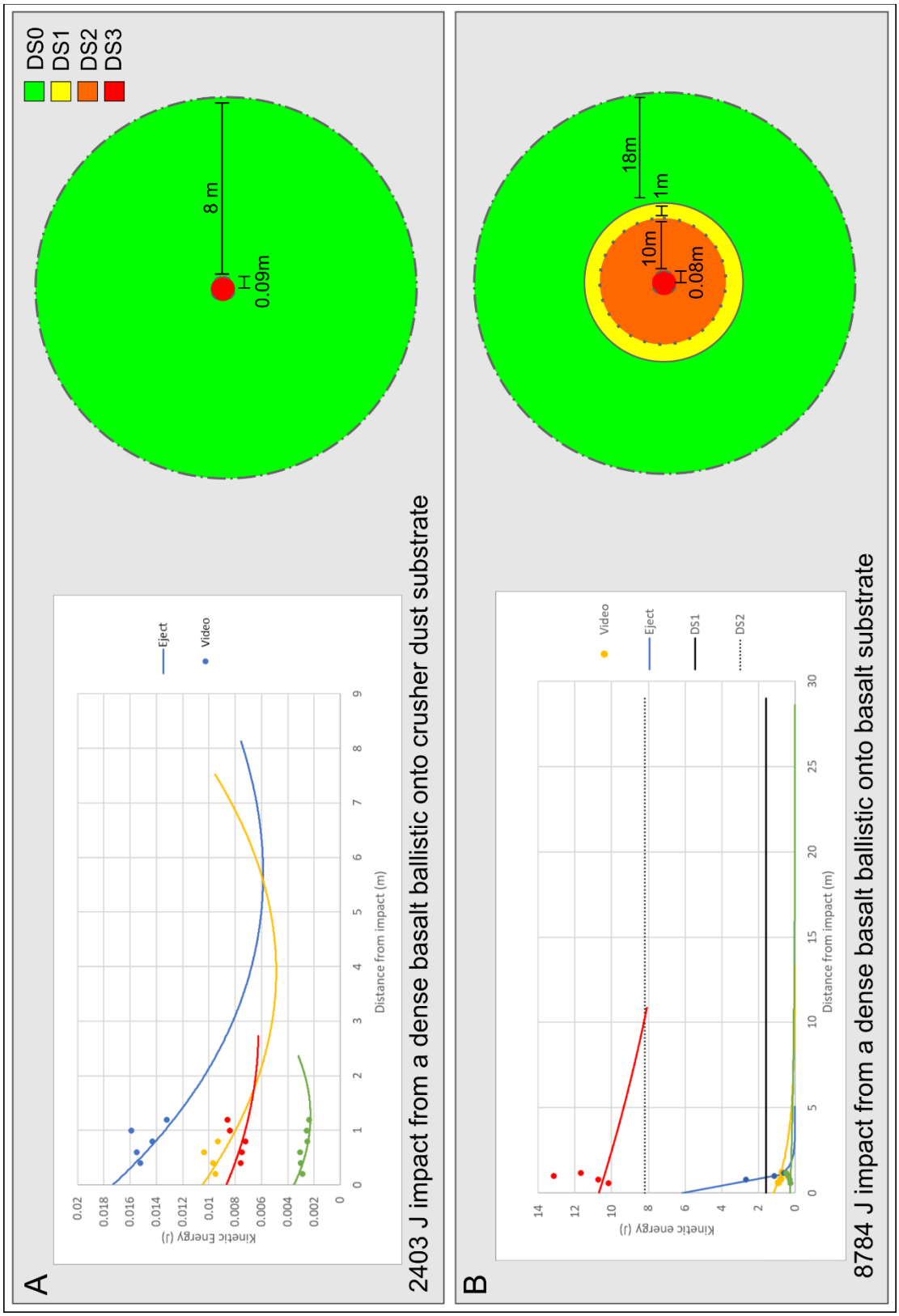

Figure 4.10 Hazard footprints zoned by damage state based on maximum kinetic energy and modelled maximum ejecta travel distance from two tests. A) 2 bar test onto crusher dust using a dense basalt ballistic, and B) a 5-bar test fired at basalt rock using a dense basalt ballistic. Each colour represents a piece of ejecta

4.7. Conclusions

Many injuries and fatalities have been recorded from volcanic ballistic projectiles. However, it was unclear which aspects of the ballistic hazard could cause these outcomes. The hazard footprint around an individual ballistic impact can be influenced by a number of factors including crater size, ballistic size, ejecta apron size, impact angle, slope, substrate and ballistic lithology. Using a pneumatic cannon, we investigated how the kinetic energy of the ballistic, the substrate impacted, and the density of the ballistic influenced whether ejecta was produced, if that ejecta was capable of causing injury or death, and over what distance. Results indicated that ballistics should not be considered as a binary hazard and that direct impact and impact ejecta can cause a range of injuries or death. Additionally, density, substrate and velocity all affected the kinetic energy of ejecta. Ejecta produced from dense ballistic impacts onto hard substrates had higher kinetic energies than ejecta from more porous ballistics and softer substrates. Experiments combined with trajectory modelling allowed for analysis of kinetic energy changes along the ejecta trajectory so that hazard intensity could be analysed over the whole ejecta hazard footprint. Four damage states were created to classify damage/injury severity and fragility functions were derived from this data to assign hazard intensity metrics to the damage states. Using the hazard intensity metrics and damage states we assessed the hazard footprint and probability of injury from ejecta from two of the cannon tests. Injury severity ranged from DS2 (serious) to DS0 (no injury) over the 207.65 m^2 and 2569.7 m^2 hazard footprints.

The damage states, hazard intensity metrics and fragility functions developed here should be built on by others to include a widened set of variables (velocity, surfaces etc.) and could be useful tools to apply in volcanic hazard and risk assessments.

4.8. Acknowledgements

We are grateful for all the experimental assistance provided by Peter Jones, Matt Cockcroft, Steph Gates, George Williams, Alex Watson, Ame McSporran, Josh Hayes, Luke Hewitson, and Ian Reeves. This work was supported by a biennial grant (16/727) from the New Zealand Earthquake Commission (EQC). RHF was supported by a Ngāi Tahu Research Centre Doctoral

Scholarship. BK was additionally supported by the “Quantifying exposure to specific and multiple volcanic hazards" programme of the New Zealand Natural Hazards Research Platform (NHRP).

4.9. References

Alatorre-Ibargüengoitia MA, Delgado-Granados H, Dingwell DB (2012). Hazard map for volcanic ballistic impacts at Popocatépetl volcano (Mexico). Bulletin of Volcanology 74(9), 2155–2169.

Alatorre-Ibargüengoitia MA, Morales-Iglesias H, Ramos-Hernández SG, Jon-Selvas J, Jiménez-Aguilar JM (2016). Hazard zoning for volcanic ballistic impacts at El Chichón Volcano (Mexico). Natural Hazards, DOI 10.1007/s11069-016-2152-0.

Allen LR (1948). Activity at Ngauruhoe, April–May 1948. N Z J Sci Tech B30, 187–193.

Andronico D, Scollo S, Cristaldi A (2015). Unexpected hazards from tephra fallouts at Mt Etna: The 23 November 2013 lava fountain. Journal of Volcanology and Geothermal Research, 304, 118-125.

Baxter P, Gresham A (1997). Deaths and injuries in the eruption of Galeras Volcano, Colombia, 14 January 1993. Journal of Volcanology and Geothermal Research, 77, 325–338.

Bernard B (2018). Rapid hazard assessment of volcanic ballistic projectiles using long-exposure photographs: insights from the 2010 eruptions at Tungurahua volcano, Ecuador. Volcanica, 1(1), 49–61. https://doi.org/https://doi.org/10.30909/vol.01.01.4961.

Biass S, Falcone J-L, Bonadonna C, Di Traglia F, Pistolesi M, Rosi M, Lestuzzi P (2016). Great balls of fire: a probabilistic approach to quantify the hazard related to ballistics — a case study at La Fossa volcano, Vulcano Island, Italy. J. Volcanol. Geotherm. Res. 325, 1–14. http://dx.doi. org/10.1016/j.jvolgeores.2016.06.006.

Bir CA, Resslar M, Stewart S (2012). Skin penetration surrogate for the evaluation of less lethal kinetic energy munitions. Forensic Science International, 220, 126 – 129.

Blong RJ (1984). Volcanic hazards: A sourcebook on the effects of eruptions. Orlando: Academic Press.

Blong R (2003). A review of damage intensity scales. Natural Hazards, 29, 57–76.

Booth B (1979). Assessing volcanic risk. Journal of the Geological Society 136(3), 331–340.

Braslau D (1970). Partitioning of energy in hypervelocity impact against loose sand targets.

Journal of Geophysical Research, 75(20), 3987 – 3999.

Breard ECP, Lube G, Cronin SJ, Fitzgerald R, Kennedy B, Scheu B, Montanaro C, White JDL, Tost M, Procter JN, Moebis A (2014). Using the spatial distribution and lithology of ballistic blocks to interpret eruption sequence and dynamics: August 6 2012 Upper Te Maari eruption, New Zealand. Journal of Volcanology and Geothermal Research 286, 373–386.

Brown SK, Jenkins SF, Sparks RSJ, Odbert H, Auker MR (2017). Volcanic fatalities database: analysis of volcanic threat with distance and victim classification. Journal of Applied Volcanology, 6, 15.

Cintala MJ, Wood CA, Head JW (1977). The effects of target characteristics on fresh crater morphology: Preliminary results for the moon and Mercury. Proceedings of the 8th Lunar and Planetary Science Conference, 3409 – 3425.

Deligne NI, Jolly GE, Taig T, Webb TH (2018). Evaluating life-safety risk for fieldwork on active volcanoes: the volcano life risk estimator (VoLREst), a volcano observatory's decision-support tool. Journal of Applied Volcanology 7, 7.

Desmoulin GT, Anderson GS (2011). Method to Investigate Contusion Mechanics in Living Humans. Journal of Forensic Biomechanics, 2, 10p.

Di Maio VJM, Copeland AR, Besant-Matthews PE, Fletcher LA, Jones A (1982). Minimal velocities necessary for perforation of skin by air gun pellets and bullets, J. Forensic Sci., JFSCA, 27, 894–898.

Dufresne A, Poelchau MH, Kenkmann T, Deutsch A, Hoerth T, Schäfer F, Thoma K (2013). Crater morphology in sandstone targets: The MEMIN impact parameter study. Meteoritics and Planetary Science, 48(1), 50–70. https://doi.org/10.1111/maps.12024.

Duma S (2005). Determination of Significant Parameters for Eye Injury Risk from Projectiles. The Journal of TRAUMA, Injury, Infection, and Critical Care, 59, 960-964.

Finlay P, Mostyn G, Fell R (1988). Landslides: Prediction of travel distance guidelines for vulnerability of persons. Proceedings of the 8th Australia New Zealand Conference on Geomechanics, 105 –113.

Fitzgerald RH, Kennedy BM, Gomez C, Wilson TM, Simons B, Leonard GS, Jolly AD, Matoza R, Garabiti E (in review). Ballistic deposition from a frequently erupting volcano: Yasur Volcano, Vanuatu. Volcanica.

Fitzgerald RH, Tsunematsu K, Kennedy BM, Breard ECP, Lube G, Wilson TM, Jolly AD,

Pawson J, Rosenberg MD, Cronin SJ (2014). The application of a calibrated 3D ballistic trajectory model to ballistic hazard assessments at Upper Te Maari, Tongariro. Journal of Volcanology and Geothermal Research, 286, 248–262.

Fudali R, Melson W (1972). Ejecta velocities, magma chamber pressure and kinetic energy associated with the 1968 eruption of Arenal volcano. Bulletin of Volcanology 35:383 – 401.

Gault DE, Greeley R (1978). Exploratory experiments of impact craters formed in viscous-liquid targets: Analogs for Martian rampart craters? Icarus, 34(3), 486–495. https://doi.org/10.1016/0019-1035(78)90040-4.

Gault DE, Heitowit ED (1963). The partition of energy for hypervelocity impact craters formed in rock. Proc. Sixth Hypervelocity Impact Symp. 2, 419-456.

Gault DE, Wedekind JA (1978). Experimental studies of oblique impact. Proceedings of the 9th Lunar and Planetary Science Conference, 3843 – 3875.

Gouhier M, Donnadieu F (2011). Systematic retrieval of ejecta velocities and gas fluxes at Etna volcano using L-Band Doppler radar. Bulletin of Volcanology, 73(9), 1139–1145. https://doi.org/10.1007/s00445-011-0500-1.

Graettinger AH, Valentine GA, Sonder I, Ross P-S, White JDL (2015). Facies distribution of ejecta in analog tephra rings from experiments with single and multiple subsurface explosions. Bulletin of Volcanology, 77(8), 66. https://doi.org/10.1007/s00445-015-0951-x.

Gurioli L, Harris AJL, Colo L, Bernard J, Favalli M, Ripepe M, Andronico D (2013) Classification, landing distribution, and associated flight parameters for a bomb field emplaced during a single major explosion at Stromboli, Italy. Geology 41(5):559–562

Harris AJL, Ripepe M, Hughes EA (2012). Detailed analysis of particle launch velocities, size distributions and gas densities during normal explosions at Stromboli. Journal of Volcanology and Geothermal Research 231-232, 109–131.

Hartmann WK (1985). Impact experiments. 1. Ejecta velocity distributions and related results from regolith targets. Icarus, 63(1), 69–98. https://doi.org/10.1016/0019-1035(85)90021-1.

Holsapple K, Giblin I, Housen K, Nakamura A, Ryan E (2002). Asteroid impacts : Laboratory experiments and scaling laws. Asteroids III, 443–462.

Jenkins SF, Spence RJS, Fonseca JFBD, Solidum RU, Wilson TM (2014). Volcanic risk

assessment: Quantifying physical vulnerability in the built environment. Journal of Volcanology and Geothermal Research 276, 105–120.

Jolly GE, Keys HJR, Procter JN, Deligne NI (2014). Overview of the co-ordinated risk-based approach to science and management response and recovery for the 2012 eruptions of Tongariro volcano, New Zealand. Journal of Volcanology and Geothermal Research 286, 184–207.

Juimo WH, Cherradi T, Abidi ML (2017). Mechanical properties of volcanic scoria for using as lightweight aggregate concrete. Proceedings from the 2nd International Conference on Bio-based Building Materials & 1st Conference on ECOlogical valorisation of GRAnular and FIbrous materials, Clermont-Ferrand, France.

Kaneko T, Maeno F, Nakada S (2016). 2014 Mount Ontake eruption: characteristics of the phreatic eruption as inferred from aerial observations. Earth, Planets and Space 68, 72-82.

Kılıç A, Atiş CD, Yaşar E, Özcan F (2003). High-strength lightweight concrete made with scoria aggregate containing mineral admixtures. Cement and Concrete Research, 33(10), 1595 – 1599.

Kimura S (2016). Mount Yasur volcano, Tanna, Vanuatu 2m from my camera. Retrieved from https://www.youtube.com/watch?v=XWeCuIC2zyw&feature=youtu.be.

Koene L, Papy A (2011). Towards a better, science-based, evaluation of kinetic non-lethal weapons. International Journal of Intelligent Defence Support Systems, 4(2), 169. https://doi.org/10.1504/ijidss.2011.039548.

Krohn K, Jaumann R, Elbeshausen D, Kneissl T, Schmedemann N, Wagner R, Voigt J, Otto K, Matz KD, Preusker F, Roatsch T, Stephan K, Raymond CA, Russell CT (2014). Asymmetric craters on Vesta: Impact on sloping surfaces. Planetary and Space Science, 103, 36 – 56.

Loftis KL, Price J, Gillich PJ (2018). Evolution of the Abbreviated Injury Scale : 1990 – 2015. Traffic Injury Prevention, 19(S2), S109–S113. https://doi.org/10.1080/15389588.2018.1512747.

Lyon DH, Bir CA, Patton BJ (1999). Injury Evaluation Techniques for Non-Lethal Kinetic Energy Munitions, Army Research Laboratory, Aberdeen Proving Ground, Report # ART-TR-1868, January.

Maeno F, Nakada S, Nagai M, Kozono T (2013). Ballistic ejecta and eruption condition of the vulcanian explosion of Shinmoedake volcano, Kyushu, Japan on 1 February, 2011. Earth,

Planets and Space 65(6), 609–621.

Manga M, Patel A, Dufek J, Kite ES (2012). Wet surface and dense atmoshpere on early Mars suggested by the bomb sag at Home Plate, Mars. Geophysical Research Letters, 39(1), L01202.

Massey CI, McSaveney MJ, Heron D, Lukovic B (2012). Canterbury Earthquakes 2010/11 Port Hills Slope Stability: Pilot study for assessing life-safety risk from rockfalls (boulder rolls), GNS Science Consultancy Report 2011/311

Mastin LG (2001). A simple calculator of ballistic trajectories for blocks ejected during volcanic eruptions. U.S. Geol. Surv. Open File Rep., 01-45.

McGetchin TR, Settle M, Chouet BA (1974). Cinder cone growth modeled after Northeast Crater, Mount Etna, Sicily. Journal of Geophysical Research, 79(23), 3257 – 3272.

Michikami T, Moriguchi K, Abe M, Hasegawa S, Fujiwara A (2001). Ejecta velocity distribution for impact cratering experiment on porous target. Proc. 34th ISAS Lunar Planet. Symp., 107–110.

Minakami T (1942). 5. On the distribution of volcanic ejecta (Part I.): The distributions of volcanic bombs ejected by the recent explosions of Asama. Bulletin of Earthquake Research Institute, 20, 65 – 92.

Nairn IA, Self S (1978). Explosive eruptions and pyroclastic avalanches from Ngauruhoe in February 1975. Journal of Volcanology and Geothermal Research 3, 36–60.

Oberbeck VR (1975). The role of ballistic erosion and sedimentation in lunar stratigraphy. Reviews of Geophysics and Space Physics, 13(2), 337–362. https://doi.org/10.1029/RG013i002p00337.

O'Keefe JD, Ahrens TJ (1985). Impact and explosion crater ejecta, fragment size, and velocity. Icarus, 62(2), 328–338. https://doi.org/10.1016/0019-1035(85)90128-9.

Osman S, Rossi E, Bonadonna C, Frischknecht C, Andronico D, Cioni R, Scollo S (2019). Exposure-based risk assessment and emergency management associated with the fallout of large clasts. Natural Hazards and Earth System Sciences, 19, 589–610. https://doi.org/10.5194/nhess-2018-91.

Petrucelli E, States JD, Hames LN (1981). The abbreviated injury scale: Evolution, usage and future adaptability. Accident, Analysis and Prevention, 13(1), 29–35.

Pierazzo E, Melosh HJ (2000). Understanding oblique impacts from experiments, observations, and modeling. Annual Review of Earth And Planetary Sciences, 28, 141–167.

https://doi.org/10.1146/annurev.earth.28.1.141

Pistolesi M, Rosi M, Pioli L, Renzulli A, Bertagnini A, Andronico D (2008). The paroxysmal event and its deposits. The Stromboli Volcano: An Integrated Study of the 2002 - 2003 Eruption. Geophysica, 317–330.

Pomonis A, Spence R, Baxter P (1999). Risk assessment of residential buildings for an eruption of Furnas Volcano, Sao Miguel, the Azores. J. Volcanol. Geotherm. Res. 92(1–2):107–131.

Porter K, Kennedy R, Bachman R (2007). Creating fragility functions for performance-based earthquake engineering. Earthquake Spectra 23, 471–489.

Radi A (2013). Human injury model for small unmanned aircraft impacts. Civil Aviation Safety Authority, 31p.

Raymond D, Van Ee C, Crawford G, Bir C (2009). Tolerance of the skull to blunt ballistic temporo-parietal impact. Journal of Biomechanics, 42(15), 2479–2485. https://doi.org/10.1016/j.jbiomech.2009.07.018.

Rosi M, Bertagnini A, Harris AJL, Pioli L, Pistolesi M, Ripepe M (2006). A case history of paroxysmal explosion at Stromboli: Timing and dynamics of the April 5, 2003 event. Earth and Planetary Science Letters, 243, 594 – 606.

Self S, Kienle J, Huot J (1980). Ukinrek Maars, Alaska, II. Deposits and formation of the 1977 craters. Journal of Volcanology and Geothermal Research, 7, 39–65.

Sellier, K.G. and Kneubuehl, B.G. (1994). Wound Ballistics and the Scientific Background, Elsevier, Amsterdam.

Schaefer LN, Kendrick JE, Oommen T, Lavallée Y, Chigna G (2015). Geomechanical rock properties of a basaltic volcano. Frontier in Earth Science, 3, 29 – 44.

Schultz RA (1993). Brittle strength of basaltic rock masses with applications to Venus. Journal of Geophysical Research, 98(E6), 10883 – 10895.

Shiroko J (2016). Patients hit by rocks during the Mt Ontake volcanic eruption in Japan: An experience of trauma cases. Journal of clinical images and case reports, 2(1).

Smedra-Kaźmirska A, Barzdo M, Kedzierski M, Antoszczyk L, Szram S, Berent J (2013). Experimental effect of shots caused by projectiles fired from air guns with kinetic energy below 17 J. Journal of Forensic Sciences, 58(5), 1200–1209. https://doi.org/10.1111/1556-4029.12251.

Smith K (2013). Environmental Hazards: Assessing Risk and Reducing Disaster. Routledge,

New York, USA.

Steinberg G, Lorenz V (1983). External ballistic of volcanic explosions. Bulletin Volcanologique 46(4), 333-348.

Sturdivan LM, Viano DC, Champion HR (2004). Analysis of injury criteria to assess chest and abdominal injury risks in blunt and ballistic impacts. Journal of Trauma, 56(3), 651–663.

Swanson DA, Zolkos SP, Haravitch B (2012). Ballistic blocks around Kīlauea Caldera: Their vent locations and number of eruptions in the late 18th century. Journal of Volcanology and Geothermal Research 231-232, 1-11.

Taddeucci J, Alatorre-Ibargüengoitia MA, Cruz-Vázquez O, Del Bello E, Scarlato P, Ricci T (2017). In-flight dynamics of volcanic ballistic projectiles. Reviews of Geophysics, 55(3), 675–718. https://doi.org/10.1002/2017RG000564.

Taddeucci J, Scarlato P, Capponi A, Del Bello E, Cimarelli C, Palladino DM, Kueppers U (2012). High-speed imaging of Strombolian explosions: The ejection velocity of pyroclasts. Geophysical Research Letters 39, L02301.

Tsunematsu K, Ishimine Y, Kaneko T, Yoshimoto M, Fujii T, Yamaoka K (2016). Estimation of ballistic block landing energy during 2014 Mount Ontake eruption. Earth, Planets and Space 68, 88.

Uehara JS, Ambroso MA, Ojha RP, Durian DJ (2003). Low-speed impact craters in loose granular media. Physical Review Letters, 90(19), 194301. https://doi.org/149902\r10.1103/PhysRevLett.91.149902.

Waitt RB, Mastin LG, Miller TP (1992). Ballistic Showers During Crater Peak Eruptions of Mount Spurr Volcano, Summer 1992. In: The 1992 eruptions of Crater Peak vent, Mount Spurr Volcano, Alaska. U.S. Geological Survey Bulletin (Vol. 2139). https://doi.org/10.1002/spe.4380120106.

Warlow T (2005). Firearms, the Law and Forensic Ballistics, CRC Press, Boca Raton.

Waza T, Matsui T, Kani K (1985). Laboratory simulation of a planetesimal collision. 2. Ejecta velocity distribution. J. Geophys. Res., 90, 1995–2011.

Whittle K, Kieser J, Ichim I, Swain M, Waddell N, Livingstone V, Taylor M (2008). The biomechanical modelling of non-ballistic skin wounding: blunt-force injury. Forensic Science, Medicine, and Pathology, 4(1), 33–39. https://doi.org/10.1007/s12024-007-0029-y

Williams GT, Kennedy BM, Wilson TM, Fitzgerald RH, Tsunematsu K, Teissier A (2017).

Buildings vs. ballistics: Quantifying the vulnerability of buildings to volcanic ballistic impacts using field studies and pneumatic cannon experiments. Journal of Volcanology and Geothermal Research 343, 171-180.

Wilson G, Wilson TM, Deligne NI, Blake DM, Cole JW (2017). Framework for developing volcanic fragility and vulnerability functions for critical infrastructure. Journal of Applied Volcanology, 6, 14–38. https://doi.org/10.1186/s13617-017-0065-6.

Wilson G, Wilson TM, Deligne NI, Cole JW (2014). Volcanic hazard impacts to critical infrastructure : A review. Journal of Volcanology and Geothermal Research, 286, 148–182.

Yamagishi H, Feebrey C (1994). Ballistic ejecta from the 1988–1989 andesitic Vulcanian eruptions of Tokachidake volcano, Japan: morphological features and genesis. Journal of Volcanology and Geothermal Research, 59(4), 269–278.

Yoganandan N, Pintar F, Sances A, Walsh PR, Ewing CL, Thomas DJ, Snyder RG (1995). Biomechanics of skull fracture. Journal of Neurotrauma, 12(4), 659–668.

Zhu T (2014). Some Useful Numbers on the Engineering Properties of Materials (Geologic and Otherwise) GEOL 615. Retrieved from https://www.jsg.utexas.edu/tyzhu/files/Some-Useful-Numbers.pdf.

Chapter Five – Conclusions

An increasing number of visitors to, and people living near, volcanoes creates increased exposure to volcanic hazards (Erfurt-Cooper, Sigurdsson and Lopes 2015). The recent disaster at Mt Ontake, Japan and the 367 deaths from ballistic impact at volcanoes around the world shows how dangerous volcanic ballistics can be (Tsunematsu et al. 2016; Brown et al. 2017). This necessitates better understanding of the hazard and its consequences so that more effective disaster risk reduction strategies can be practiced. These strategies should be based on appropriate and targeted scientific data and use a risk-based approach.

In comparison to other volcanic hazards (e.g. ashfall) volcanic ballistics have received little research attention despite being the most common cause of fatalities for visitors and scientists on volcanoes (Brown et al. 2017). There is a plethora of data recording how far ballistics can travel (Minakami 1942; Nairn and Self 1978; Blong 1984; Kilgour et al. 2010; Alatorre-Ibargüengoitia et al. 2012) but little data on how they are distributed and their spatial density within this area. This can be attributed to the inherent risk to scientists mapping time-sensitive ballistic deposits where there may be further eruptions. As such, when ballistics have been included in hazard and risk assessments and management decisions, ballistic hazard has traditionally been considered by placing a precautionary zone around the volcano, often based on the maximum travel distance of ballistics (e.g. Coombs et al. 2008; Alatorre-Ibargüengoitia et al. 2012). This management approach is relatively crude and potentially unsuitable to many risk contexts, particularly with increasing tourist activity and other livelihood pressures necessitating access to active volcanoes. Additionally, little work has been done to determine the hazard footprint of an individual ballistic. When assessing risk in the past, only a direct hit by a ballistic has been considered (Jolly et al. 2014; Deligne et al. 2018). However, there are many other aspects of a ballistic impact that make up the hazard footprint. The hazard footprint area is used by risk managers to calculate the probability of someone being hit by a ballistic while on the volcano (Jolly et al. 2014; Deligne et al. 2018). It is essential to know the potential size of the hazard footprint that a person could be affected by and the hazard intensity that may be experienced.

Within this context, this thesis has sought to better understand: ballistic hazard and risk and how it is assessed, managed and communicated, providing an overview of the topic area, knowledge gaps to guide the more in-depth hazard research that follows and recommendations for future management and communication (Objective 1); how ballistics are distributed within a ballistic field and their spatial hazard intensity (Objective 2); the temporal deposition of ballistics and how this is influenced by eruption dynamics (Objective 3); the factors that contribute to the hazard footprint from an individual ballistic (Objective 4); and the hazard intensity from impact ejecta within the individual hazard footprint (Objective 5). Improving our understanding of ballistic hazard in the aforementioned ways will improve our ability to assess hazard and risk and subsequently apply appropriate disaster risk reduction measures.

5.1. Key findings from each thesis chapter

Understanding how ballistic hazard and risk is communicated and managed, how ballistics are distributed in space and time, and how hazard intensity changes over the hazard footprint vastly improve our ability to assess ballistic hazard and risk. This section summarises the major findings of each chapter, supported by a summary table (Table 5.1) detailing the key findings for each objective.

5.1.1. Chapter 2

Ballistic hazard and risk changes depending on the eruptive state of the volcano, exposure of assets and people, and their vulnerability, and ballistic risk management and communication strategies applied at volcanoes should also reflect this. A literature review of ballistic hazard characteristics and current knowledge, consequences to society, and management and communication methods used for both ballistic hazard and other volcanic hazards resulted in recommendations for how to improve ballistic hazard communication and management. To manage and communicate ballistic risk effectively, recommended methods and actions to take include: 1) Hazard and risk assessments specific to the volcano, which, if appropriate, include ballistics. These assessments should be accessible by emergency managers and decision makers with authors/scientists available to answer questions and advise where necessary and practical;

2) The inclusion of ballistic hazard zones in hazard maps with accompanying advice on actions to take. Maps should be updated in a crisis with new information and readily available through a range of media. These maps should continue to be updated after an eruption when detailed scientific studies are complete; 3) Volcano monitoring systems to monitor volcanic activity and indicate volcano unrest; 4) Signage around the volcano to communicate ballistic hazard and risk to visitors, in addition to other hazard advice such as warning systems where practical, with a focus on effectiveness of communication; 5) Volcanic alert bulletins, media releases or reports to communicate ballistic hazard and risk in crisis phases; and 6) Open, sufficiently frequent communication between scientists, stakeholders, emergency managers and local communities.

5.1.2. Chapter 3

Yasur Volcano, Vanuatu was used as a case study to assess how ballistic distribution and intensity change over a ballistic field. It was found that ballistic hazard can vary over relatively small areas. The ballistic spatial density and mean ballistic diameter decreased with distance from the crater. Analysis of the spatial density across the field revealed higher densities in the S – SSE compared to the rest of the field. Video, geophysical data and topographic analysis show that this was due to preferential directionality in explosions. However, directionality was found to vary over time when two data sets over different timescales were compared. To get the highest resolution understanding of the spatial and temporal aspects of the hazard and make the most effective risk management decisions, assessments should be conducted over as much of the volcano as possible and address a timeframe relevant to the longevity of the hazard assessment, i.e. includes all temporal hazard changes that may occur in the relevant timeframe. It is also important to map ballistics as quickly as possible to get an accurate assessment of the hazard because Yasur ballistics were buried by further eruption deposits over time. Without this consideration, the ballistic hazard could be underestimated or distorted.

5.1.3. Chapter 4

The size of the hazard footprint from an individual impact and the intensity (kinetic energy) are also important considerations when assessing hazard and risk to humans. The hazard footprint is the area around a ballistic impact in which a person is in potential danger and is used by risk

managers to calculate probability of casualty from a ballistic impact, while the kinetic energy/hazard intensity is used to calculate vulnerability. The size of the footprint depends on the impact energy of the ballistic, ballistic diameter, crater diameter, ejecta travel distance, ejecta impact energy, ballistic density, substrate hardness, impact angle and slope. Pneumatic cannon experiments showed that ejecta from ballistic impacts was an important part of the hazard footprint. Some ejecta produced on impact had sufficient kinetic energy to cause fatality or injury, though this was highly dependent on the hardness of the substrate impacted, the density of the ballistic, the impact energy, and the distance along the ejecta trajectory. Ejecta typically did not retain kinetic energy levels over the entire trajectory, indicating that hazard intensity changed over the hazard footprint. Kinetic energy is therefore a suitable hazard intensity metric for individual ballistic hazard footprints.

Table 5.1 Key findings and thesis objectives from each chapter

Chapter	Thesis objective	Key findings
Chapter 2: The communication and risk management of volcanic ballistic hazards	6) Review ballistic hazard and risk characteristics, management and communication to provide an overview of the topic and provide recommendations for how management and communication could be improved.	Recommended strategies to manage and communicate ballistic risk effectively: 1A) Accessible hazard and risk assessments specific to the volcano, which, if appropriate, include ballistics 1B) The inclusion of ballistic hazard zones in hazard maps with accompanying advice on actions to take. Maps should be updated with changing levels of crisis with new information and readily available through a range of media 1C) Targeted volcano monitoring systems to monitor volcanic activity and indicate volcano unrest 1D) Signage and warning systems around the volcano to communicate ballistic hazard and risk to visitors 1E) Volcanic alert bulletins, media releases or reports to communicate ballistic hazard and risk in crisis phases 1F) Open, sufficiently frequent communication between scientists, stakeholders, emergency managers and local communities.
Chapter 3: Ballistic deposition from a frequently	7) Determine the size and spatial distribution of ballistics from a complex,	2A) The spatial density of the ballistics decreased with increasing distance away from the crater

erupting volcano: Yasur Volcano, Vanuatu	cumulative ballistic field through detailed mapping, to understand the spatial and temporal distribution of hazard intensity across the hazard footprint. 8) Using an integrative approach, assess temporal ballistic hazard and how this is affected by eruption dynamics.	2B) The mean ballistic diameter decreased with distance from the crater. 2C) Higher spatial densities of ballistics are seen in the S-SSE than in other directions due to explosion directionality. 3A) A different directionality was observed in the GoPro videos than in the daily observations and ballistics mapped from aerial photos, representing the short-term and long-term directionality trends respectively. 3B) Field preservation issues are observed, with the burial of ballistics by further deposition of tephra over time. Therefore, ballistic mapping is time sensitive after an eruption and delays in mapping will likely be accompanied by decrease in field preservation and result in an underestimation of ballistic hazard.
Chapter 4: Using pneumatic cannon experiments to understand ejecta hazard intensity within ballistic hazard footprints	9) Review and understand the factors that contribute to the hazard footprint from an individual ballistic impact 10) Quantify the size and hazard intensity from impact ejecta associated with ballistics of different density and different substrates to the individual hazard footprint to improve ballistic hazard and risk assessments	4A) Contributing factors to ballistic hazard footprint size include: ballistic kinetic energy, ballistic size, crater size, ejecta apron size, slope, impact angle, ballistic density, and substrate hardness 5A) Ballistic density, substrate and velocity affect the kinetic energy of ejecta. 5B) Ejecta produced from dense ballistic impacts onto hard substrates had higher kinetic energies than ejecta from more porous ballistics and softer substrates 5C) Kinetic energy is an appropriate hazard intensity metric for ballistic impact and, combined with the damage states and fragility functions, can be used to assess exposure and vulnerability in the future.

5.2. Future work

This research has identified a number of avenues for future work. Wider ballistic research should look to focus on:

1) Using an integrated approach to monitor and forecast ballistic hazard. Chapter 3 highlighted how acoustic data is highly complementary to visual observation of eruption size/energy. There may be potential to use geophysical networks to monitor and forecast the expected area of ballistic deposition. A larger eruption ejects ballistics further, therefore greater magnitude acoustic waves could indicate greater ballistic hazard. However, these data remain relatively un-calibrated. Appendix A describes the effectiveness of acoustic monitoring in recording eruptive activity at Yasur.
2) Improving understanding of human exposure to ballistic hazard. The number of people that visit a volcano may be known, but little is understood about human behaviour in terms of movement on a volcano during non-eruption and rapid onset eruption situations (including evacuation dynamics).
3) Improving understanding of vulnerability within ballistic risk assessments. Human vulnerability research is scant for ballistic impacts. All that is known is the types and severity of injuries that can be sustained from direct ballistic impact (Baxter and Gresham 1997; Shiroko 2016). Research is needed to determine which areas of the body are most exposed and the likelihood of injury occurring with varying hazard intensity (i.e. fragility functions) for different parts of the body. This research should be conducted by someone with a medical background who understands injury severity. In addition to human vulnerability, further research is also needed on building and infrastructure vulnerability to ballistic impact. Some work has been done to assess building vulnerability (see Appendix D and references therein), however further building typologies and other infrastructure should also be analysed, and fragility functions created.
4) Systematic and robust collection of damage data for both people and the built environment to inform exposure and vulnerability calculations and fragility functions. Chapter 4 reviews the limited literature available for human impacts, however further research into other similar causes of injury, further experiments, and better recording of ballistic impacts that occur on volcanoes (including the nature of the injury, the location/distance from vent that the injury occurred at, and any information on the size and characteristics of the ballistic) is needed. Additionally, Appendix D provides some damage data for buildings, though there is a lack of data for other infrastructure. Similarly to human impacts, useful data to collect for building and infrastructure

includes descriptions of the damage observed, descriptions of the asset affected i.e. building type and element damaged, location or distance from the vent, and ballistic size and characteristics.

5) Including ballistics in volcanic multi-hazard assessments where appropriate. Often ballistics are left out as the hazard footprint of other hazards (PDCs and ash) are larger and engulf the ballistic footprint. However, ballistics are often the most damaging and dangerous hazard produced in unheralded and small (e.g. phreatic, Strombolian) eruptions, as seen at Mt Ontake (Kaneko et al. 2016; Tsunematsu et al. 2016) and Upper Te Maari (Fitzgerald et al. 2014). Appendix C describes eruptions scenarios, that include ballistic modelling, created to assess consequences and risk from eruptions in the Auckland Volcanic Field. Effective Disaster Risk Reduction (DRR) should to be underpinned by effective understanding of the potential hazard and risks (UNISDR 2015).
6) Improving ballistic risk management and communication to reduce consequences. This should take into account volcanoes that are highly visited and/or settled, unheralded eruptions, volcanoes with poorly understood eruptive histories, volcanoes with limited monitoring resources, and engagement between authorities and stakeholders.

More specific suggestions of future work directions for ballistic hazard include:

- Increasing the breadth of data available on ballistic distribution within a field, especially from varying eruptions styles and sizes (see Appendix B for preliminary mapping from a multi-vent phreatic and phreatomagmatic eruption). More quality size, distribution and spatial density data available on a wide variety of ballistic fields will result in a more accurate and detailed understanding of the hazard and how this varies between different volcanoes and eruption styles.
- Expanding ejecta hazard footprint size and intensity testing to refine the footprint and hazard intensity metrics. In this thesis, only three lithologies, two surfaces and velocities between 12 and 70 m/s were tested. Further testing could include other surfaces such as scoria and concrete/asphalt that represents carparks and paths around volcanoes; more lithologies such as more crystalline ballistics (andesitic or dacitic lavas) and obsidian (as seen at Puyahue-Cordon Caulle following the 2011 eruption); and an extended velocity range.

- More research to understand and quantify the other factors described in Chapter 4 that influence hazard footprint size. This may be experimental or from fieldwork.
- A model that can incorporate all factors of hazard footprint to produce expected footprint size and hazard intensity over different areas/changing volcanic landscapes. This could then be quickly used by risk managers to calculate vulnerability and risk.
- Mapping over longer time scales and at varying periodicities both at Yasur and at other volcanoes. The ballistic mapping at Yasur only encompasses three months of explosions and within that time eruption directionality changed. Better understanding of the short term and long-term spatial hazard is needed.

This will lead to a much better understanding of ballistic hazard from any eruption, more accurate risk assessments, and more targeted risk management strategies.

5.3. References

Alatorre-Ibargüengoitia MA, Delgado-Granados H, Dingwell DB (2012). Hazard map for volcanic ballistic impacts at Popocatépetl volcano (Mexico). Bulletin of Volcanology 74(9), 2155–2169

Baxter P, Gresham A (1997). Deaths and injuries in the eruption of Galeras Volcano, Colombia, 14 January 1993. Journal of Volcanology and Geothermal Research 77, 325–338

Blong RJ (1984). Volcanic hazards: A sourcebook on the effects of eruptions. Orlando: Academic Press

Brown SK, Jenkins SF, Sparks RSJ, Odbert H, Auker MR (2017). Volcanic fatalities database: analysis of volcanic threat with distance and victim classification. Journal of Applied Volcanology, 6, 15

Coombs ML, McGimsey RG, Browne BL (2008). Preliminary Volcano-Hazard Assessment for Gareloi Volcano , Gareloi Island. Alaska Scientific Investigations Report 2008-5159

Deligne NI, Jolly GE, Taig T, Webb TH (2018). Evaluating life-safety risk for fieldwork on active volcanoes: the volcano life risk estimator (VoLREst), a volcano observatory's decision-support tool. Journal of Applied Volcanology 7, 7

Erfurt-Cooper P, Sigurdsson H, Lopes RMC (2015). Volcanoes and Tourism. In: Sigurdsson H (ed), The Encyclopedia of Volcanoes, Academic Press, 1295-1311

Fitzgerald RH, Tsunematsu K, Kennedy BM, Breard ECP, Lube G, Wilson TM, Jolly AD, Pawson J, Rosenberg MD, Cronin SJ (2014). The application of a calibrated 3D ballistic trajectory model to ballistic hazard assessments at Upper Te Maari, Tongariro. Journal of Volcanology and Geothermal Research 286, 248–262

Jolly GE, Keys HJR, Procter JN, Deligne NI (2014). Overview of the co-ordinated risk-based approach to science and management response and recovery for the 2012 eruptions of Tongariro volcano, New Zealand. Journal of Volcanology and Geothermal Research 286, 184–207

Kaneko T, Maeno F, Nakada S (2016). 2014 Mount Ontake eruption: characteristics of the phreatic eruption as inferred from aerial observations. Earth, Planets and Space 68, 72-82

Kilgour G, Della Pasqua F, Hodgson KA, Jolly GE (2010). The 25 September 2007 eruption of Mount Ruapehu, New Zealand: Directed ballistics, surtseyan jets, and ice-slurry lahars. Journal of Volcanology and Geothermal Research 191(1-2), 1–14

Minakami T (1942). 5. On the distribution of volcanic ejecta (Part I.): The distributions of volcanic bombs ejected by the recent explosions of Asama. Bulletin of Earthquake Research Institute 20, 65 – 92

Nairn IA, Self S (1978). Explosive eruptions and pyroclastic avalanches from Ngauruhoe in February 1975. Journal of Volcanology and Geothermal Research 3, 36–60

Shiroko J (2016). Patients hit by rocks during the Mt Ontake volcanic eruption in Japan: An experience of trauma cases. Journal of clinical images and case reports, 2(1)

Tsunematsu K, Ishimine Y, Kaneko T, Yoshimoto M, Fujii T, Yamaoka K (2016). Estimation of ballistic block landing energy during 2014 Mount Ontake eruption. Earth, Planets and Space 68, 88

UNISDR (2015). Sendai Framework for Disaster Risk Reduction (2015-2030). United Nations International Strategy for Disaster Reduction, Geneva, Switzerland. Retrieved from http://www.unisdr.org/we/coordinate/sendai-framework

Appendix A: Capturing the Acoustic Radiation Pattern of Strombolian Eruptions using Infrasound Sensors Aboard a Tethered Aerostat, Yasur Volcano, Vanuatu

Arthur D. Jolly[1], Robin S. Matoza[2], David Fee[3], Ben M. Kennedy[4], Alexandra M. Iezzi[3], Rebecca H. Fitzgerald[4], Allison C. Austin[2], and Richard Johnson[5]

[1]GNS Science, Lower Hutt, New Zealand

[2]Department of Earth Science and Earth Research Institute, University of California, Santa Barbara, CA, USA

[3]Geophysical Institute, University of Alaska Fairbanks, Fairbanks, AK, USA,

[4]Department of Geological Sciences, University of Canterbury, Christchurch, New Zealand,

[5]GNS Science, Wairakei Research Centre, Taupo, New Zealand

Journal: Geophysical Research Letters

Submitted: 16 July 2017

Accepted: 14 September 2017

Online: 25 September 2017

(See Electronic Appendices)

Appendix B: A progress report on the assessment of ballistic hazard and impacts from the 2000 eruption of Usu, Japan and the 2014 eruption of Mt Ontake, Japan

Rebecca Fitzgerald[1], George Williams[1,2], Ben Kennedy[1], Thomas Wilson[1], Graham Leonard[3], Kae Tsunematsu[4], Hiromu Okada [5], Koshun Yamaoka [6]

[1] University of Canterbury, Private Bag 4800, Christchurch 8140, New Zealand

[2] Earth Observatory of Singapore, Nanyang Technological University, 50 Nanyang Ave, 639798, Singapore

[3] GNS Science, PO Box 30368, Lower Hutt 5040, New Zealand

[4] Mount Fuji Research Institute, Yamanashi Prefectural Government, 5597-1 Kenmarubi Kamiyoshida, Fujiyoshida-shi, Yamanashi 403-0005, Japan

[5] Hokkaido University, N10W5 Sapporo, Hokkaido 060-0810, Japan

[6] Earthquake and Volcano Research Centre, Graduate School of Environmental Studies, Nagoya University, Furo-cho, Chikusa-ku, Nagoya 464-8601, Japan

Journal: Earthquake Commission research funding report

Submitted: 30 January 2018

(See Electronic Appendices)

Appendix C: The DEVORA Scenarios: Multi-hazard eruption scenarios for the Auckland Volcanic Field

Josh L. Hayes[1], Sophia W. Tsang[2], Rebecca H Fitzgerald[1], Daniel M. Blake[1], Natalia I. Deligne[3], Angela Doherty[4], Jenni L. Hopkins[5], Tony W, Hurst[3], Nicolas Le Corvec[6], Graham S. Leonard[3], Jan M. Lindsay[2], Craig A. Miller[7], Karoly Nemeth[8], Elaine Smid[2], James D.L. White[9], Thomas M. Wilson[1]

[1]University of Canterbury, Private Bag 4800, Christchurch, New Zealand
[2]University of Auckland, Private Bag 92019, Auckland, New Zealand
[3]GNS Science, PO Box 30-368, Lower Hutt, New Zealand
[4]Auckland Council, Bledisloe House, Auckland, New Zealand
[5]Victoria University of Wellington, PO Box 600, Wellington, New Zealand
[6]Laboratoire Magmas et Volcans, Université Clermont Auvergne—CNRS—IRD, OPGC, 6 Avenue Blaise Pascal, 63178, Aubière Cedex, France
[7]GNS Science, Private Bag 2000, Taupo, New Zealand
[8]Massey University, Private Bag 11-222, New Plymouth, New Zealand
[9]Otago University, 362 Leith Street, Dunedin, New Zealand

Journal: GNS Science Report
Online: September 2018

(See Electronic Appendices)

Appendix D: Buildings vs. ballistics: Quantifying the vulnerability of buildings to volcanic ballistic impacts using field studies and pneumatic cannon experiments

George T. Williams[1], Ben M. Kennedy[1], Thomas M. Wilson[1], Rebecca H. Fitzgerald[1], Kae Tsunematsu[2], Adrian Teissier[1]

[1] Department of Geological Sciences, University of Canterbury, Private Bag 4800, Christchurch, New Zealand

[2] Mount Fuji Research Institute, Yamanashi Prefectural Government, 5597-1 Kenmarubi Kamiyoshida, Fujiyoshida-shi, Yamanashi 403-0005, Japan

Journal: Journal of Volcanology and Geothermal Research
Submitted: 16 March 2017
Accepted: 30 June 2017
Online: 2 July 2017

(See Electronic Appendices)